THE ROLE OF CCL5 (RANTES) IN THE IMMUNE RESPONSE AGAINST *Mycobacterium tuberculosis* IN THE GUINEA PIG

A Dissertation

by

TROY ARTHUR SKWOR

Submitted to the Office of Graduate Studies of
Texas A&M University
in partial fulfillment of the requirements for the degree of

DOCTOR OF PHILOSOPHY

December 2004

Major Subject: Medical Sciences

THE ROLE OF CCL5 (RANTES) IN THE IMMUNE RESPONSE AGAINST

***Mycobacterium tuberculosis* IN THE GUINEA PIG**

A Dissertation

by

TROY ARTHUR SKWOR

Submitted to Texas A&M University
in partial fulfillment of the requirements
for the degree of

DOCTOR OF PHILOSOPHY

Approved as to style and content by:

David N. McMurray (Chair of Committee)	Jane Welsh (Member)
Jonathan T. Skare (Member)	John M. Quarles (Head of Department)
Vernon L. Tesh (Member)	

December 2004

Major Subject: Medical Sciences

ABSTRACT

The Role of CCL5 (RANTES) in the Immune Response Against *Mycobacterium tuberculosis* in the Guinea Pig. (December 2004)

Troy Arthur Skwor, B.S., University of Wisconsin – Madison

Chair of Advisory Committee: Dr. David N. McMurray

Tuberculosis is the second leading cause of morbidity and mortality worldwide due to an infectious disease. Development of a new tuberculosis (TB) vaccine would be facilitated by a better understanding of the mechanisms of protection induced by the current TB vaccine, *Mycobacterium bovis* BCG. Recombinant guinea pig (rgp)CCL5 and anti-rgpCCL5 were developed and characterized. The biological activity of rgpCCL5 was determined in a chemotaxis assay using T lymphocytes and pleural exudate cells. The specificity of rabbit anti-rgpCCL5 polyclonal antibody was confirmed by Western blot. RgpCCL5 was used to stimulate alveolar and peritoneal macrophages *in vitro.* and cytokine/chemokine gene expression was evaluated using real-time PCR. RgpCCL5 stimulated TNFα, IL-1β, CCL2, and CXCL8 mRNA expression and TNFα protein production (as assessed in the L929 cell bioassay) in macrophages. The effect of BCG-vaccination on CCL5 expression and production in leukocytes infected with *M. tuberculosis* was examined *in vitro* and *in vivo.* Polyclonal anti-rgpCCL5 was used to develop an ELISA assay to quantify gpCCL5 protein levels, and real-time PCR was used to detect CCL5 mRNA. Leukocytes isolated from BCG-vaccinated guinea pigs and infected *in vitro* with virulent *M. tuberculosis* demonstrated

significantly elevated gpCCL5 mRNA and protein compared to cells from naive animals. The response of gpCCL5 to *M. tuberculosis in vivo* was studied in tuberculous pleural effusions, where peak levels of CCL5 mRNA and protein were reached at day 4 post-induction. Disease severity, cellular differentiation, histology, and cytokine/chemokine mRNA levels in pleural cells and granulomas were analyzed on day 4 in guinea pigs induced with tuberculous pleurisy and treated with either rgpCCL5 or anti-rgpCCL5 by direct intra-pleural injection. In these studies, neutralizing CCL5 resulted in reduced macrophage accumulation, diminished levels of IFNγ, TNFα, and CCL5 mRNA in pleural effusion cells, and reduced spontaneous lymphocyte proliferation. Together these studies suggest an important role for gpCCL5 in activating leukocytes during *M. tuberculosis* infection.

ACKNOWLEDGEMENTS

I would first like to acknowledge and thank Dr. David McMurray for his guidance, support, and belief in me. He has provided moral support throughout my graduate studies, and has been a good mentor throughout my research experience. I would also like to thank all the previous and present laboratory members in Dr. David McMurray's laboratory for the wonderful working environment they created. Dr. Shannon Sedberry Allen has been wonderful co-worker throughout my years at Texas A&M University. She has been an excellent source to converse with regarding numerous scientific ideas pertaining to my studies, as well as anything on my mind. I would like to acknowledge her help in optimizing the real-time PCR methodology, as well as numerous components involved in the pleuritic guinea pig model. Hyosun Cho has donated numerous hours performing bioassays detecting bioactive TNFα protein in many of my samples She has also been a wonderful person in providing support and discussing scientific theories. Dr. Christine McFarland has been responsible for bringing many smiles to my face during difficult periods in my graduate studies. She has also provided moral support, as well as giving beneficial advice regarding many of my studies. I would like to thank Dr. Ammini Jeevan for her development of many guinea pig reagents and assays, and would like to thank her for her support and prayers. I would also like to thank other previous and current members of the laboratory, Kirti Sawant, Dr. Todd Lasco, Dr. Mark Lyons, Dr. Toshiko Yamamoto, and Susan Phalen for their support, fellowship, and assistance throughout my graduate studies.

I would like to acknowledge and thank my family who have been so supportive throughout this difficult journey in my life. I am extremely thankful to my parents who have been with me throughout my trials and tribulations and who always believed in me. My brothers, Cory and Shane Skwor, and their wives, Amy and Amy, have been a blessing throughout my life in everything I do. My family was crucial in my successful completion of my doctorate degree. My nephew, Brendan Skwor, and my goddaughter/niece, Makenna Skwor, though too little to know, have given me strength to continue during difficult times always reminding me that no matter how difficult and confusing my studies appeared, life is beautiful and precious.

I also would like to thank all the high school kids and core team members involved in Keysis at St. Joseph's, my piano students and their families, and the seniors at St. Joseph Manor for the moral support and prayers throughout my graduate studies. I am also indebted to them for allowing me to see the important things in life.

TABLE OF CONTENTS

CHAPTER Page

LIST OF FIGURES

FIGURE Page

FIGURE Page

LIST OF TABLES

CHAPTER I

INTRODUCTION

TUBERCULOSIS EPIDEMIOLOGY

Tuberculosis has plagued mankind for thousands of years. Archeological evidence has displayed uncontested evidence of tuberculosis in Dynasty mummies as far back as 1000 B.C. Today the causative agent, *Mycobacterium tuberculosis*, is still estimated to infect one-third of the world's population and claims more than 2 million lives a year (56). The majority of these cases occur in sub-Saharan Africa and Southeast Asia, however, due to the increased international travel this disease presents as a global threat. Until the mid–1980s, tuberculosis appeared to be declining in many developed countries (31). It is believed that the resurgence of tuberculosis was related to the development of the HIV pandemic. Numerous areas with high prevalence of tuberculosis correlated with endemic areas of HIV, with Africa reporting up to one-third of TB cases being HIV-positive (56).

PATHOGENESIS OF *M. tuberculosis*

The pathogenesis of tuberculosis begins when a droplet nucleus (< 5μm in size) containing *M. tuberculosis* is inhaled by the host and proceeds down the airway until reaching the distal end of the respiratory tree, where the organisms enter the alveolar space. In the alveolus, resident macrophages phagocytose 'foreign invaders' and what

---

This dissertation follows the style and format of Infection and Immunity.

occurs next determines the outcome of *M. tuberculosis* infection. In the presence of an activated macrophage, the microbe is destroyed by reactive oxygen and nitrogen intermediates (ROIs and RNIs) (1, 42, 104). If the alveolar macrophage is not activated, the microbe will remain in the lag phase for a few days and then proceed to undergo numerous rounds of replication (18-24 h per replication cycle) within the macrophage resulting in host cell death and the release of a plethora of organisms into the surrounding environment. Products of these infected macrophages will attract numerous blood leukocytes to the site of infection, and the extracellular bacteria can then be internalized by incoming blood monocytes (21), neighboring alveolar macrophages (72), alveolar epithelial cells (20, 21, 71), neutrophils (97), and possibly M cells lining the bronchi (194). The blood monocytes which ingest *M. tuberculosis* can mature into macrophages, but are unable to kill the microbe. As a result, the organisms continue to replicate in these inflammatory cells, eventually destroying the cells resulting in the release of more bacteria into the environment. This process is repeated continually until ~ 2-3 weeks into infection when bacteria and/or their antigens are taken to draining lymph nodes via dendritic cells and presented to T cells. Upon development of T cell immunity, antigen-specific T lymphocytes enter into inflamed foci, proliferate, and release interferon-γ (IFNγ), which synergistically works with tumor necrosis factor-α (TNFα) to activate surrounding macrophages enabling them to produce anti-mycobacterial compounds (45, 62) . These events result in the formation of a primary lesion (granuloma) and halt the logarithmic growth of the mycobacteria. However,

mycobacteria escape from the primary lesion and get into the blood or lymph, thus disseminating to neighboring lymph nodes and/or other organs (spleen, liver, etc.), as well as reseeding the apical regions of the lung. In healthy, HIV-negative individuals, around 90% of tuberculosis infections end here and do not progress to active disease.

MACROPHAGE VERSUS *M. tuberculosis*

Most likely the first encounter of mycobacteria with the host is the engulfment of the bacilli by alveolar macrophages. It has been previously shown that *M. tuberculosis* binds to complement receptors (CR1, 3, and 4) (178, 179), Fc receptors (58), mannose receptors (155, 179), toll-like receptors (TLR2 and 4) (114, 131, 160, 202), scavenger receptors (216), fibronectin (151), and surfactant protein A (72, 124, 150). These receptors act in an independent or concerted manner facilitating the uptake of *M. tuberculosis.* It has been demonstrated that the method of internalization can affect the outcome of *M. tuberculosis* viability within the macrophage (199). Once the tubercle bacillus is within the macrophage and residing in a phagosome, the fate of the pathogen lies with its ability to prevent fusion with the lysosome. This organelle contains numerous degradative hydrolytic enzymes, as well as a lethal intravesicular acidic pH (~ 4.5 – 5.0), that aid in the destruction of *M. tuberculosis* (15). Previous studies have shown that viable, virulent *M. tuberculosis* can prevent phagosome-lysosome fusion and replicate within the phagosome (126), as well as preventing the development of a proton-ATPase on the vacuolar membrane. However, attenuated *M. tuberculosis* H37Ra, *M. bovis* Bacille Calmette Guerin (BCG), and heat-killed H37Ra or H37Rv all

fail to inhibit lysosomal fusion resulting in destruction by ROI, RNI, and acidic environments.

HOST RESPONSE TO *M. tuberculosis*

Once *M. tuberculosis* is internalized by the alveolar macrophage, one of the host responses is to inform the neighboring cells of its presence. This is accomplished by releasing an arsenal of molecules (i.e. cytokines and chemokines) to activate neighboring leukocytes, attract new inflammatory cells to the focus of infection, and regulate the host immune response. The first cytokines released are a group of pro-inflammatory cytokines, which include TNFα, interleukin-1β (IL-1β), and IL-6. TNFα is released from macrophages/monocytes (106), dendritic cells (74), and neutrophils (119) in response to either direct binding of the bacteria to the leukocyte or via secretory proteins from *M. tuberculosis*, including Ag85 (117), heat-shock protein 70 (207), and culture filtrate protein (CFP-10) (196). The release of TNFα results in leukocyte activation via autocrine and paracrine pathways. Previous studies have shown that humans and mice deficient in TNFα production have abnormal granuloma formation, succumb to tuberculosis infection more readily, and have elevated risk of tuberculosis reactivation (32, 63, 136). IL-1β deficiencies display similar defects in infection control mechanisms. In murine studies, it has been shown that the lack of IL-1 or absence of IL-1 receptor results in granuloma abnormalities, and enhanced mycobacterial outgrowth (89). In contrast, the impact of the other pro-inflammatory cytokine, IL-6, has been controversial. This cytokine plays a regulatory role by reducing the production TNFα

and IL-1β (177). In the absence of IL-6, mice expressed less IFNγ and more IL-4 resulting in more rapid mortality from tuberculosis. Interestingly, absence of IL-6 had no significant effect on bacterial burdens in the lung, liver, or spleen when mice were infected with BCG (102).

After the first 2-3 weeks of infection, memory T lymphocytes begin to appear at the foci of infection. At this stage, it is essential for the host phagocytes to release cytokines favoring the differentiation of CD4+ T helper cells into Th1 effector cells. The production of IL-12, IL-18, and IL-23 are pivotal in this step. These cytokines induce naive and memory T lymphocytes to release IFNγ (39, 96, 144, 200) which activates neighboring macrophages. This is a crucial step in the cross-talk between macrophages and T lymphocytes, which work together to develop a protective, well-localized granuloma (152). The interaction of IFNγ with macrophages results in elevated levels of anti-mycobacterial molecules, including ROI and RNIs (50, 51, 152). Inside the granulomas, IFNγ also causes monocytes/macrophages to fuse, resulting in the formation of epithelioid and multi-nucleated giant cells around the nucleus of the granuloma (26). These cells contain enhanced anti-mycobacterial components and are beneficial to the host defenses due to the heighten ability to secrete cytokines, ROIs, and RNIs.

As the infection progresses, it is beneficial for *M. tuberculosis* to attempt to induce the secretion of anti-inflammatory cytokines to suppress the anti-mycobacterial response. This category of cytokines, including IL-4, IL-10, and transforming growth factor-β (TGFβ), can down-regulate TNFα, IFNγ, and IL-12 levels thus rendering the

host more susceptible to mycobacterial infection. The interaction of lipoarabinomannans (LAM), which are cell wall components of mycobacteria, with human macrophages resulted in the production of the anti-inflammatory cytokine, TGFβ (41). Other studies have demonstrated that the presence of TGFβ during *M. tuberculosis* infections can result in abrogated T cell blastogenesis (76) and increased bacterial replication within human monocytes (77). Although IL-4 and IL-10 are Th2 cytokines with the potential to diminish IFNγ, TNFα, and IL-12, their impact on disease pathogenesis has been controversial (61, 199).

CHEMOKINES AND *M. tuberculosis*

In addition to the release of cytokines in response to *M. tuberculosis* proteins, an arsenal of chemokines are released by host cells following direct contact with *M. tuberculosis* or its products. Chemokines are a group of small molecular weight (8-12 kDa) proteins known for their chemotactic properties, and more recently associated with an array of diverse biological activities. They are categorized into 4 groups based on the position of the first two cysteine residues. The majority of inflammatory chemokines are in the α- (one amino acid separating the first two cysteine residues –CXC) or β- (adjacent cysteine residues –CC) chemokine families. Human tuberculosis patients have heightened levels of chemokines CXCL8 (IL-8), CCL5, and CCL2 (MCP-1) in bronchoalveolar lavage fluid during acute and convalescent stages with more pronounced levels appearing during the acute phase (101). Other studies described similar findings in the bronchoalveolar lavage fluid and serum, including CCL4 (MIP-

1β) and IFN-inducible protein 10 (IP-10) (90, 167). The first cells likely to interact with *M. tuberculosis* are alveolar macrophages and epithelial cells (20, 71). Previous studies have shown human alveolar macrophages release CCL2, CCL3 (MIP-1α), CCL4, CCL5, IP-10, and CXCL8 (167, 174) when infected with *M. tuberculosis*. The component of *M. tuberculosis* responsible for chemokine secretion in macrophages has been further elucidated in other studies. Lipoarabinomannan (LAM) has been shown to induce CXCL8, CCL2, and CCL4 in monocytes/macrophages (90, 118). In macaque peripheral blood mononuclear cells (PBMCs), *M. tuberculosis* heat shock protein 70 (hsp70) induced CCL3 and CCL5 production (207). Soluble tuberculosis factor was also shown to stimulate human alveolar macrophages to release CCL5 (88). *M. tuberculosis* infection of the human alveolar epithelial cell line A549 resulted in CCL2, CXCL8, and CCL5 secretion (111, 173, 210). Thus, the infection of these cell types results in a concerted release of chemokines, which could result in a chemotactic stimulus for leukocytes leading to the development of an anti-mycobacterial environment. Some studies have characterized the variation of chemokine expression in mycobacterial (type-1) versus schistosomal (type-2) antigen-elicited pulmonary granulomas in mice. These studies demonstrated an enhanced mRNA expression and production of 6 chemokines, including IP-10, CCL3, CCL4, and CCL5 in type 1 granulomas compared to type 2 (35, 158), suggesting the importance of chemokines populations during protective mycobacterial granuloma formation.

ROLE OF CCL5 DURING A *M. tuberculosis* INFECTION

The availability of chemokine knock-out mice and neutralizing antibodies have facilitated the study of the role of chemokines during tuberculosis pathogenesis and their contribution to host protection. Chensue et al. have shown that type 1 granulomas (PPD induced) in IFNγ -/- mice revert to a type 2 phenotype with diminished levels of CCL5 production (34). Neutralization of CCL5 with anti-CCL5 antibody resulted in diminished type 1 (PPD) granulomas while enhancing type 2 (*Schistosoma mansoni* egg) granulomas (35). Treatment of mice the rhCCL5 resulted in significantly enhanced IFNγ, IL-2, IL-5, and IL-13 protein in PPD stimulated cells harvested from the mediastinal lymph nodes of PPD-immunized animals (35).

Saukkonen et al. demonstrated increased viability of *M. tuberculosis* in human alveolar macrophages co-cultured with anti-CCL5 (174). Whether this anti-mycobacterial environment is the result of CCL5 directly or indirectly is an area of interest. Locati et al. performed an elaborate study on the ability of rhCCL5 to activate human nonadherent blood monocytes. They showed an up-regulation in mRNA expression levels of 114 genes out of 5600 human genes tested. These genes were involved in many diverse physiological activities, including cytokine production, membrane receptors, regulators of tissue invasion, enzymes, signal transducers, nuclear proteins, and cytoskeleton-related proteins (113). It is apparent that many of the genes grouped into tissue invasion, cytoskeleton-related proteins, and membrane receptors (including CD44, which has been associated with *M. tuberculosis* uptake (108)) are associated with chemotactic function. However, many of these genes are associated

with cytokines and signal transducers that might be capable of further activating monocytes/macrophages and neighboring leukocytes. Other studies have demonstrated the activating properties of CCL5 on T lymphocytes resulting in enhanced IL-2 and IFNγ production, as well as increased proliferative and cytotoxic activity (11, 14, 121, 193). The elevated levels of IFNγ can further activate macrophages resulting in the production of anti-mycobacterial compounds (50, 51). Together these results suggest a possible role for CCL5 in eliciting mechanisms crucial for the development of a protective anti-mycobacterial environment.

REGULATION OF CCL5

Bi-directional communication occurs between CCL5 and cytokines. It has been previously demonstrated that TNFα and IFNγ can act synergistically to enhance the production of CCL5 protein in endothelial and epithelial cells (29, 122, 189). Casola et al. used a human alveolar epithelial cell line to demonstrate that TNFα induced CCL5 mRNA promptly, and IFNγ enhanced the transcriptional level and stabilized the CCL5 mRNA transcripts (29). Of the studies to date, regulation of CCL5 expression in T lymphocytes is perhaps the best understood. The transcription of CCL5 varies considerably from other chemokines in that is enhanced days after T cell activation, making it a 'late' transcript (187). The upstream CCL5 promoter in T lymphocytes is composed of numerous sequences for DNA-binding proteins, including RANTES factor of late activated T lymphocytes-1 (RFLAT), interferon regulatory factor 3 (IRF-3), nuclear factor of IL-6 (NF-IL-6), NF-κB, rel p50/p50, and rel p50/p65 (140, 141, 187).

CCL5 has also been shown to be induced by type 1 IFNs via IFN-stimulated response element (ISRE) – like mechanisms (40). The Th1 cytokine, IL-12, also can induce CCL5 secretion in CD4+ and CD8+ T cell clones (116). Together these data suggest that cross-talk between cytokines and chemokines is necessary to orchestrate a protective immune response against *M. tuberculosis.*

In these studies we attempted to further elucidate the contributions of gpCCL5 to the anti-mycobacterial immune response.

CHAPTER II

RECOMBINANT GUINEA PIG CCL5 (RANTES) DIFFERENTIALLY MODULATES CYTOKINE PRODUCTION IN ALVEOLAR AND PERITONEAL MACROPHAGES*

INTRODUCTION

During an infection, the leukocytes which are recruited to and reside in the tissues are constantly in contact with chemokines. As these cells leave the circulation and enter the site of infection, they encounter increasing chemokine concentrations. This plays a role in attracting the cells to the infectious focus, but recent studies suggest that chemokines have effects on leukocyte functions which go beyond chemotaxis. CCL5, CCL3 (MIP-1α), and CCL4 (MIP-1β) have all been shown to activate macrophages (10, 27, 54, 203) and T lymphocytes (10, 11, 14, 120, 121, 193). The differentiation of helper T lymphocytes into polarized Th1 and Th2 cytokine-producing subpopulations has been shown to be regulated by numerous chemokines, including CCL5 (54). This chemokine is chemotactic for eosinophils (4), basophils (22), dendritic cells (43), macrophages/monocytes (27, 175), and T lymphocytes (175), including those of the Th1 phenotype (94).

The diverse physiological roles of CCL5 might be due to the large family of receptors through which it can signal. Many of these receptor interactions are

---

*Reprinted with permission from "Recombinant guinea pig CCL5 (RANTES) differentially modulates cytokine production in alveolar and peritoneal macrophages" by Skwor, T. A., H. Cho, C. Cassidy, T. Yoshimura, and D. N. McMurray, 2004, Journal of Leukocyte Biology vol 76.

Determined by the concentration of CCL5 present. CCL5 has been shown to interact with the G coupled protein receptors CCR1, 3, 4 and 5 at low concentrations (12), while at higher concentrations it appears to bind to glycosoaminoglycans (GAG) (80) and CD44 (165). These various receptor interactions may allow CCL5 to trigger diverse cellular responses.

Lipopolysaccharide (LPS) induces a pronounced inflammatory response, which can eventually lead to septic shock syndrome (49). Previous studies have demonstrated that LPS upregulates numerous cytokines and chemokines in naive macrophages (28, 46, 99, 115, 118). These molecules proceed to activate neighboring cells, resulting in a cascade of events leading to the recruitment of leukocytes to the site of infection. Chemokines are the primary inducers of leukocyte accumulation. It is likely that leukocytes leaving the circulation to enter an inflammatory tissue focus would encounter host chemokines before interacting with products of an invading pathogen.

Previously, we have demonstrated that guinea pig CXCL8 (IL-8), CCL2 (MCP-1), and CCL5 mRNA expression and/or secretion were enhanced in macrophages cultured with LPS or *Mycobacterium tuberculosis* (85, 118). In the present studies, the ability of CCL5 to induce TNFα, IL-1β, CCL2, and CXCL8 expression in alveolar and peritoneal macrophages was evaluated. In addition, we examined the effect of pretreatment with CCL5 on the ability of macrophages to respond to subsequent stimulation with LPS.

MATERIALS AND METHODS

Production and purification of recombinant guinea pig (rgp) CCL5. The sequence encoding the mature form of the protein, described by Campbell, et al. (27), was subcloned into the Novagen (Milwaukee, WI) pET30-Xa/LIC vector using the cDNA clone for gpCCL5, according to the protocol from Novagen. The vector was transformed into *E. coli* BL21 (DE3) (Novagen) cells, which were grown in 1L of Luria-Bertani broth (Becton Dickinson, Sparks, Maryland) with 50ug/ml kanamycin at 37°C. The production of rgpCCL5 was performed using a slightly modified protocol from Laurence, et al. (107). Briefly, the cells were induced with 0.1mM isopropyl-beta-D-thiogalactopyranoside (IPTG) for 4 hours. The cells were centrifuged and the pellet was resuspended in 500mM NaCl, 20 mM Tris, 1 mM ethylenediaminetetraacetic acid (EDTA), 5 mM benzamidine, and 5 mM β-mercaptoethanol at pH 7.4. The suspension was exposed to two rounds of lysis in a French Press at 18,000-20,000 psi, and centrifuged at 18,500 × g for 60 minutes. The pellet was then resuspended in denaturing buffer (5M guanidine hydrochloride, 50mM Tris, 50mM NaCl, 3mM EDTA, pH 7.4, and 5mM β-mercaptoethanol) and left for 2 h at room temperature. Centrifugation of the denatured protein was performed at 18,500 × g for 60 min. The supernatant was added to dilution buffer (50mM Tris, 50mM NaCl, pH 7.4, and 5mM β-mercaptoethanol) in a drop wise manner and allowed to sit for 4 h to refold the protein. The solution was centrifuged for 30 min at 13,000 × g and purified by C4 reverse phase chromatography, using a Vydac column (Hesperia, CA). The purified fractions were then lyophilized and

resuspended in 20mM Tris, 2mM CaCl, pH 7.4, and 100mM NaCl until an A_{280nm}=0.3. Factor Xa (Novagen) was used for proteolysis at 2U/ml and incubated at room temperature for 24 h, followed by re-purification over a C4 column using reverse phase chromatography. The samples were tested for purity by SDS-PAGE analysis using 10-20% tris-tricine gels (Invitrogen, Carlsbad, CA) stained with Coomassie brilliant blue R250. Edman degradation was performed on the cleaved protein to verify the N-terminal sequence using G1000A Automated Protein Sequencer (Hewlett Packard, Albertville, MN). The protein concentration of the rgpCCL5 preparation was determined by the Bradford protein assay (Bio-Rad, Richmond, CA) following manufacturer's instructions. Endotoxin levels were less 0.05ng/ug of recombinant protein using *Limulus* Amebocyte Lysate assay (Cape Cod Inc., Falmouth, MA).

Animals. Specific-pathogen-free, outbred, male and female Hartley guinea pigs from Charles River Breeding Laboratories, Inc. (Wilmington, MA), were used in this study. They were housed in polycarbonate cages within an air-filtered environment under a 12 h light-dark cycle. Food (Ralston Purina, St. Louis, MO) and tap water were supplied to the animals *ad libitum*. All procedures were reviewed and approved by the Texas A&M University Laboratory Animal Care Committee.

Isolation of macrophages. Guinea pigs were euthanized by two 1.5 ml intramuscular injections of sodium pentobarbital (100mg/ml) (Sleepaway Euthanasia Solution; Fort Dodge Laboratories, Inc., Fort Dodge, IA). To obtain peritoneal exudate cells (PEC), guinea pigs were injected intraperitoneally with 5 ml of 3% sodium thioglycollate (Becton Dickinson, Cockeysville, MD) four days before euthanasia.

Guinea pigs not injected with sodium thioglycollate were used as a source of resident peritoneal macrophages. The abdominal and thoracic cavities were opened aseptically. The peritoneal cavity was flushed twice with 30ml of cold phosphate-buffered saline (PBS) with 10U/ml heparin and 2% FBS to obtain PEC or resident peritoneal macrophages. Alveolar macrophages were obtained by exposing the trachea and inserting an 18-gauge cannula fixed to a 20 ml syringe. The bronchoalveolar lavage (BAL) was performed by filling the lungs with cold 12mM lidocaine in PBS with 3% FBS as previously described (118). Cells were pelleted by centrifuging at 380 × g for 10 minutes. These pellets were washed twice with RPMI-1640 medium without phenol red, supplemented with 10% FBS, 10μM 2-mercaptoethanol, and 2μM L-glutamine (RPMI complete medium). The cells were resuspended in 1ml RPMI complete medium, and viable cells were enumerated on a hemacytometer by the trypan blue exclusion method. Cells from BAL were resuspended at 1×10^6 cells/ml, resident peritoneal cells at 1.5×10^6 cells/ml, and PEC at a concentration of 5×10^6 cells/ml in RPMI complete medium.

Chemotaxis assay for rgpCCL5 bioactivity. Chemotaxis was performed using ChemoTx (Neuroprobe, Inc., Gaithersburg, MD) disposable chemotaxis systems containing 5μm pore size polycarbonate filters, following modified instructions from the manufacturer. Briefly, PECs were resuspended in RPMI 1640 with 0.1% bovine serum albumin (RPMI-BSA) at a concentration of 5×10^6 cells/ml. Dilutions of N-formyl-Met-Leu-Phe (fMLP) (Sigma, St. Louis, MO) and rgpCCL5 were made in RPMI-BSA and added to the wells of a 96-well plate. The polycarbonate filter was then placed on the plate and checked to ensure that the fluid in each well was in contact with the filter.

The cells were then added to the top of the filter in a 50µl volume containing 2.5×10^5 cells/well. Chemotaxis was performed at 37°C in 5% CO_2 for 2 h. Fluid on top of the filter was aspirated, and cold PBS with 0.5M EDTA was added and incubated at 4°C for 30 min. Cotton swabs were used to wipe off any cells remaining on the top of the filters. Plates were centrifuged for 430 × g for 10 minutes to dislodge any remaining cells bound to the underside of the filter. The filter plate was removed and 150ul aspirated from each well. A tetrazolium salt, 3-(4,5-dimethylthiazolyl-2)-2,5-diphenyltetrazolium bromide (MTT) (Sigma, St. Louis, MO), was added at 5mg/ml to each well and allowed to incubate for 2 h at 37°C in 5% CO_2. Plates were centrifuged at 140 × g for 5 min and supernatants were aspirated. Warm lysis buffer (50% 2-2 Dimethylformamide and 20% SDS at pH 4.7) was added to each well and allowed to incubate for 4 h at 37°C and 5% CO_2. This colorimetric assay was then read at 570nm using a Dynatech MR5000 automated plate reader and analyzed with Biolinx Software, version 2.1 (Dynatech Laboratories, Inc., Chantilly, VA).

Macrophage stimulation. Cells from the BAL and peritoneal cavity were plated on 96 well plates and allowed to adhere for 1.5 h at 37°C in 5% CO_2 incubator. Nonadherent cells were aspirated and the adherent cells were washed with RPMI complete medium. Adherent macrophages were stimulated with rgpCCL5 at different concentrations (1.35, 405, 1350, and 4050ng/ml) for 2 and 6 h. To examine the priming effect of rgpCCL5 on the response to LPS, macrophages were pre-incubated with 1350ng/ml rgpCCL5 for 2 h. The cells were then exposed to LPS (10ng/ml) and samples were collected at 2 and 6 h post-LPS exposure. At each time point, supernatants

were collected and stored at –70°C until analyzed for TNFα by the L929 bioassay, and total RNA was isolated using the RNeasy kit (QIAGEN, Valencia, CA) with the addition of Rnase-free DNase according to the manufacturer's instructions.

Real-time PCR on cytokine mRNA. Reverse transcription was performed on 1-5μg of total RNA using TaqMan Reverse Transcription Reagents (Applied Biosystems, Foster City, CA). Negative controls were performed to ensure PCR amplification of cDNA was not due to contaminating genomic DNA. RT-PCR analysis was performed on the cDNA using SYBR Green I (Applied Biosystems) following a previously published protocol (118). Primer Express software (Applied Biosystems) was used to design the sequences for guinea pig hypoxanthine phosphoribosyltransferase (HPRT) (forward primer, AGGTGTTTATCCCTCATGGACTAATT; reverse primer, CCTCCCATCTCCTTCATCACAT) and guinea pig IL-1β (forward primer, GCCCAGGCAACAGCTCTC; reverse primer, GGAGTCTCTACCAGCTCAACTTGG). The sequences for TNFα, CXCL8, and CCL2 primers were previously described (8, 118). Real-time PCR was performed using the Applied Biosystems Prism 7700 sequence detector following the manufacturer's instructions. Results were expressed as fold induction of mRNA, which was determined by normalizing cytokine threshold cycle (C_t) values against HPRT values. This was further normalized against samples from unstimulated cells at 0 h.

L929 bioassay. The concentration of bioactive TNFα protein in macrophage culture supernatants was measured by cytotoxicity on L929 fibroblasts (106). Briefly, L929 cells were plated into 96-well plates in RPMI 1640 without phenol red

supplemented with 2μM L-glutamine, 100 U/ml of penicillin, 100μg/ml streptomycin/ml, and 2% FBS. Serial two-fold dilutions of supernatants in 8μg/ml actinomycin D were added to each well and incubated for 20 h. Cells were incubated for an additional 2 h at 37°C + 5% CO_2 after the addition of WST-1 (6mM) / 1-methoxymethyl phenazium methylsulfate (0.4mM) (Dojindo, Kumamoto, Japan). The color development was halted with 1N H_2SO_4 and the optical densities were measured at OD_{450} and OD_{630}. Human recombinant TNFα (R&D Systems, Inc., Minneapolis, MN) was used to derive a standard curve and all samples were expressed as the 50% cytotoxicity value based on the standard curve.

Statistical analysis. Analysis of variance was used to determine statistical significance between mean differences of rgpCCL5-treated and untreated macrophages at a 95% confidence interval using Duncan post hoc analysis. A two-tailed t-test was used to determine statistical significance at a 95% confidence interval between rgpCCL5 prestimulated group and naive macrophages cultured with LPS. The statistical tests were performed using SAS software (release 8.01; SAS Institute, Inc., Cary, NC).

RESULTS

Expression and bioactivity of recombinant guinea pig (rgp) CCL5. Figure 1 illustrates the expression and purification of rgpCCL5. Large amounts of CCL5 were induced using low levels of IPTG (0.1mM) (Fig. 1A, lane 3). The fusion protein was absent in the soluble fraction following cell lysis via French Press (fig. 1A, lane 5).

Inclusion bodies contained abundant rgpCCL5 (fig. 1A, lane 6), therefore, we treated the insoluble fraction with high concentrations of guanidine hydrochloride to solubilize the

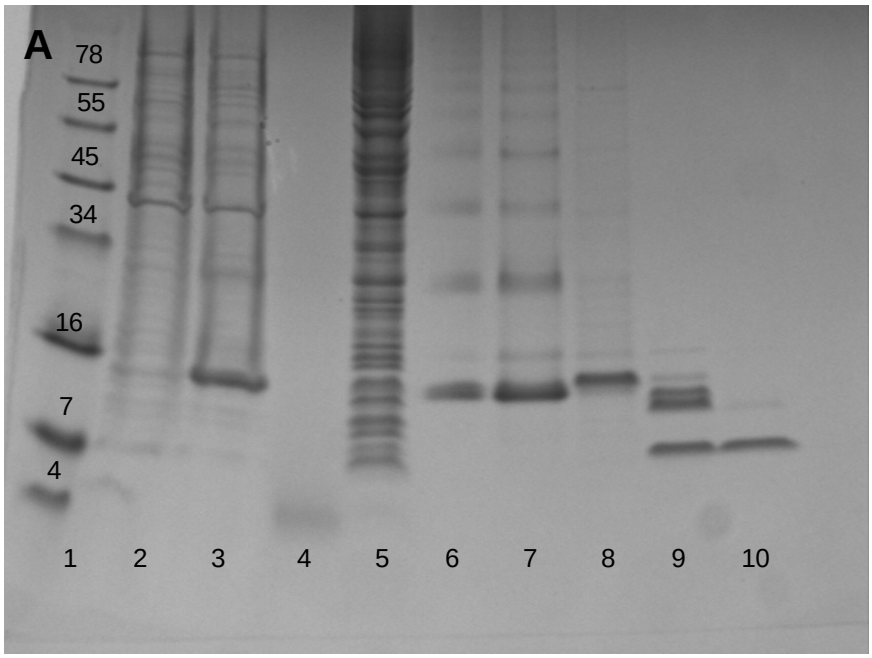

Figure 1: SDS-PAGE analysis was used to trace rgpCCL5 through the expression and purification process. (A) Lane 1, low molecular weight ladder; lane 2, uninduced total *E. coli* proteins; lane 3, cellular proteins from 0.1mM IPTG induced *E. coli*; lane 4, secreted proteins from induced cultures; lane 5, soluble proteins from *E. coli* lysate; lane 6, insoluble proteins from *E. coli* lysate; lane 7, proteins after refolding; lane 8, purification of rgpCCL5 uncut from inclusion body proteins after reverse phase HPLC (B); lane 9, protein obtained from peak a (C); lane 10, mature rgpCCL5 purified from peak b (C) after reverse phase HPLC (recombinant gpCCL5). Reverse phase HPLC displayed purification of rgpCCL5 with fusion peptide between 40-50% acetonitrile concentrations (B). Following cleavage with Factor Xa, the fusion peptide and mature rgpCCL5 were separated by running solution over reverse phase-HPLC (C).

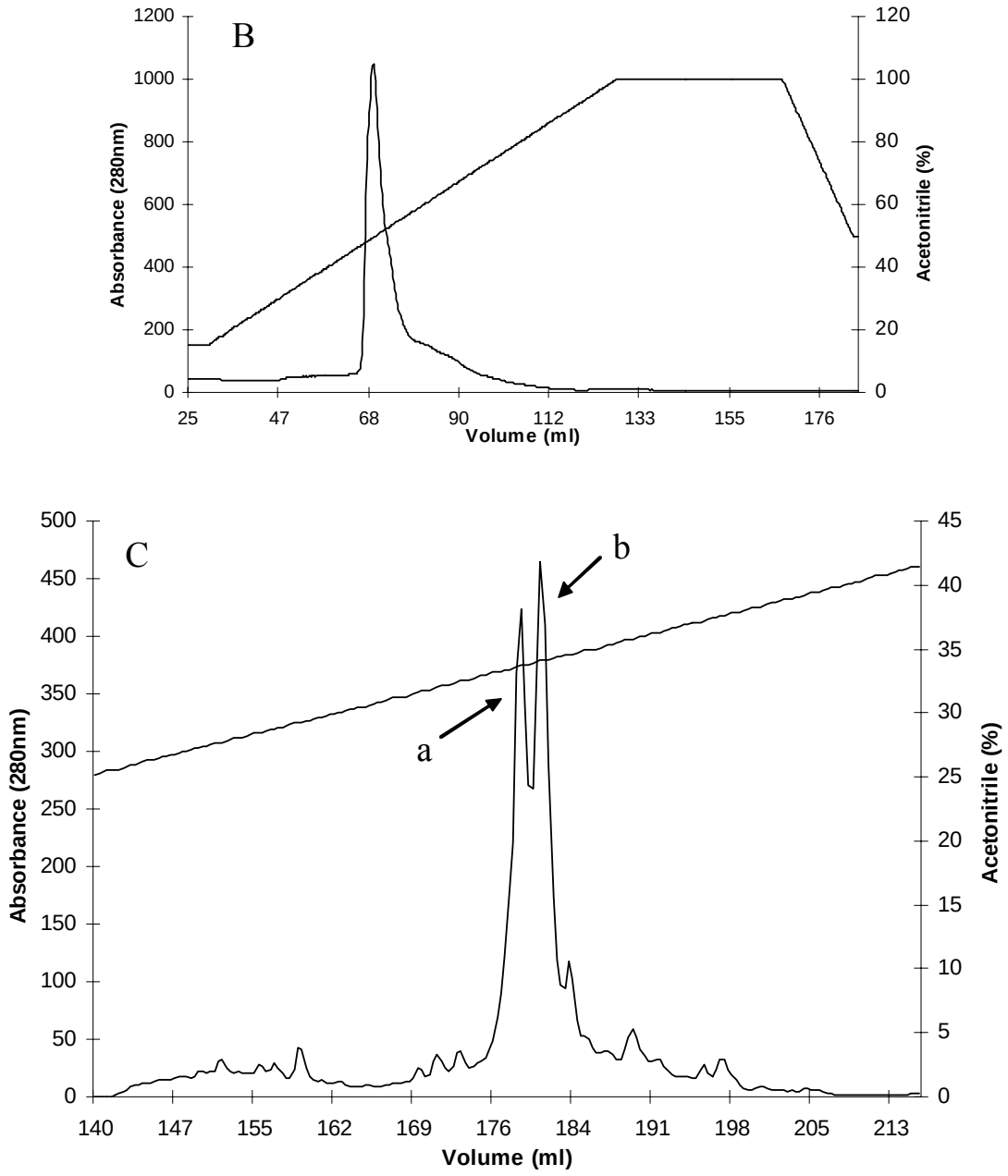

Figure 1 continued.

protein. The separation of CCL5 from other *E. coli* proteins was achieved using reverse phase HPLC. The fusion protein came off the C4 column as one peak between 45-50% acetonitrile concentrations (fig. 1B). The protein was visualized as a distinct band at ~ 14kDa on a 10-20% tris-tricine gel after SDS-PAGE analysis (fig. 1A, lane 8). The fusion protein was then exposed to Factor Xa protease to obtain the mature form of gpCCL5. Cleavage by the endoproteinase resulted in three bands on SDS-PAGE analysis (fig. 1A, lane 9) suggesting an uncut, improperly cut, and mature recombinant protein. The amino acid compositions were determined using Edman degradation. The improperly cut protein (~12 kDa) appeared to have a 5'- terminal amino acid sequence GSGMKE, which suggested the protein was improperly cleaved at the thrombin site found in the fusion peptide. The ~8 kDa mature protein was sequenced and contained SPYASD hexa-peptide on the 5' end, verifying it was the mature form of gpCCL5. Separation of these proteins was performed by retarding the acetonitrile gradient between 25-42% on reverse phase HPLC resulting in two distinct peaks (fig. 1C). The first peak appeared to contain all three forms of the recombinant protein after SDS-PAGE analysis (fig. 1A, lane 9). However, the second peak contained mature CCL5 alone at greater than 99% purity (fig. 1C peak b; fig. 1A, lane 10).

The bioactivity of rgpCCL5 was demonstrated in a chemotaxis assay using guinea pig PEC. Figure 2 illustrates that significant PEC migration was induced by rgpCCL5 and the positive control, fMLP, compared to media alone. In these experiments, cells were added to the upper chamber of a chemotaxis assay at a ratio of 2.5 cells/pore. The chemotactic agent was added to the lower chamber and after two

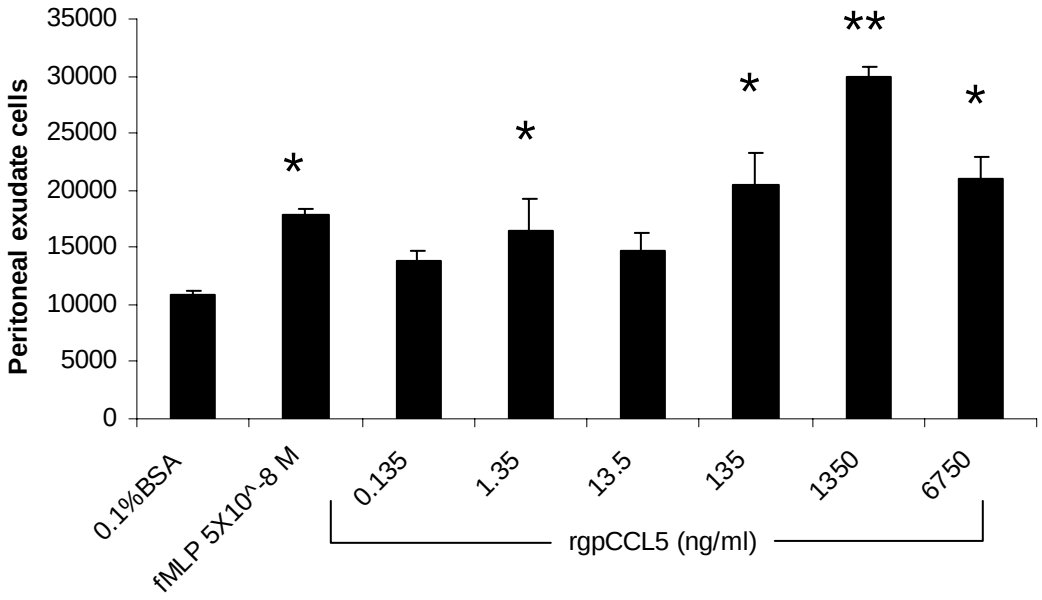

Figure 2: Chemotactic properties of rgpCCL5 to PEC. Chemotactic abilities of rgpCCL5 were assessed by determining the migration of guinea pig PEC *in vitro* to varying concentrations of recombinant protein and fMLP against media (RPMI + 0.1%BSA) alone. Cell migration was determined using the MTT viability assay after the cells were dislodged from the filters. Results are displayed as the mean $\pm$ SEM for three experiments, each containing quadruplicate wells per concentration tested. * Significant differences ($p < 0.05$) were seen in migration with chemotactic agents compared to media alone, and ** ($p < 0.05$) displayed significance between rgpCCL5 concentrations using ANOVA.

hours of incubation migration was detected using the MTT viability assay. The migration was concentration-dependent, with 1350ng/ml being significantly greater than other concentrations tested (fig. 2). At concentrations higher than 1350ng/ml, the chemotactic effect of gpCCL5 was diminished.

Effect of rgpCCL5 on cytokine expression in macrophages. Guinea pig resident peritoneal macrophages were exposed to varying concentrations of rgpCCL5, and the levels of mRNA of inflammatory cytokines and chemokines were assessed using real time PCR. Figure 3 shows that the mRNA levels of two proinflammatory guinea pig cytokines, TNFα and IL-1β, were significantly enhanced at two hours post-rgpCCL5 exposure compared to media alone (fig. 3A and 3B). This effect was optimal at 1350ng/ml of rgpCCL5 compared to the other concentrations tested. After six hours, TNFα mRNA levels swiftly declined, but IL-1β levels tapered off to a lesser extent (fig.3A and 3B). In comparison, LPS (10ng/ml) stimulation of resident peritoneal macrophages resulted in 42.62 $\pm$ 11.95 and 11.21 $\pm$ 4.57 fold induction for TNFα mRNA at 2 h and 6 h, respectively, and IL-1β mRNA increased to 6.87 $\pm$ 0.64 and 5.99 $\pm$ 1.32 fold induction at similar time intervals.

Sequences for the guinea pig chemokines are limited, however, CXCL8 and CCL2 are available (213, 214). The kinetics of mRNA levels for these genes in response to rgpCCL5 mirrored the enhancement seen in TNFα and IL-1β mRNA. At two hours post-exposure to rgpCCL5, both CXCL8 and CCL2 mRNA levels were significantly elevated compared to untreated cells. The stimulatory effect was short-lived and at six hours these levels had declined (fig. 3C and 3D). LPS (10ng/ml) was used as a positive

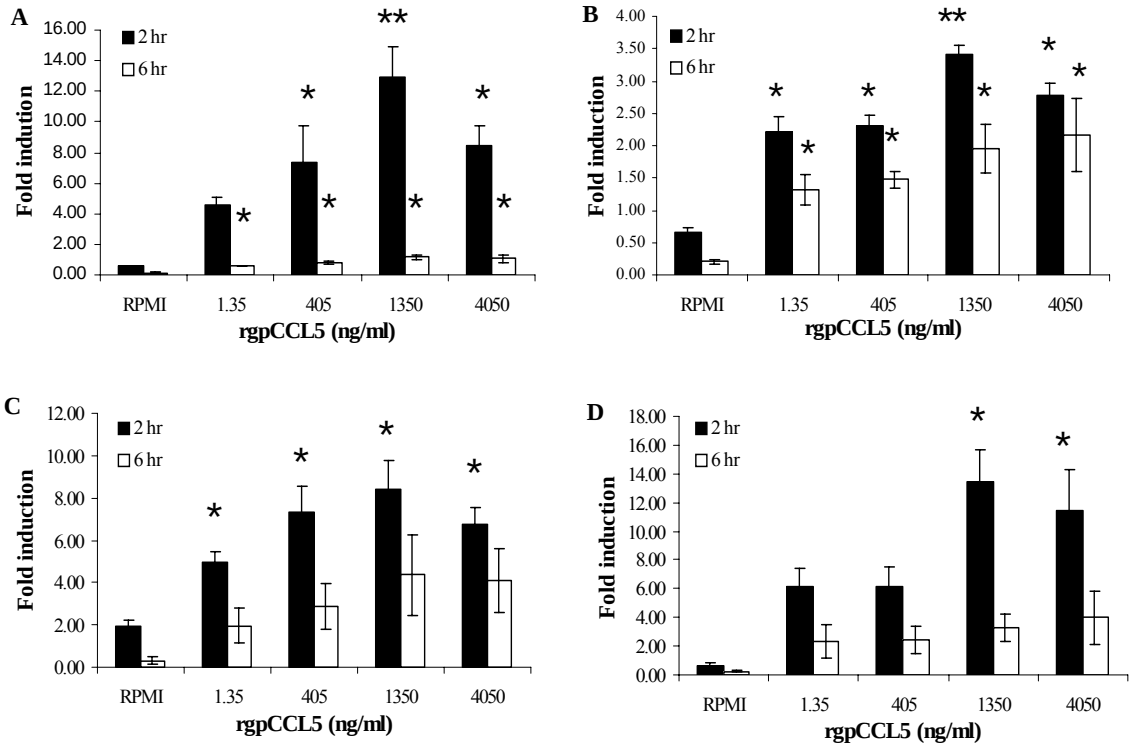

Figure 3: Peritoneal macrophage activation by rgpCCL5 as evaluated by cytokine and chemokine mRNA expression. Expression of TNFα (A), IL-β (B), CCL-2 (C), and CXCL-8 (D) mRNA was determined at two and six hours after rgpCCL5 (1.35, 405, 1350, and 4050ng/ml) stimulation via real-time PCR. Data represent the mean ± SEM for 3-4 experiments with an asterisk representing significant differences ($p < 0.05$) between rgpCCL5 and media alone (RPMI + 10% FBS). Double asterisks represent significance ($p < 0.05$) between different concentrations of rgpCCL5 at same time points. Statistical analysis was performed using ANOVA.

Control, stimulating 7.22 ± 2.78 and 7.44 ± 3.3 CCL2 mRNA fold induction at 2 h and 6 h, respectively, from unstimulated resident peritoneal macrophages. CXCL8 mRNA fold induction levels were also heightened in LPS-treated cells to 23.26 ± 5.00 and 18.48 ± 7.16 at similar time points.

The diverse biological properties of different macrophage populations (70, 130, 168, 205) prompted us to extend our studies of the stimulatory effect of gpCCL5 to alveolar macrophages, a cell type which we have studied previously and which is relevant to our focus on the pathogenesis of pulmonary tuberculosis in the guinea pig model (118, 215). Figure 4 illustrates mRNA levels for TNFα, IL-1β, CCL2, and CXCL8 in alveolar macrophages stimulated with rgpCCL5. At 1350ng/ml, rgpCCL5 significantly enhanced mRNA levels of TNFα and IL-1β compared to all other concentrations tested (fig. 4A and 4B). At six hours, these levels fell in a manner similar to that observed in resident peritoneal macrophages. However, this kinetic pattern was not repeated with alveolar macrophages stimulated with LPS (10ng/ml). TNFα mRNA fold induction levels increased from 2 h (67.1 ± 33.53), to 6 h (108.45 ± 27.02), and IL-1β mirrored similar patterns with mRNA fold induction levels increasing from 28.38 ± 11.55 to 112.98 ± 39.95 at 2 h and 6 h, respectively. Chemokines were evaluated in alveolar macrophages in response to rgpCCL5 stimulation. CXCL8 mRNA levels were enhanced significantly with rgpCCL5 at 1350ng/ml in alveolar macrophages at two and six hours following stimulation, a kinetic pattern which differed from peritoneal macrophages. Fold induction levels of CXCL8 mRNA from LPS (10ng/ml) stimulated alveolar macrophages were 52.92 ± 23.34 at 2 h, and 234.83 ± 88.28 at 6 h. CCL2

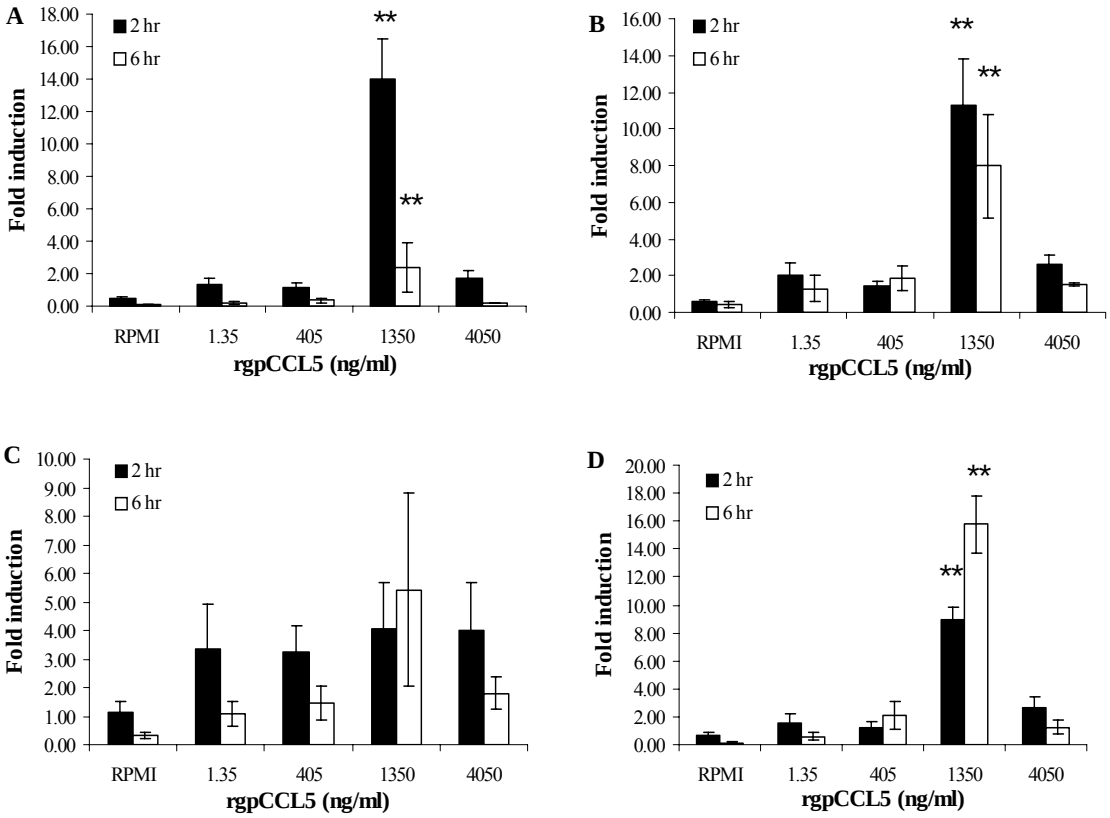

Figure 4: Alveolar macrophage activation by rgpCCL5 as determined by enhanced mRNA levels of cytokine and chemokine genes. Stimulation was assessed at two and six hours for TNFα (A), IL-β (B), CCL-2 (C), and CXCL-8 (D) mRNA using real-time PCR. Data represent the mean ± SEM of three experiments. Double asterisks represent significance ($p < 0.05$) between rgpCCL5 concentrations and media alone. Significance was determined by ANOVA analysis.

MRNA expression was not increased significantly by stimulation with rgpCCL5 compared to media alone, although mRNA levels were higher at all concentrations tested. In contrast, LPS stimulated alveolar macrophages produced elevated levels of CCL2 mRNA at 2h (5.33 $\pm$ 1.21), and at 6 h (14.15 $\pm$ 3.95).

In figure 5, bioactive TNFα levels were assessed in macrophages treated with rgpCCL5. Resident peritoneal macrophages stimulated with rgpCCL5 displayed significantly enhanced levels of bioactive TNFα protein at both two and six hours following stimulation with all concentrations of rgpCCL5 tested (1.35, 405, 1350, and 4050ng/ml) compared to media alone (fig. 5A). However, in alveolar macrophages exposed to the same stimulants, TNFα protein levels followed the same narrow rgpCCL5 concentration kinetics as seen in mRNA levels with significantly higher levels of protein at two hours in response to 1350ng/ml rgpCCL5 compared to all other lower concentrations tested (fig. 5B). At six hours, this pattern was repeated and 1350ng/ml rgpCCL5 induced significantly higher TNFα protein levels than all other concentrations tested (fig. 5B).

Effect of CCL5 prestimulation on the responses of macrophages to LPS.

Figure 6 shows the ratio of mRNA levels for TNFα, IL-1β, CCL2, and CXCL8 in resident peritoneal macrophages prestimulated with rgpCCL5 (1350ng/ml) for two hours and then exposed to a low concentration of LPS (10ng/ml) for two or six hours. Two hours and six hours post-LPS stimulation, TNFα mRNA was diminished by nearly 40% in peritoneal macrophages prestimulated with rgpCCL5 compared to mRNA levels in cells not exposed to rgpCCL5 (fig. 6A). CCL2 mRNA was modestly enhanced (30%

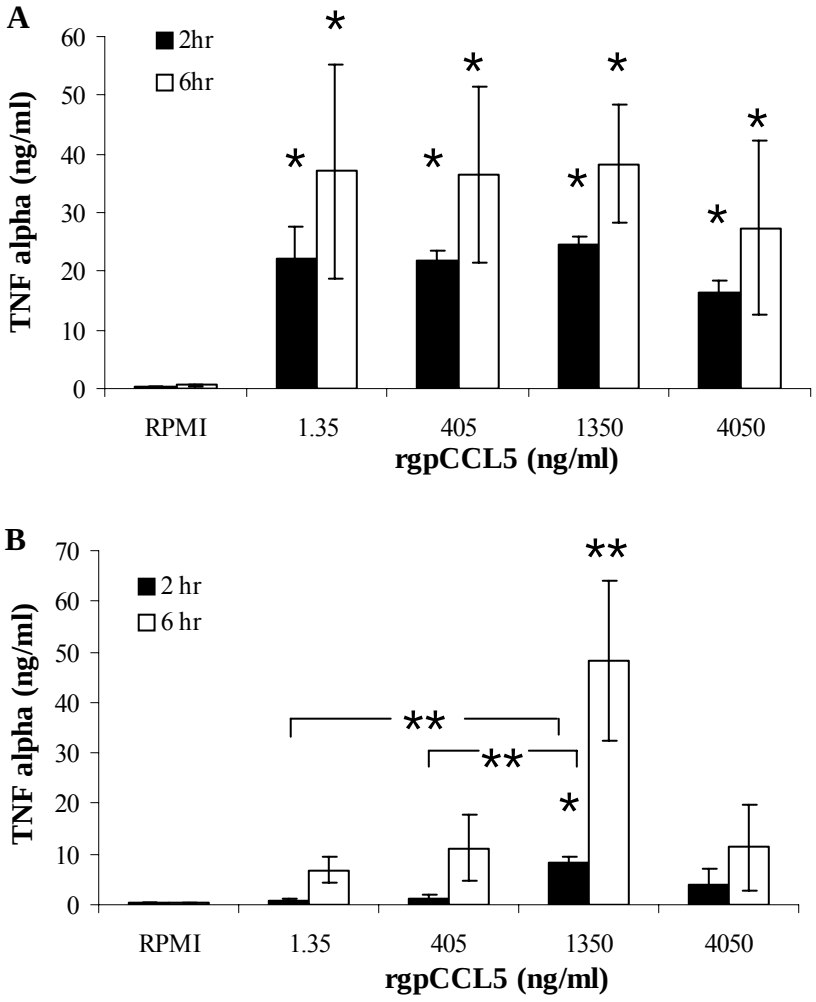

Figure 5: TNFα protein levels from guinea pig peritoneal and alveolar macrophages stimulated with rgpCCL5. The L929 bioassay was used to determine TNFα protein concentrations in alveolar (A) and peritoneal (B) macrophages stimulated with rgpCCL5 for two and six hours. Data represent mean $\pm$ SEM from 3-4 experiments. Significance ($p < 0.05$) of rgpCCL5 compared to media alone is depicted by an asterisk. Significance ($p < 0.05$) between concentrations is denoted as two asterisks. Statistical analysis was performed using ANOVA.

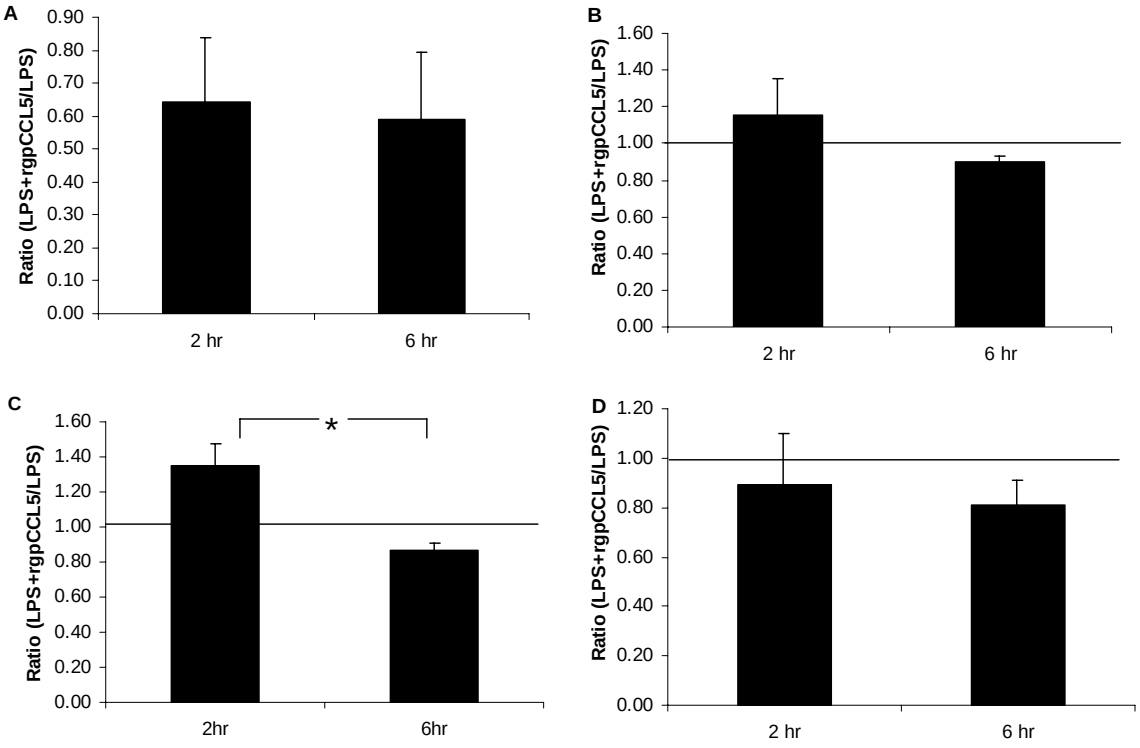

Figure 6: Regulation of LPS-induced cytokine and chemokine mRNA expression in guinea pig peritoneal macrophages by pretreatment with rgpCCL5. Expression of TNFα (A), IL-β (B), CCL-2 (C), and CXCL-8 (D) mRNA was assessed by real-time RT-PCR. Cells were pretreated with 1350ng/ml rgpCCL5 for two hours, and then stimulated with LPS (10ng/ml) for two or six hours. Results are expressed as mean $\pm$ SEM of the ratios of mRNA in rgpCCL5-pretreated over untreated cells of 3-4 experiments. Significance ($p < 0.05$) between ratios at different time points was determined using Student's t test and is denoted by an asterisk.

Increased) in the rgpCCL5-pretreated macrophages at two hours post-LPS stimulation, however, by six hours the levels had fallen significantly (fig. 6C). Levels of mRNA for IL-1β and CXCL8 were minimally affected by rgpCCL5 pretreatment at two hours, but at six hours post-LPS stimulation they were modestly diminished in rgpCCL5 pretreated cultures (fig. 6B and D).

Since the effect of priming with CCL5 on the responses of different macrophage populations to LPS was of interest, alveolar macrophages were pretreated with rgpCCL5 in a similar fashion. In figure 7, TNFα mRNA levels were reduced by 40% at two hours post-LPS stimulation in rgpCCL5 pretreated macrophages compared to untreated LPS-stimulated alveolar macrophages (fig. 7A). However, IL-1β, CCL2, and CXCL8 mRNA levels displayed a different trend. At two hours, rgpCCL5 pretreated alveolar macrophages had slightly higher mRNA levels than alveolar macrophages not exposed to rgpCCL5. This trend was reversed at six hours post LPS-stimulation when all rgpCCL5 pretreated macrophages expressed lower mRNA levels compared to LPS alone. This change in mRNA expression levels between two and six hours is significant in pretreated alveolar macrophages for CXCL8 ($p<0.02$).

Figure 8 shows the concentrations of TNFα protein produced between alveolar and peritoneal macrophages pretreated with rgpCCL5 or untreated, following stimulation with LPS. Resident peritoneal macrophages produced significantly more bioactive TNFα protein levels at two hours post-LPS stimulation following pretreatment with rgpCCL5 (fig. 8A). However, this pattern was reversed at six hours with TNFα levels were unaltered in rgpCCL5 pretreated macrophages compared to the enhanced

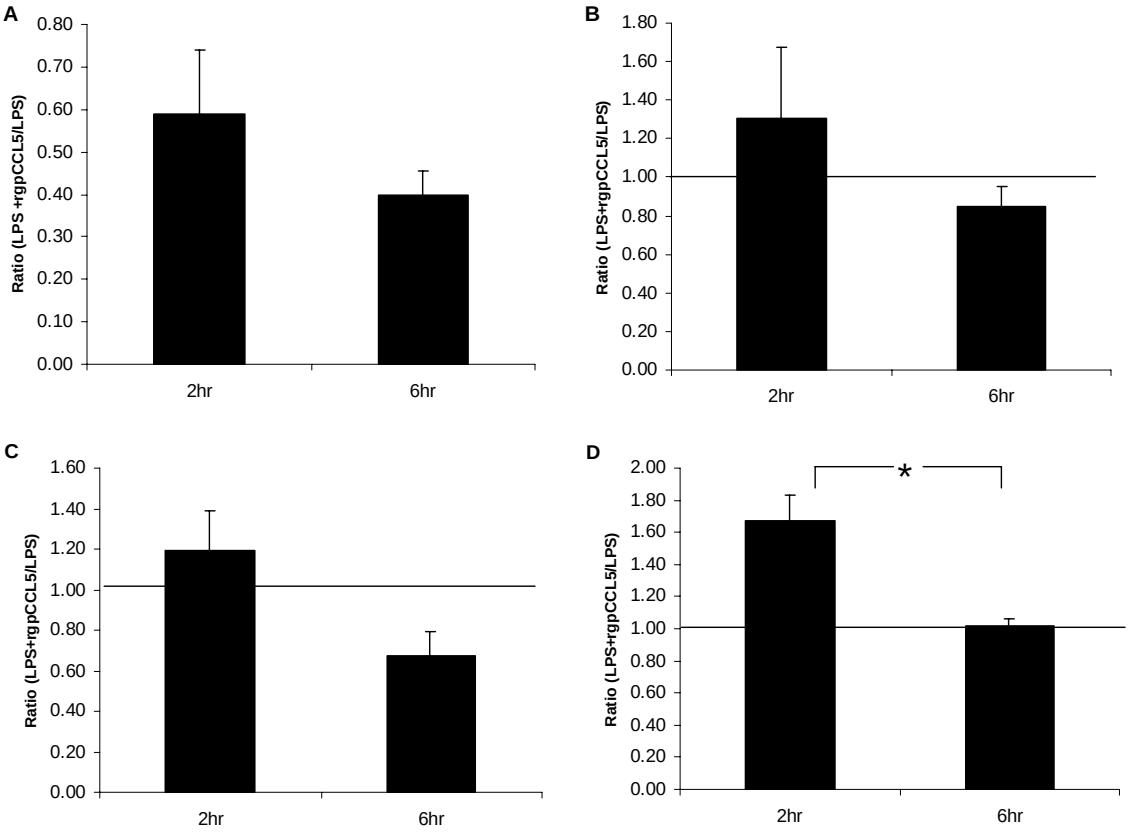

Figure 7: Regulation of LPS-induced cytokine and chemokine mRNA expression in guinea pig alveolar macrophages by pretreatment with rgpCCL5. Expression of TNFα (A), IL-β (B), CCL-2 (C), and CXCL-8 (D) mRNA was assessed by real-time RT-PCR. Cells were pretreated with 1350ng/ml rgpCCL5 for two hours, and then stimulated with LPS (10ng/ml) for two or six hours. Results are expressed as mean $\pm$ SEM of the ratios of mRNA in rgpCCL5-pretreated over untreated cells of 3-4 experiments. Significance ($p < 0.05$) between ratios at different time points was determined using Student's t test and is denoted by an asterisk.

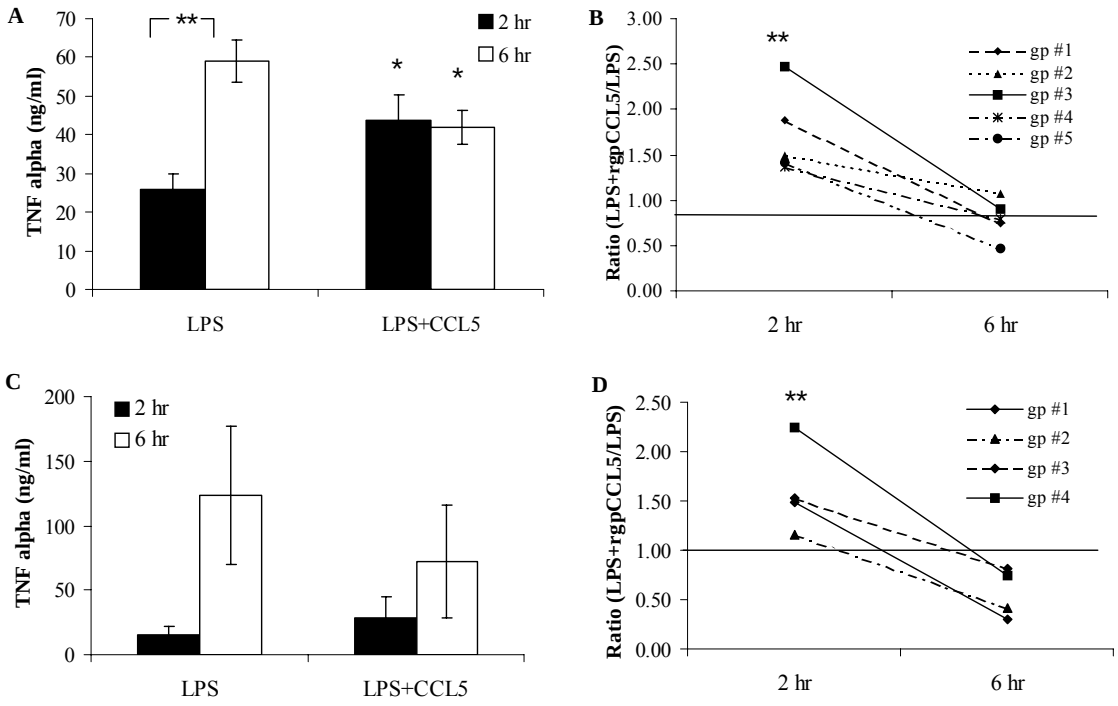

Figure 8: Regulation of LPS-induced TNFα protein production by rgpCCL5-pretreatment in peritoneal and alveolar macrophages. Alveolar (A) and peritoneal (B) macrophages were pretreated with 1350ng/ml rgpCCL5 for two hours followed by stimulation with 10ng/ml LPS for two or six hours. Supernatants were assessed for TNFα protein levels using the L929 bioassay. Data in A and C are the mean $\pm$ SEM of TNFα protein concentrations (ng/ml) from four experiments. The ratios of TNFα protein concentration of rgpCCL5-pretreated/untreated cells are represented in B (peritoneal) and D (alveolar). An asterisk represents significance differences ($p < 0.05$) between LPS stimulated macrophages from rgpCCL5 pretreated versus LPS alone at similar time points. A double asterisk denotes significance ($p < 0.005$) between TNFα protein production at two versus six hours with the same stimulus (fig. 8A and C) or significance between the average ratios (LPS+rgpCCL5/LPS) of two and six hours (fig. 8B and D). Statistics were performed using the Student's t test.

Expression in macrophages exposed to LPS alone. This trend was present in alveolar macrophages as well but, due to the variability between animals, statistical significance was not reached (fig. 8C). Both macrophage populations displayed minimal alterations in TNFα protein levels at six hours post-LPS stimulation in cells primed with rgpCCL5 (1350ng/ml) compared to two hours (fig. 8A and 8C). A significant difference was seen when comparing the ratios TNFα protein in rgpCCL5 pretreated versus untreated macrophages following LPS stimulation. The ratio (treated/untreated) at two hours was significantly greater than at six hours (fig. 8B and 8D), suggesting CCL5 had the ability to enhance TNFα protein production immediately, however, production declined thereafter. This trend was seen in both macrophage populations.

DISCUSSION

In this study, we tested the ability of rgpCCL5 to enhance the proinflammatory responses in guinea pig macrophages. The current dogma suggests that CCL5 attracts leukocytes to the site of inflammation via signaling through seven transmembrane G-coupled protein receptors (12, 169) and glycosoaminoglycan (GAG) receptors (157). It has been shown that the interaction of CCL5 with GAG on T cells results in prolonged calcium influx (14) in response to signaling via protein tyrosine kinases (33). This suggests CCL5 may have the ability to activate many cellular responses due to the promiscuity in receptor binding and the activation of numerous signaling pathways.

Our data show that rgpCCL5 significantly enhanced IL-1β and TNFα mRNA levels (fig. 3A, 3B, 4A, and 4B), as well as TNFα protein production (fig. 5A and B),

compared to media alone in both resident peritoneal and alveolar macrophages isolated from guinea pigs. This is the first time CCL5 has been shown to stimulate the expression of both proinflammatory cytokines in tissue specific macrophages. The ability of CCL5 to enhance IL-1β mRNA is in agreement with a previous study looking at human nonadherent monocytes exposed to recombinant CCL5 (113). Human recombinant CCL5 alone, at varying concentrations, was able to significantly heighten IL-1β mRNA levels in nonadherent human monocytes (113). However, in that study, increased IL-1β protein synthesis was not seen. Other studies have shown that adherence enhances IL-1β mRNA in macrophages, however, this priming results in earlier and enhanced IL-1β synthesis in human peripheral blood mononuclear cells stimulated with LPS (176). Due to the absence of reagents for the guinea pig, IL-1β protein levels could not be measured in our study.

For the first time in any species, enhanced expression and secretion of bioactive TNFα was documented when resident peritoneal and alveolar macrophages were incubated with rgpCCL5 (fig. 3A, 4A, 5A, and 5B). These findings contrast with the previous report in which no increase in TNFα protein levels were observed in nonadherent human monocytes treated with CCL5 (113). This apparent contradiction may be related to species or macrophage differences. The previous study used human nonadherent monocytes compared to the adherent guinea pig resident tissue macrophages examined in this study. Another plausible explanation may be that our macrophages were slightly activated due to adherence to plastic, which may have enhanced the stimulatory effect of rgpCCL5 on macrophage production of TNFα. The

study of macrophages which have been slightly activated by adherence may mimic what is occurring *in vivo,* since these macrophages are migrating along chemokine concentration gradients to arrive at the site of inflammation. It has been shown previously that cytokines, including TNFα, IL-1β, and/or IFNγ, enhance CCL5 mRNA and/or protein in human synovial fibroblasts (159), human endothelial cells (122), murine macrophages (212), and human monocytes (123). These data suggest that CCL5 and cytokines may cooperate to enhance each other's expression.

Stimulation with rgpCCL5 significantly enhanced CCL2 mRNA expression by resident peritoneal macrophages, but not alveolar macrophages (fig. 3C and 4C). Levels of CXCL8 mRNA were increased significantly in both macrophage types by stimulation with rgpCCL5 (fig. 3D and 4D). These chemokines are chemotactic for T lymphocytes (139), neutrophils (112), and monocyte/macrophages (163, 188). CCL2 has previously been shown to induce IL-1 and IL-6 protein in human monocytes (87), and to enhance Th2 polarization in mice (47). CXCL8 has been suggested to play a role in providing protection against infection because enhanced levels of expression are observed in vaccinated compared to naive animals (118). In a study where the IL-8 receptor (CXCR2) was knocked out, the mice were more susceptible to gastric and acute systemic candidiasis (17, 120). A previous study showed that CCL2 and CXCL8 mRNA levels were enhanced in human nonadherent monocytes when exposed to CCL5 alone, and CCL2 protein levels mimicked mRNA expression (113). In our studies, CCL5 enhanced both CXCL8 and CCL2 mRNA levels. These results suggest CCL5, while

attracting the macrophages to the site of infection, is priming macrophages for an encounter with microbes by enhancing cytokine and chemokine expression levels.

Differences observed in this study between peritoneal and alveolar macrophages have also been documented with regard to a variety of biological responses (53, 70, 82, 192, 201). However, very few studies have looked at the response of different resident macrophage populations to chemokines alone. Our results show that alveolar macrophages were less sensitive to stimulation with rgpCCL5 than peritoneal macrophages. Alveolar macrophages displayed a significant enhancement in TNFα, IL-1β, and CXCL8 mRNA expression (fig. 4) and TNFα protein (fig. 5B) only when stimulated with 1350ng/ml rgpCCL5 compared to media alone. In contrast, peritoneal macrophages displayed significant enhancement of TNFα, IL-1β, CCL2, and CXCL8 mRNA expression (fig. 3) and TNFα protein (fig. 5A) at lower concentrations of rgpCCL5. This might be due to different expression levels of CCL5 receptors and/or differences in signal transduction pathways. Differences between macrophage populations were seen also in the degree of stimulation of chemokine mRNA levels post-rgpCCL5 exposure. CCL2 mRNA was not significantly enhanced in alveolar macrophages exposed to rgpCCL5 (fig. 4C), whereas it was significantly increased in peritoneal macrophages (fig. 3C). Also, the kinetics of CXCL8 mRNA alterations differed between the two cell types. Alveolar macrophages expressed increasing levels of CXCL8 mRNA at 6h compared to 2h, in contrast to peritoneal macrophages in which expression of CXCL8 mRNA was diminished at 6hr. These data contribute to a better

understanding of the variation between different resident macrophage populations in terms of their responses to CCL5.

It has been shown in previous studies that LPS induces the expression of many chemokines, including CCL5, *in vitro* (37, 93, 99) and *in vivo* (99). In an attempt to better understand the effect of CCL5 exposure on the response of macrophages to LPS, alveolar and peritoneal macrophages were pretreated with rgpCCL5 and then stimulated with low levels of LPS. We observed a significant reduction in the ratio (LPS + rgpCCL5/ LPS) of CCL2 mRNA in peritoneal macrophages (fig. 6C), and CXCL8 mRNA in alveolar macrophages (fig. 7D) between two and six hours. TNFα exhibited diminished levels of mRNA at 2 h post-LPS stimulation in the rgpCCL5 pretreated macrophages (fig. 6A and 7A), however, the bioactive TNFα protein levels appeared slightly enhanced at 2 h followed by a reduction at 6h (fig. 8). One explanation for these findings might be the presence of endogenous TNFα produced by the macrophages before exposure to LPS. We have shown that CCL5 alone can induce bioactive TNFα protein as early as two hours post-CCL5 exposure (fig. 5). This production, plus the additional TNFα produced by macrophages upon activation by LPS, might result in the production of the immunoregulatory cytokine, IL-10. Previous studies have shown that TNFα alone induces IL-10 expression and production in human monocytes (208) and enhances IL-10 secretion when the cells are co-cultured with LPS (64, 156, 208). IL-10 suppresses many proinflammatory cytokines and chemokines in human monocytes, including TNFα, IL-1β, and CXCL8 (44). Human monocytes incubated with IL-10 and LPS exhibited a profound reduction in TNFα production compared to LPS alone (64)

and this effect appeared to be dependent on adherence to plastic (153). Pretreatment of monocytes with TNFα has resulted in partial cross-tolerance to LPS by suppressing ERK phosphorylation and increasing NFκB p50 homodimers (59), which are associated with LPS-tolerance. The topic of TNFα induced LPS tolerance has resulted in numerous contradicting publications suggesting both the inability and ability to induce cross-tolerance to LPS (59, 64, 66, 133). We plan to investigate the controversial role of endogenous TNFα by blocking TNFα activity in the cultures using anti-rgpTNFα antiserum. The contribution of IL-10 to the CCL5-induced hyporesponsiveness of macrophages to LPS will have to wait until rgpIL-10 and anti-gpIL-10 are available.

Another plausible explanation for the altered cytokine expression in CCL5 pretreated macrophages following LPS exposure may be the ability of IL-1β to induce LPS tolerance. In our experiments, IL-1β mRNA was induced within 2h of CCL5 treatment of both alveolar and peritoneal macrophages (Fig. 3B and 4B). Previous experiments have shown that IL-1β is regulated at the transcriptional and translational levels and that two signals are needed for IL-1β protein production (176). Due to the lack of guinea pig reagents, IL-1β protein levels were not assessed. However, it has been demonstrated that adherence of macrophages alone induces IL-1β mRNA levels (176) and stimulation of human nonadherent monocytes with CCL5 triggers IL-1β mRNA synthesis (113). Pretreatment of macrophages with IL-1β has resulted in LPS tolerance in many studies (9, 59, 133). This may be the result of common signaling intermediates between the LPS receptor (TLR4) and IL-1 receptor (IL-1R), such as

MyD88, IL-1R-associated kinase (IRAK), TNFR-associated factor-6, and NF-κB-inducing kinase (134). Another explanation for this cross-tolerance involves the ability of IL-1β to down-regulate TLR4 expression in peritoneal macrophages (9). It has also been shown that TNFα and IL-1β synergistically enhance LPS-induced production of the immunoregulatory cytokine, IL-10 (64). These data suggest that IL-1β and TNFα are induced in guinea pig macrophages by pretreatment with rgpCCL5 and lead to a state of tolerance when macrophages are exposed subsequently to LPS.

A novel direct role of CCL5 may account for the altered cytokine expression in CCL5 pretreated macrophages. Interactions between the signal transduction pathways elicited by CCL5 following engagement with seven transmembrane G protein-coupled receptors (CCR1, 3, 4, and 5) and glycosaminoglycans (GAG) might affect the ability of LPS to induce exceedingly high levels of cytokines and chemokines. A previous study induced nonadherent monocytes with rhCCL5 and observed the upregulation of 114 genes involved in various biological activities (113). Many of these genes have not been analyzed for their ability to alter the response of the cells to LPS.

These results suggest that CCL5 may directly or indirectly regulate the host phagocytic cell responses to prevent uncontrollable release of dangerous concentrations of proinflammatory cytokines. We plan on further elucidating the mechanisms by which CCL5 pre-treatment alters macrophage responses to bacterial products, and the role it may play in host-pathogen interactions, especially in the response of the guinea pig to *Mycobacterium tuberculosis.*

CHAPTER III

ACTIVATION OF ANTI-MYCOBACTERIAL FUNCTIONS IN MACROPHAGES AND LYMPHOCYTES BY rgpCCL5

INTRODUCTION

Tuberculosis (TB) has continued to plague mankind for millennia, and *Mycobacterium tuberculosis* currently infects over one third of the world's population (56). The development of new vaccines is in great demand due to the varying efficacy of the current BCG vaccine (13, 38, 73). Designing an improved TB vaccine will require a better understanding of the host immune response to TB. Currently, the guinea pig is an excellent model in which to test new tuberculosis vaccines because of the degree of protection BCG provides against pulmonary and disseminated tuberculosis in this species (186), and the similarities of guinea pigs to humans with regard to similar delayed type hypersensitivity (PPD) reactions, pulmonary physiology, granuloma composition and structure, and the ability to infect with a few bacilli via aerosolized droplet nuclei (16, 127).

Chemokines play an important role in eliciting a protective immune response against *M. tuberculosis* by participating in the formation of a well-defined and localized granuloma (35, 181), contributing to a delayed type hypersensitivity reaction (34, 35, 48, 121), attracting protective inflammatory cells to the site of infection (12, 27, 166, 209), and assisting in the differentiation of CD4+ T cells into a Th1 phenotype (54, 125, 217). The beta-chemokine, CCL5 (RANTES), is unique among the chemokines because of its

diverse biological activities. The role of CCL5 during the inflammatory response has been elucidated in cell lines and animal models. At low concentrations (ng/ml), CCL5 is chemotactic to numerous leukocytes, including eosinophils (4), CD4+ and CD8+ T lymphocytes (52, 166, 209), and monocyte/macrophages (12, 27, 142, 198, 209). It has also been demonstrated that CCL5 not only attracts these cell types to the foci of infection, but activates them as well. At high CCL5 concentrations (μg/ml), such as those most likely found at the foci of infection, T lymphocytes have been shown to be activated, resulting in IL-2 (121, 193) and IFNγ production (110, 121), as well as proliferation (14, 121, 193) . Previous studies have demonstrated the induction of reactive oxygen species (ROS) in eosinophils in response to CCL5 (36, 79, 91, 170). However, the chemotactic properties of CCL5 on eosinophils is diminished in the presence of peroxynitrite (171), suggesting reverse roles of CCL5 at high concentrations in eosinophils. The use of CCL5 as a gene adjuvant in DNA vaccines resulted in enhanced cytotoxic T lymphocyte activity and proliferation (95). Furthermore, *M. tuberculosis* viability inside human alveolar macrophages was increased when the cells were co-cultured with anti-human CCL5 (174).

In these studies, we elucidated the activation of guinea pig immune cells by gpCCL5. We examined the ability of CCL5 to modulate PPD-induced T lymphocyte proliferation, to affect the production of reactive oxygen species by macrophages in response to *M. tuberculosis* infection, and to alter *M. tuberculosis* viability within macrophages.

MATERIALS AND METHODS

Mycobacteria preparation. *Mycobacterium tuberculosis* H37Rv (ATCC 27294; American Type Culture Collection, Manassas, VA) and H37Ra (ATCC 25177) stored at –80°C were rapidly thawed, vortexed, and sonicated for 60s with an Ultrasonics sonicator (Heat Systems-Ultrasonics, Inc., Plainview, NY) at an output setting of 8.0 to remove clumps.

Animals and vaccination. Specific-pathogen-free, outbred, male and female Hartley guinea pigs from Charles River Breeding Laboratories, Inc. (Wilmington, MA) were housed in polycarbonate cages within an air-filtered environment under a 12 h light-dark cycle. Food (Ralston Purina, St. Louis, MO) and tap water were supplied to the animals ad libitum. Vaccination of guinea pigs was performed via intradermal injection of 0.1ml (10^3 CFU) of viable *Mycobacterium bovis* BCG (Danish 1331 strain, Statens Seruminstitut, Copenhagen, DK) into the left inguinal region. All procedures were reviewed and approved by the Texas A&M University Laboratory Animal Care Committee.

Necropsy and macrophage isolation. Guinea pigs were euthanized by two 1.5 ml intramuscular injections of sodium pentobarbital (100mg/ml) (Sleepaway Euthanasia Solution; Fort Dodge Laboratories, Inc., Fort Dodge, IA). The abdominal and thoracic cavities were opened aseptically and resident peritoneal macrophages were obtained by flushing the peritoneal cavity twice with 30ml of cold sterile phosphate-buffered saline (PBS) with 10U/ml heparin and 2% fetal bovine serum (FBS) (Atlanta Biologicals, Norcross, GA). Alveolar macrophages were obtained by exposing the trachea and

inserting an 18-gauge cannula fixed to a 20 ml syringe. The bronchoalveolar lavage (BAL) was performed by filling the lungs with cold 12mM lidocaine in PBS with 3% FBS as previously described (118). Cells were pelleted by centrifuging at 320 × g for 15 minutes at 4°C. These pellets were washed once with cold PBS. The cells were resuspended in 1ml of RPMI-1640 medium with phenol red (Irvine Scientific, Santa Anna, CA), 10μM 2-mercaptoethanol, 2 μM L-glutamine, 100 U/ml of penicillin, 100μg/ml of streptomycin, and 10% heat-inactivated FBS (RPMI 1640 complete medium). Viable cells were enumerated on a hemacytometer by Trypan blue exclusion (Gibco Life Technologies, Grand Island, NY). Cells from BAL were resuspended at 1×10^6 cells/ml and resident peritoneal macrophages at 2×10^6 cells/ml. Macrophage populations were added at 200μl/well in a 96-well polystyrene plate for 2 h. Nonadherent cells were removed by washing with warm RPMI 1640 complete medium.

Preparation of splenocytes. Spleens were removed aseptically from the peritoneal cavity and placed in RPMI-1640 complete medium. Spleens were homogenized and erythrocytes were lysed with ACK lysis buffer (0.14M NH_4Cl, 1.0mM $KHCO_3$, 0.1mM Na_2EDTA [pH 7.2 – 7.4]). Splenocytes were washed twice and resuspended in RPMI 1640 complete medium at a concentration of 2 X 10^6 cells/ml determined by excluding dead cells using Trypan blue exclusion and enumerating splenocytes on a hemacytometer. Splenocytes were added to a 96-well polystyrene plate in a volume of 100μl.

Macrophage stimulation and hydrogen peroxide detection. Resident peritoneal and alveolar macrophages from BCG-immunized or non-immunized guinea

pigs were rested for 18 h and infected with an attenuated strain of *M. tuberculosis* H37Ra at varying MOIs with added rgpCCL5, rgpTNFα (105), rabbit anti-gpTNFα (105), or RPMI 1640 complete media alone for varying periods of time. Media was removed and replaced with 100μl of H_2O_2 assay solution (0.2 ml phenol red stock (28mM), 0.2 ml horse-radish peroxidase (1000U/ml) (Sigma, St. Louis, MO), and 9.6ml Hanks balanced salt solution without phenol red (Sigma)) and incubated at 37°C in 5% CO_2 for 90 minutes. The reaction was interrupted by the addition of 10μl of 1N NaOH to each well. Absorbance was measured using a Dynatech MR5000 automated plate reader (Dyantech Laboratories, Inc., Chantilly, VA) at 630nm after 3 minutes. A standard curve was derived using two-fold dilutions of H_2O_2 (0.78 – 100μM) to quantify H_2O_2 concentrations in samples.

Lymphoproliferation. Splenocytes were incubated with rgpCCL5 (see Chapter II for preparation) or rabbit anti-rgpCCL5 (see Chapter V for preparation) with or without PPD (12.5 or 25 μg/ml) or ConA for different time periods. [H^3] thymidine was added at 1 μCi/well for the final 24 h of incubation. Splenocytes were harvested onto glass fiber filters, and proliferation was determined by the number of counts per minute with a liquid scintillation counter (LS8000; Beckman Instruments, Inc., Fullerton, CA).

***M. tuberculosis* viability assay.** Resident alveolar and peritoneal macrophages from naive and BCG-vaccinated guinea pigs were pretreated with rgpCCL5, rabbit anti-rgpCCL5, or media alone and infected with *M. tuberculosis* H37Rv (MOI 1:5) for 2 h at 37°C in 5% CO_2. Extracellular bacteria were aspirated and fresh RPMI 1640 medium with 10μM 2-mercaptoethanol, 2 μM L-glutamine, 10% FBS, and gentamycin

(200μg/ml) was added to each well for varying periods of time. [^{3}H] uracil at 1 μCi/well was added during the last 24 h of incubation. After each time interval, live *M. tuberculosis* was heat-killed by incubating at 80°C for 30 minutes. Macrophages were harvested onto glass fiber filters, and *M. tuberculosis* proliferative activity was determined by the number of counts per minute with a liquid scintillation counter.

RESULTS

Effect of gpCCL5 on hydrogen peroxide production. Figure 9 illustrates the effect of rgpCCL5 and rgpTNFα on H_2O_2 production in alveolar and peritoneal macrophages isolated from naive and BCG-vaccinated guinea pigs. Figure 9A demonstrates the inability of rgpTNFα or rgpCCL5 to induce H_2O_2 in rested resident peritoneal or alveolar macrophages. In figure 9B, attenuated *M. tuberculosis* H37Ra (MOI 5:1) was shown to induce H_2O_2 after only 90 minutes of incubation. The pretreatment of macrophages with rgpTNFα (50ng/ml) or rgpCCL5 (1,250-12,500ng/ml) for 2 h before infection did not affect significantly H_2O_2 production from *M. tuberculosis* H37Ra infected macrophages. It was demonstrated that infection with *M. tuberculosis* H37Ra was not altered in the presence of anti-rgpTNFα during the 90-minute infection. Macrophages were also studied following infection for longer periods of time (24 h and 48 h), however, H_2O_2 production appeared to be greater during earlier time points (data not shown).

The effect of rgpCCL5 on *M. tuberculosis* viability in macrophages. Previous studies have demonstrated increased viability of *M. tuberculosis* in the presence of anti-

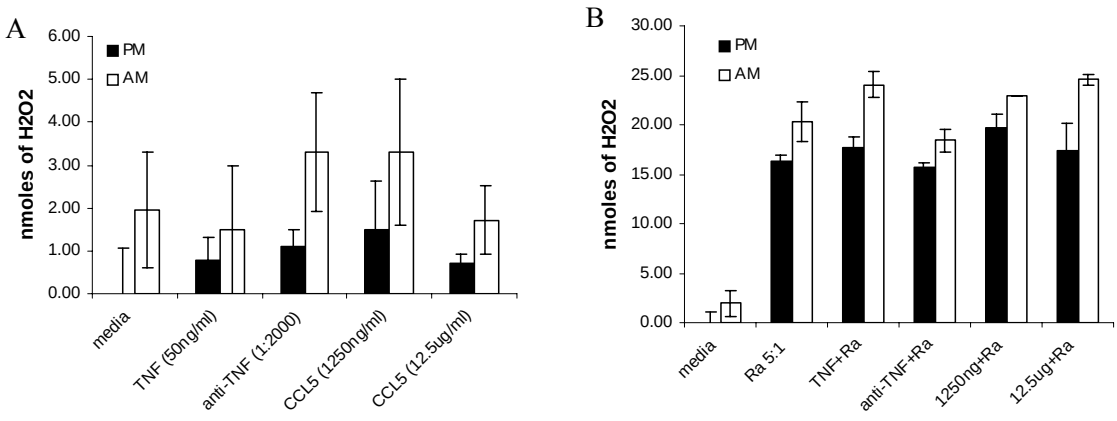

Figure 9: The effect of rgpTNFα and rgpCCL5 on H_2O_2 production in macrophages infected with *M. tuberculosis.* Resident alveolar and peritoneal macrophages were isolated from BCG-vaccinated guinea pigs and stimulated with rgpTNFα (50ng/ml), rabbit anti-rgpTNFα (diluted 1:2000), or rgpCCL5 (1250ng/ml or 12.5ug/ml) for 2 h followed by the addition of H_2O_2 assay medium for 90 minutes (A). The effect of rgpTNFα and rgpCCL5 on H_2O_2 production in macrophages infected with *M. tuberculosis* H37Ra (MOI 5:1) is displayed in panel B. Cells were pretreated with rgpTNFα or rgpCCL5 for 2 h, or co-cultured with anti-rgpTNFα and infected with H37Ra for 90 minutes in H_2O_2 assay medium. H_2O_2 was assessed as discussed in Materials and Methods. Results are presented as the mean $\pm$ SD of triplicate wells from one experiment.

Human CCL5 (174). Figure 10 illustrates the effect of gpCCL5 on virulent *M. tuberculosis* viability within macrophages. Macrophages isolated from BCG-vaccinated guinea pigs were infected with *M. tuberculosis* H37Rv (MOI 1:5) for 7 days. In figure 10A, it appears CCL5 does not affect *M. tuberculosis* viability within alveolar macrophages. Resident peritoneal macrophages appeared to limit *M. tuberculosis* replication in the presence of rgpCCL5 (1250ng/ml and 62.5μg/ml) (Fig. 10B). It is also apparent that high concentrations of anti-rgpCCL5 IgG has an inhibitory effect against bacterial viability in peritoneal macrophages.

Figure 11 demonstrates the difference in *M. tuberculosis* viability within macrophages obtained from BCG-vaccinated versus naive guinea pigs. Macrophages were infected with *M. tuberculosis* H37Rv (MOI 1:1 or 1:5) for 7 days. Pretreatment of infected macrophages with rgpCCL5 (1250ng//ml and 12.5μg/ml) for 2 h or co-culture with rgpCCL5 (12.5μg/ml) did not seem to affect bacterial viability. The co-culture of infected macrophages with anti-rgpCCL5 IgG (1:50) resulted in no differences. However, alveolar macrophages isolated from BCG-vaccinated guinea pigs had an enhanced ability to control *M. tuberculosis* growth *in vitro* compared to macrophages isolated from naive animals, regardless of the alteration of CCL5 activity in the cultures.

Effect of rgpCCL5 on splenocyte proliferation. Figure 12 demonstrates the effect of rgpCCL5 on splenocyte proliferation . Figure 12A suggests rgpCCL5 has a minimal effect on spontaneous proliferation of splenocytes taken from naive guinea pigs and cultured for 2 or 3 days. Peak splenocyte proliferation was apparent with 1ug/ml of rgpCCL5 with levels ~ 1.5 fold higher than media alone. At higher concentrations, this

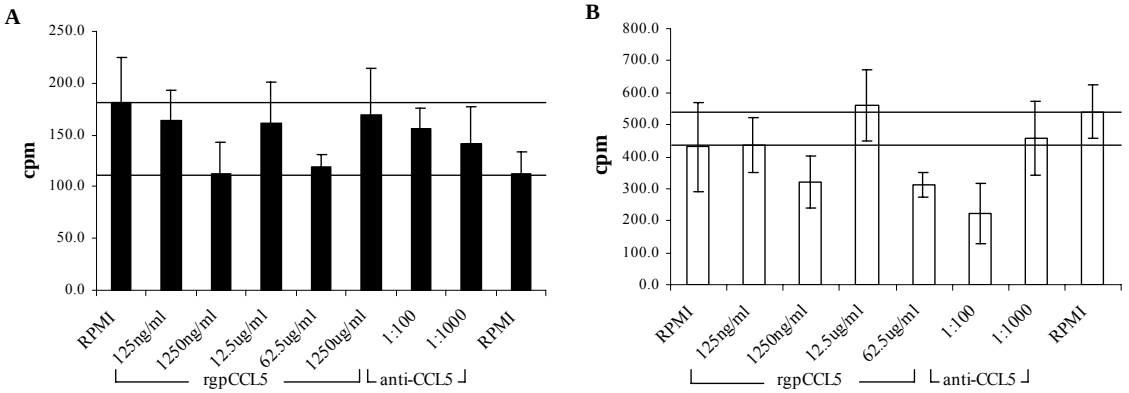

Figure 10: The effect of rgpCCL5 on *M. tuberculosis* viability within macrophages isolated from BCG-vaccinated guinea pigs. Alveolar macrophages (A) and resident peritoneal macrophages (B) were stimulated with rgpCCL5 (125ng/ml – 1250ug/ml) or anti-CCL5 (1:100 and 1:1000) and infected with *M. tuberculosis* H37Rv (MOI 1:5) for 7 days with 1μCi/well of [^{3}H] uracil being added 24 h before harvesting the cells. Cells were harvested onto glass fiber filters and read with a liquid scintillation counter. Each set of data represent mean $\pm$ SEM of triplicate wells from one experiment.

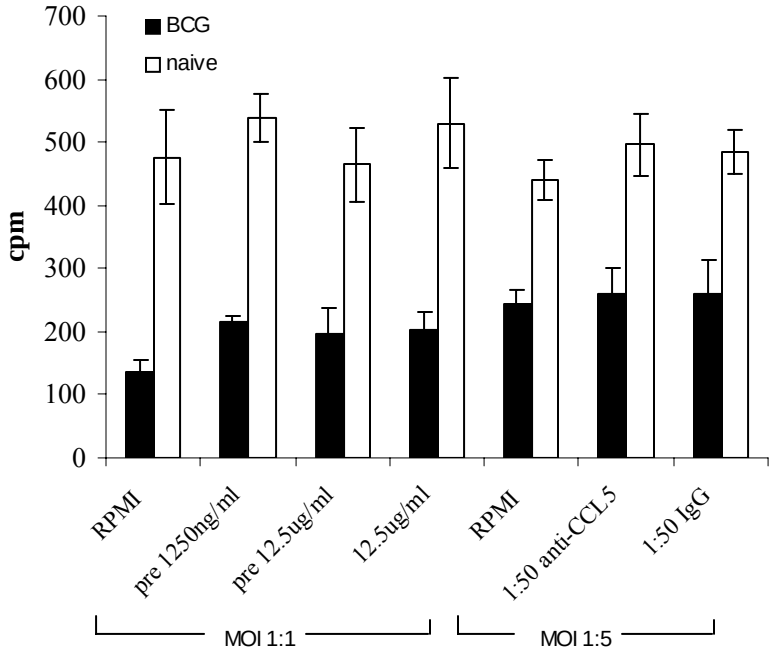

Figure 11. The effect of BCG-vaccination status on *M. tuberculosis* viability within alveolar macrophages. Alveolar macrophages were isolated from BCG-vaccinated and naive guinea pigs and either pretreated with rgpCCL5 (1250ng/ml or 12.5ug/ml) for 2 h or co-cultured with CCL5 (12.5ug/ml), anti-CCL5, guinea pig IgG, or media and infected with *M. tuberculosis* H37Rv (MOI 1:5 and 1:1) for 7 days. During the last 24 h of incubation 1μCi/well of [^{3}H] uracil was added and cells were harvested onto glass fiber filters. Radioactivity was quantitated using a liquid scintillation counter and the results are displayed as counts per minute (cpm). Results are representative of the means ± SEM of triplicate wells from one experiment.

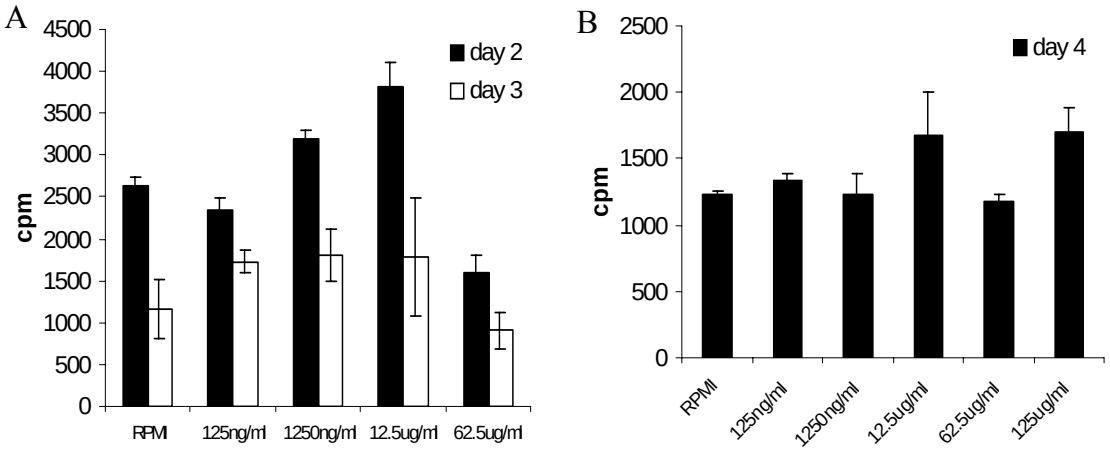

Figure 12: The effect of rgpCCL5 on splenocyte proliferation. In panel A, splenocytes were obtained from naive guinea pigs and stimulated with rgpCCL5 (125ng/ml – 62.5μg/ml) for 2 or 3 days. Panel B displays proliferation from splenocytes obtained from BCG-vaccinated animals and stimulated with rgpCCL5 for 4 days. During the last 6 h (panel A) or 24 h (panel B) of incubation, 1 μCi/ml [^{3}H] thymidine was added to each well. Cells were harvested and proliferative activity determined by counts per minute (cpm). Results are representative of the mean $\pm$ SEM of triplicates per treatment group from one experiment.

Effect was lost. In figure 12B, splenocytes obtained from BCG-vaccinated animals were cultured for 4 days in the presence of 12.5μg/ml and 125μg/ml of rgpCCL5. No statistically significant effect on splenocyte proliferation was observed.

The effect of rgpCCL5 on splenocyte proliferation to PPD was evaluated from cells taken from BCG-vaccinated guinea pigs (Fig. 13). RgpCCL5 (1250ng/ml) enhanced proliferative activity slightly at day 4, but was not different from media alone at days 1-3. Blocking gpCCL5 function by co-cultures with anti-rgpCCL5 did not appear to affect splenocyte proliferative activity during the time intervals examined.

DISCUSSION

During *M. tuberculosis* infection, the development of a protective immune response likely requires the migration of proper leukocyte populations, the development of Th1 response, and the ability of macrophages to be activated to produce anti-mycobacterial compounds (reactive oxygen and nitrogen intermediates). Recent studies have suggested that chemokines are involved in many of these host immune responses (54, 142, 174). Here we examined the contribution of gpCCL5 to these non-chemotactic functions during *M. tuberculosis* infections in the guinea pig.

We demonstrated that rgpCCL5 slightly enhanced H_2O_2 production within macrophages infected with *M. tuberculosis* (Fig. 9). Previous studies have reported ROS production in response to CCL5 in eosinophils (36, 79, 91) but, to our knowledge, there is an absence of data supporting a direct link between CCL5 stimulation and macrophage ROS production. However, recent reports of enhanced *M. tuberculosis* viability in

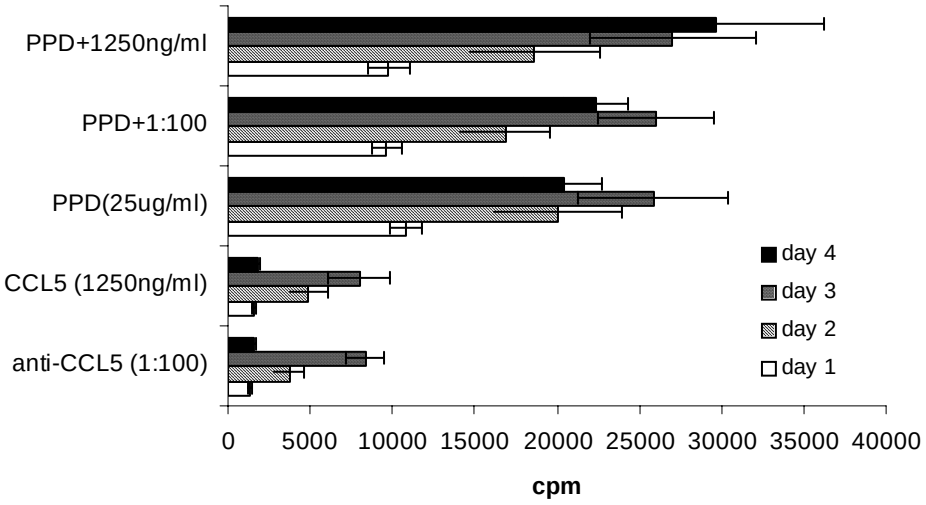

Figure 13: The effect of rgpCCL5 on T lymphocyte proliferation to PPD. Splenocytes were obtained from BCG-vaccinated guinea pigs and stimulated with rgpCCL5 (1250ng/ml) or anti-rgpCCL5 IgG (1:100) and co-cultured with or without PPD (25ug/ml) for 1-4 days. [^{3}H] thymidine at 1μCi/well was added to each well 24 h (days 1-3) or 6 h (day 4) before incubation time. Cells were harvested and proliferative activity determined by counts per minute. Results are representative of the mean $\pm$ SEM from two independent experiments with triplicates performed with each treatment group.

Human alveolar macrophages in the presence of anti-human CCL5 (174) suggest that CCL5 induces anti-mycobacterial products (i.e. ROS) in these cells. We were disappointed, therefore, to observe that gpCCL5 did not appear to affect *M. tuberculosis* viability in guinea pig resident alveolar macrophages, and only minimally affected mycobacterial viability in resident peritoneal macrophages (Fig. 10). These preliminary studies need to be repeated at different MOIs to verify these observations. The data suggest that CCL5 might stimulate ROIs in eosinophils through different host receptors compared to macrophages. Another plausible explanation is that eosinophil CCRs interact with other receptors within their lipid rafts, thus resulting in varying transmembrane signaling compared to macrophages.

In Fig. 11, macrophages obtained from BCG-vaccinated guinea pigs displayed an enhanced ability to limit *M. tuberculosis* growth compared to macrophages isolated from naive guinea pigs. A previous study indicated that alveolar macrophages isolated from BCG-vaccinated guinea pigs produce more H_2O_2 than naive macrophages when infected with H37Ra (84), suggesting a mechanism of how alveolar macrophages from BCG-vaccinated guinea pigs can limit the growth of *M. tuberculosis in vitro.*

The ability of naive splenic lymphocytes to proliferate when stimulated with rgpCCL5 was evaluated. We found that rgpCCL5 enhanced splenocyte proliferation minimally at 1250ng/ml, 12.5μg/ml, and 125μg/ml in splenocytes isolated from naive and/or BCG-vaccinated guinea pigs alone (Fig. 12). Preliminary studies examining the effect of rgpCCL5 on antigen-specific lymphocyte proliferation to PPD in cells from BCG-vaccinated animals revealed minimal differences following treatment with

rgpCCL5 or anti-rgpCCL5 (Fig. 13). This is in contrast with previous studies supporting CCL5's ability to act in a mitogen-like manner by inducing T lymphocyte proliferation (14, 121, 193). However, the published studies were performed with freshly isolated human T cells and human T cell clones. In our studies, we used whole splenocytes instead of purified T lymphocytes to assess the role of gpCCL5 on naive and PPD-specific lymphocyte proliferation. No previous studies to our knowledge have reported splenocyte proliferation induced by CCL5. Future studies looking at proliferation of guinea pig nylon wool purified T lymphocyte in the presence of rgpCCL5 will be performed to further evaluate differences and similarities among species. A previous study performed by Campbell, et al. demonstrated variability between human and guinea pig eosinophils. There was an absence of chemotactic properties associated with rgpCCL5 or rhCCL5 to guinea pig eosinophils (27). This is in contrast with human studies, which have shown rhCCL5 to be chemotactic to eosinophils (4). In these studies, there was a diminished ability of rgpCCL5 to induce splenocyte proliferation. Previous studies have exhibited human and murine CCL5's ability to induce T lymphocytes proliferation (14, 121, 193). This suggest the possibility of variability and selective differences between chemokines and/or leukocytes between guinea pigs and humans but, since we did not examine purified T lymphocytes in this study, further experiments need to be performed before these conclusions are accepted.

CHAPTER IV

VACCINATION ENHANCES IL-12p40 mRNA LEVELS IN GUINEA PIG ALVEOLAR MACROPHAGES INFECTED WITH *Mycobacterium tuberculosis*

INTRODUCTION

Mycobacterium tuberculosis continues to be one of the top three infectious killers in the world and claims two million lives a year. The immune response plays a critical role in the development of the disease, specifically granuloma formation. The granuloma is formed by a collection of cells, including macrophages and T lymphocytes, aggregating around the foci of infection. The formation of a protective granuloma is partially dependent on the concentration and timing of chemokines and cytokines. These proteins are responsible for attracting and activating leukocytes at the site of infection. IL-12 has long been known to be a crucial Th1 cytokine secreted by macrophages and responsible for differentiating CD4+ T lymphocytes into the Th1 phenotype. These Th1 effector cells release IFNγ, which results in macrophage activation and the production of elevated levels of anti-mycobacterial compounds, including reactive oxygen and nitrogen intermediates (23, 172).

More recently it has been shown that the IL-12p40 chain is involved in the composition of two Th1 cytokines, IL-12 and IL-23 (144). These cytokines share a common receptor subunit, IL-12 Rβ1 (148), but interact with different T lymphocyte subpopulations. IL-12 has been associated with the activation of naive T lymphocytes, whereas IL-23 is associated with the activation of memory T lymphocytes (103). The

interaction of T cells with either IL-12 or IL-23 results in IFNγ production. The IL-12p40 subunit plays an important role during mycobacterial infections (39, 78) . IL-12p40 knockout mice infected with *M. tuberculosis* had higher bacterial burdens, abrogated delayed type hypersensitivity reactions, and a reduction in IFNγ production compared to wild type mice were observed (39, 78). Together these data strongly support the necessity of the IL-12p40 subunit in eliciting a protective immune response to tuberculosis infection.

In this study, the expression of IL-12p40 mRNA levels was analyzed in guinea pig alveolar macrophages infected with virulent or attenuated strains of *Mycobacterium tuberculosis,* and the effect of BCG-vaccination on this response was documented.

MATERIALS AND METHODS

Animals and BCG vaccination. Specific-pathogen-free, outbred, male and female Hartley guinea pigs from Charles River Breeding Laboratories, Inc. (Wilmington, MA) were housed in polycarbonate cages within an air-filtered environment under a 12 h light-dark cycle. Food (Ralston Purina, St. Louis, MO) and tap water were supplied to the animals ad libitum. Vaccination of guinea pigs was performed via intradermal injection of 0.1ml (10^3 CFU) of viable *Mycobacterium bovis* BCG (Danish 1331 strain, Statens Seruminstitut, Copenhagen, DK) into the left inguinal region. All procedures were reviewed and approved by the Texas A&M University Laboratory Animal Care Committee.

Necropsy and alveolar macrophage isolation. Four weeks after vaccination, guinea pigs were euthanized by two 1.5 ml intramuscular injections of sodium pentobarbital (100mg/ml) (Sleepaway Euthanasia Solution; Fort Dodge Laboratories, Inc., Fort Dodge, IA). Bronchoalveolar lavage cells were obtained by placing an 18-gauge cannula fixed to a 20ml syringe intra-tracheally. Bronchoalveolar lavage was performed with 50ml of PBS containing 3% fetal bovine serum (FBS) and 12mM lidocaine. These cells were washed with PBS and resuspended in RPMI 1640 with 10μM 2-mercaptoethanol, 2μM L-glutamine, and 10% FBS (C-RPMI). Alveolar macrophages (AM) were isolated by adherence to a 96-well plastic culture plate during 1-2 hours of incubation at 37°C in a 5% CO_2 in air atmosphere. The cell cultures were washed twice with warm RPMI to remove nonadherent cells. C-RPMI 1640 was added to the wells and the cells were rested for an additional 24 hours.

Mycobacterium preparation. *Mycobacterium tuberculosis* H37Rv (ATCC 27294; American Type Culture Collection, Manassas, VA) and H37Ra (ATCC 25177) stored at –80°C were rapidly thawed, vortexed, and sonicated for 60s with an Ultrasonics sonicator (Heat Systems-Ultrasonics, Inc., Plainview, NY) at an output setting of 8.0 to remove clumps.

Cell cultures. Alveolar macrophages were infected with H37Ra or H37Rv at a MOI 1:5 in C-RPMI with no antibiotics for 2 h. Extracellular mycobacteria were removed by aspirating the media and washing the cells once. Fresh C-RPMI was added to the wells and these samples were used as 0 h time point. At each time interval, media was aspirated and cells were lysed with buffer RLT (Qiagen) and frozen at –80°C.

RNA isolation and real-time PCR. RNA was isolated using QIAshredder followed by the RNeasy kit from Qiagen. Reverse transcription was performed using Taqman reverse transcription reagents (Applied Biosystems). Primer Express software (Applied Biosystems) was used to design the sequences for guinea pig 18S (forward primer, 5'-TGCATGGCCGTTCTTAGTTG – 3'; reverse primer, 5'-AGTTAGCATGCCAGAGTCTCGTT – 3') and IL-12p40 (forward primer, 5'-GTGGTAGAGTTGGATTGGCACA – 3'; reverse primer, 5'-TCCTCAGCAGTGTTGCAGGT – 3'). Real time PCR was performed using SYBR Green PCR Supermix and the ABI Prism 7700 Sequence Detector from Applied Biosystem. Fold induction levels of mRNA were obtained by analyzing cycle threshold (Ct) levels normalized to 18S Ct values and further normalized against values at 0 h.

Statistical analysis. The differences between groups were analyzed for statistical significance using the Student's t test with a two-tailed distribution. The probability levels were set at 95%.

RESULTS

The effect of BCG-vaccination on *M. tuberculosis* infected alveolar macrophage expression of IL-12p40. Figure 14 illustrates the effect of BCG-vaccination on IL-12p40 mRNA expression in alveolar macrophages infected with *M. tuberculosis.* In Fig. 14A, alveolar macrophages from naive and BCG-vaccinated guinea

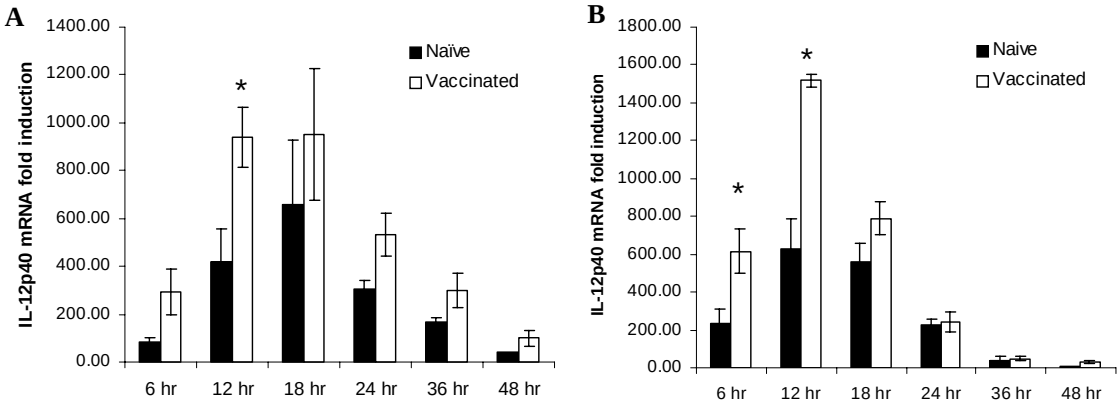

Figure 14: Alveolar macrophages exhibit enhanced IL-12p40 mRNA levels from BCG-vaccinated compared to naïve guinea pigs. Rested AM were infected with attenuated H37Ra (A) and virulent H37Rv (B) *M. tuberculosis* (MOI 1:5) for 6, 12, 28, 24, 36, and 48 h. Differences in IL-12p40 mRNA were analyzed in *M. tuberculosis* infected macrophages obtained from naive (black bars) or BCG-vaccinated (white bars) animals. At each time interval, RNA was isolated from cells and reverse transcribed into cDNA. Real time analysis of the cDNA was performed in duplicates, and IL-12p40 mRNA fold inductions were determined by normalizing IL-12p40 threshold cycle (C_t) values against 18S values. This was further normalized against mRNA from infected macrophages at 0 h. The bars above represent the mean ± SEM of three animals. Statistical analysis was done analyzing H37Ra versus H37Rv at each time point and values of $p < 0.05$ (*) were considered significant.

Pigs were isolated and infected with an attenuated strain of *M. tuberculosis* (H37Ra) at a MOI 1:5 for 6, 12, 18, 24, 36, and 48 h. At each time interval RNA was isolated, reverse transcribed into cDNA, and analyzed by real-time PCR. As early as 6 h, elevated levels of IL-12p40 mRNA appeared in macrophages obtained from BCG-vaccinated compared to naive animals. Significant ($p < 0.05$) differences between the treatment groups were apparent at 12 h with about 2-fold higher expression levels in macrophages obtained from BCG-vaccinated guinea pigs. The mRNA fold induction levels, though not statistically significant, remained slightly elevated in macrophages obtained from BCG-vaccinated animals compared to naive throughout the course of the experiment. In fig. 14B, live virulent *M. tuberculosis* (H37Rv) was used to infect alveolar macrophages. This resulted in significant ($p < 0.05$) enhancement of IL-12p40 mRNA in macrophages obtained from BCG-vaccinated animals as early as 6 h. A three-fold difference between the groups was observed at 12 h, however, at 18 h the expression level of IL-12p40 mRNA in macrophages from vaccinated animals declined to levels similar to naive macrophages.

Differences between IL-12p40 mRNA expression in alveolar macrophages infected with an attenuated versus virulent strain of *M. tuberculosis.* Figure 15 illustrates the variation in IL-12p40 mRNA expression between alveolar macrophages infected with an attenuated (H37Ra) or a virulent (H37Rv) strain of *M. tuberculosis.* In figure 15A, alveolar macrophages were obtained from naive guinea pigs and infected for 6, 12, 18, 24, 36, and 48 h with either *M. tuberculosis* H37Ra or H37Rv at a MOI 1:5. IL-12p40 mRNA expression was determined by real-time PCR analysis. Although not

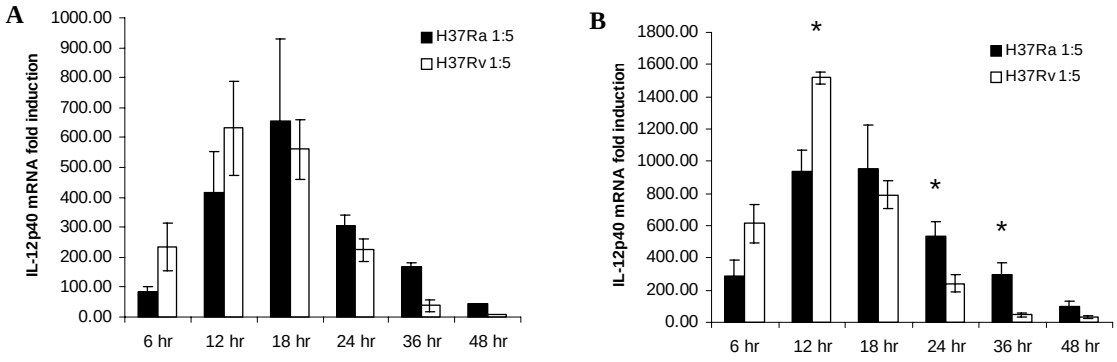

Figure 15: Virulent *M. tuberculosis* H37Rv induces a more rapid upregulation of IL-12p40 mRNA than an attenuated (H37Ra) strain. AM were isolated from naive (A) and BCG-vaccinated (B) guinea pigs and infected with attenuated H37Ra (black bars) or virulent H37Rv (white bars) strains of *M. tuberculosis* (MOI 1:5) for 6, 12, 28, 24, 36, and 48 h. At each time interval, RNA was isolated from cells and reverse transcribed into cDNA. Real time analysis of the cDNA was performed in duplicates, and IL-12p40 mRNA fold inductions were determined by normalizing IL-12p40 threshold cycle (C_t) values against 18S values. This was further normalized against mRNA from infected macrophages at 0 h. Statistical analysis was done analyzing H37Ra versus H37Rv at each time point. The bars above represent the mean ± SEM of three animals. Values of $p < 0.05$ (*) were considered significant.

Statistically significant, H37Rv induced IL-12p40 mRNA to a greater extent early (6 and 12 h) during the infection, while H37Ra induced higher levels throughout the rest of the experiment. In figure 15B, alveolar macrophages were isolated from BCG-vaccinated guinea pigs and infected with either H37Ra or H37Rv. A similar kinetic pattern was observed in macrophages obtained from naive and vaccinated animals, however, H37Rv induced significantly ($p < 0.05$) elevated IL-12p40 mRNA compared to H37Ra at 12 h post-infection. As the infection proceeded, this pattern was reversed and at 24 and 36 h H37Ra induced IL-12p40 mRNA levels which were significantly ($p < 0.05$) higher than those induced by H37Rv.

DISCUSSION

The current tuberculosis vaccine, BCG, though varying in efficacy, provides a degree of protection especially against the dissemination of *M. tuberculosis* (65). The development of a more protective vaccine would be facilitated by an understanding of the mechanisms of protection elicited by BCG. Considering the multitude of similarities shared between the pathogenesis of tuberculosis in guinea pigs and humans (127), guinea pigs provide a useful model to test new vaccines against tuberculosis. BCG vaccination induces significant protection against disseminated disease in the guinea pig (129), thus it is important to dissect the protective immune response elicited in BCG-vaccinated compared to naive guinea pigs (7, 106, 118).

In these studies, we elucidated the effect of BCG-vaccination on IL-12p40 mRNA expression in alveolar macrophages obtained from guinea pigs. We

demonstrated a significantly enhanced expression of IL-12p40 mRNA in macrophages isolated from BCG-vaccinated guinea pigs, suggesting the importance of this cytokine subunit in eliciting a protective immune response against *M. tuberculosis*. These findings further support previous results demonstrating the importance of IL-12 and IL-23 in providing protection against *M. tuberculosis* in mice (39, 78, 96) and humans (2, 69, 197). Due to lack of available guinea pigs reagents, studies focusing on IL-12 and IL-23 protein production could not be carried out. The story is incomplete without these data. However, our IL-12p40 mRNA results strengthen the potential importance of these Th1 cytokines in providing protection against tuberculosis and display another similarity between humans and guinea pigs. Previous studies in our lab have demonstrated enhanced CXCL8, CCL2, CCL5, IFNγ, TNFα, and IL-1β mRNA and/or protein in *M. tuberculosis*-infected leukocytes from BCG-vaccinated guinea pigs *in vitro* compared to cells from naive animals (85, 86, 106, *118*). These findings aid in the understanding of which cytokines/chemokines are involved in eliciting a protective immune response against tuberculosis.

Previous studies in our lab have demonstrated differences in the induction of inflammatory cytokines and chemokines between virulent (H37Rv) and attenuated (H37Ra) strains of *M. tuberculosis* (106, *118*), suggesting bacterial virulence is related to the macrophage response. In these studies, macrophages obtained from naive guinea pigs had similar IL-12p40 mRNA levels when infected with H37Ra or H37Rv. However, alveolar macrophages isolated from BCG-vaccinated guinea pigs displayed a significant difference in IL-12p40 mRNA expression after infection with attenuated

versus virulent strains of *M. tuberculosis.* H37Rv induced a rapid upregulation of IL-12p40 mRNA as early as 6 h with significant enhancement over H37Ra by 12 h. This elevated response was transient and by 24 h IL-12p40 expression levels declined over 30 fold. In contrast, levels of IL-12p40 mRNA in H37Ra infected macrophages dropped slightly over 3 fold between 12 h to 48 h. This suggests that virulent *M. tuberculosis* might down-modulate the production of IL-12/IL-23, leading to an attenuation of the host immune response, thus, ensuring its own persistence. Previous studies in our lab have demonstrated the ability of virulent *M. tuberculosis* to induce significantly lower CXCL8 mRNA levels in alveolar macrophages than the attenuated strain (*118*) . However, in that study, CXCL8 protein levels were not affected. Therefore, it is important that we measure IL-12/IL-23 protein levels before drawing any definitive conclusions. It is also possible that an increase in bacterial uptake by the macrophage occurs with virulent compared to attenuated *M. tuberculosis*. This may result in more immediate expression of IL-12p40 mRNA. However, the kinetic patterns of IL-12p40 mRNA between the two strains is particularly interesting because infections with H37Rv results in rapid decline in IL-12p40 mRNA levels after 12 h (Fig. 15B). These findings may be due to a reduction in macrophage viability, however, this effect was not examined in the present study. Unpublished studies in our lab have demonstrated unaltered macrophage viability in cells infected with *M. tuberculosis* at MOIs of 1:5 or less, suggesting that the aforementioned explanation is unlikely. In contrast, at 24 and 36 h, attenuated *M. tuberculosis* induced significantly higher levels of IL-12p40 mRNA compared to the virulent strain (Fig. 15B). This rapid decline in IL-12p40 mRNA in

virulent *M. tuberculosis*-infected alveolar macrophages could be associated with a survival mechanisms developed by the bacteria. However, protein data for IL-12 and IL-23, as well as a correlation with bacterial viability, need to be obtained before these conclusions can be drawn.

CHAPTER V

EFFECT OF BCG VACCINATION ON CCL5 PRODUCTION *IN VITRO* AND *IN VIVO* IN RESPONSE TO *Mycobacterium tuberculosis* IN THE GUINEA PIG

INTRODUCTION

Millennia have passed and still tuberculosis (TB) persists in our world, infecting one third of the world's population and claiming ~ 2 million lives per year (56). We are in great need of a new vaccine against tuberculosis due to the varying efficacy (0-80%) of the current BCG vaccine (38, 162). The development of a better tuberculosis vaccine has been the focus of concerted studies throughout the world, including protection trials in numerous animal models, such as mice, rabbits, guinea pigs, and monkeys (128, 132). Guinea pigs display protection following vaccination with BCG, disease progression similar to that of humans and potent delayed-type hypersensitivity, following infection with a low aerosol dose of *M. tuberculosis*. Therefore, guinea pigs are considered to be an excellent animal model in which to study novel TB vaccines (145).

To better design a more efficacious vaccine against TB, we need to further develop our understanding of the guinea pig immune response elicited by BCG vaccination in response to *M. tuberculosis* infection. A pivotal step in the containment of infection is the formation of a protective granuloma, which is dependent on many components of the

Host immune response, including numerous cytokines and chemokines. Abnormal granuloma formation has been observed in the absence of TNFα (24, 161), IL-12 (78), and IFNγ (34, 190). Chemokines have also been suggested to play a crucial role in granuloma formation (5, 34, 35, 68, 158, 161), due to their chemotactic properties for macrophages/monocytes and T lymphocytes. Of particular interest is the CC chemokine, CCL5 (RANTES), because of its ability to attract T lymphocytes and macrophages, which are involved in protection against *M. tuberculosis* (14, 142, 175, 209), to induce a Th1 response (54, 125, 217), to activate and expand populations of T lymphocytes (11, 14, 54, 193, 209), and to augment the delayed type hypersensitivity response (34, 35, 48, 121). Recently, CCL5 has been shown to play a role in diminishing *M. tuberculosis* viability in macrophages (174). Previous studies have shown elevated levels of CCL5 in the bronchoalveolar lavage fluid from individuals with human pulmonary tuberculosis (81, 101, 167) and reduced levels in those co-infected with immunosuppressive diseases, like HIV/AIDS, suggesting an important role of this chemokine in providing protection against tuberculosis. Human monocytes (167), monocyte-derived dendritic cells (206), and alveolar macrophages (167, 174) have been shown to secrete CCL5 in response to *M. tuberculosis* infection.

Due to the lack of reagents for the guinea pig, much remains to be elucidated regarding the immune response against *M. tuberculosis* and the protective effect of BCG vaccine. Previous work in our laboratory has revealed enhanced expression and production of TNFα (106) and CXCL8 (IL-8) (*118*) from different cell populations isolated from BCG-vaccinated guinea pigs compared to non-immunized animals. We

have also observed heightened mRNA levels of IL-1β (85) and CCL5 (85) in *M. tuberculosis*-infected macrophages isolated from BCG-vaccinated guinea pigs. In these studies, the effect of BCG vaccination on CCL5 mRNA expression and protein production from different guinea pig leukocyte populations infected with *M. tuberculosis in vitro* was elucidated. This is the first time gpCCL5 protein has been detected and quantified in the guinea pig. BCG vaccination enhanced the levels of CCL5 mRNA and secreted protein from macrophages and splenocytes infected with *M. tuberculosis* (H37Rv). The well-established guinea pig model of tuberculosis pleurisy (154) was used to quantify levels of CCL5 *in vivo.* High concentrations of CCL5 mRNA and protein were observed in pleural exudate cells and fluid aspirated from the pleural cavity.

MATERIALS AND METHODS

***Mycobacterium* preparation.** *Mycobacterium tuberculosis* H37Rv (ATCC 27294; American Type Culture Collection, Manassas, VA) stored at –80°C was rapidly thawed, vortexed, and sonicated for 60s with an Ultrasonics sonicator (Heat Systems-Ultrasonics, Inc., Plainview, NY) at an output setting of 8.0 to remove clumps.

Production of polyclonal anti-guinea pig CCL5. Recombinant guinea pig CCL5 was obtained as previously described (184). Rabbits were injected three times with rgpCCL5 (0.1mg) with TiterMax Gold adjuvant (Sigma, St. Louis, MO) at three week intervals. Blood was collected by exsanguination and centrifuged at 200 × g for 30

minutes to obtain total serum. The specificity of the anti-serum was detected against recombinant guinea pig (rgp) CCL5 using Western blot analysis.

SDS-PAGE analysis and Western blot. Recombinant gpCCL5 was analyzed by SDS-PAGE using 10-20% tris-tricine gels (Invitrogen, Carlsbad, CA). The protein was transferred to polyvinylidene difluoride (PVDF) membranes (Invitrogen, Carlsbad, CA) using 350 mAmps from a Power Pac 300 (Bio-rad, Hercules, CA). The membrane was than washed to eliminate any transfer buffer. Western blot was performed using rabbit anti-rgpCCL5 serum and the Western Breeze Chromogenic Immunodetection Kit (Invitrogen, Carlsbad, CA) following the user manual.

Animals and vaccination. Outbred male and female Hartley guinea pigs from Charles River Breeding Laboratories, Inc. (Wilmington, MA) were housed in polycarbonate cages within an air-filtered environment under a 12 h light-dark cycle. Food (Ralston Purina, St. Louis, MO) and tap water were supplied to the animals *ad libitum*. Vaccination of guinea pigs was performed via intradermal injection of 0.1ml (10^3 CFU) of viable *Mycobacterium bovis* BCG (Danish 1331 strain, Statens Seruminstitut, Copenhagen, DK) into the left inguinal region. All procedures were reviewed and approved by the Texas A&M University Laboratory Animal Care Committee.

Necropsy and macrophage isolation. Guinea pigs were euthanized by two 1.5 ml intramuscular injections of sodium pentobarbital (100mg/ml) (Sleepaway Euthanasia Solution; Fort Dodge Laboratories, Inc., Fort Dodge, IA). The abdominal and thoracic cavities were opened aseptically and resident peritoneal macrophages were obtained by

flushing the peritoneal cavity twice with 30ml of cold phosphate-buffered saline (PBS) with 10U/ml heparin and 2% fetal bovine serum (FBS) (Atlanta Biologicals, Norcross, GA). Alveolar macrophages were obtained by exposing the trachea and inserting an 18-gauge cannula fixed to a 20 ml syringe. The bronchoalveolar lavage (BAL) was performed by filling the lungs with cold 12mM lidocaine in PBS containing 3% FBS as previously described (*118*). Cells were pelleted by centrifuging at 320 × g for 15 minutes at 4°C. These pellets were washed twice with cold PBS. The cells were resuspended in 1ml of Macrophage-SFM (Invitrogen, Carlsbad, CA), and viable cells were enumerated on a hemacytometer by Trypan blue exclusion (Gibco Life Technologies, Grand Island, NY). Cells from BAL and peritoneal cavity were resuspended at 1×10^6 cells/ml and 500µl/well were added to a 48-well polystyrene plate.

Preparation of splenocytes. Spleens were removed aseptically from the peritoneal cavity after resident peritoneal cells were harvested and placed in RPMI-1640 medium (Irvine Scientific, Santa Anna, CA) with 10µM 2-mercaptoethanol, 2 µM L-glutamine, and 10% heat-inactivated FBS. Spleens were homogenized and erythrocytes were lysed with ACK lysis buffer (0.14M NH_4Cl, 1.0mM $KHCO_3$, 0.1mM Na_2EDTA [pH 7.2 – 7.4]). Splenocytes were washed twice in RPMI medium without fetal bovine serum, and resuspended in Macrophage-SFM at a concentration of 1×10^6 cells/ml determined by excluding dead cells using Trypan blue exclusion and enumerating splenocytes on a hemacytometer. Splenocytes were added to a 24-well polystyrene plate in a volume of 1ml/well.

Cell stimulation. Alveolar and peritoneal macrophages were isolated via adherence to polystyrene plates for 1.5 – 2 h at 37°C. Nonadherent cells were removed by washing wells with warm Macrophage – SFM media. Purified macrophages were infected with *M. tuberculosis* H37Rv at a multiplicity of infection (MOI) of 1:5 for 2 h at 37°C. Extracellular bacteria were aspirated and fresh Macrophage-SFM was added to each well (time = 0h). Splenocytes were infected with *M. tuberculosis* H37Rv at MOI 1:5. At the appropriate time points, supernatants were aspirated, centrifuged at 8,000 × g for 5 minutes, and stored at –80°C until analyzed for CCL5 by ELISA.

Tuberculous pleurisy experiment. *M. tuberculosis* H37Rv was heat-killed by exposure to 80°C water bath for 2 h and resuspended at 5.5×10^7 CFU/ml in sterile, endotoxin-free 0.9% sodium chloride solution (Sigma, St. Louis, MO). Pleurisy was induced 5 wks post-BCG-vaccination by the administration of 1 ml of heat-killed *M. tuberculosis* H37Rv bilaterally into the pleural cavity (day 0) of anesthetized vaccinated guinea pigs. Anesthesia was performed following a previous protocol (154). At daily intervals post-pleurisy induction, guinea pigs were euthanized and fluid in the pleural cavity was aspirated and centrifuged at 200 × g for 15 min to remove inflammatory cells. The fluid was transferred to a new tube and centrifuged at 1400 × g for 20 min and supernatants were stored at –80°C until tested for CCL5 protein by ELISA.

Total RNA isolation and real-time PCR. Total RNA was isolated from adherent and nonadherent cell populations using the RNeasy kit (QIAGEN, Valencia, CA) with the addition of Rnase-free DNase according to the manufacturer's instructions. Reverse transcription was performed on 1-5μg of total RNA using TaqMan Reverse

Transcription Reagents (Applied Biosystems, Foster City, CA). Negative controls were included to ensure PCR amplification of cDNA was not due to contaminating genomic DNA. Real-time PCR analysis was performed on the cDNA using SYBR Green I (Applied Biosystems) following a previously published protocol (*118*). Primer Express software (Applied Biosystems) was used to design the sequences for guinea pig hypoxanthine phosphoribosyltransferase (HPRT) (forward primer, AGGTGTTTATCCCTCATGGACTAATT; reverse primer, CCTCCCATCTCCTTCATCACAT) and guinea pig CCL5 (forward primer, CTGGCCCACTGCTTAGCAAT; reverse primer, CCTTGCTTCTTTGCCTTGAAA). Real-time PCR was performed using the Applied Biosystems 7500 Real-Time PCR System following the manufacturer's instructions. Results were expressed as fold induction of mRNA, which was determined by normalizing CCL5 threshhold cycle (C_t) values against HPRT values. This was further normalized against pooled mRNA of cells obtained from non-vaccinated animals and infected with *M. tuberculosis* at time zero. For pleurisy studies, CCL5 was normalized against HPRT values, and further normalized against C_t values from pleural cells derived from BCG-vaccinated, pleuritis-free (not antigen-injected) animals.

Enzyme-linked immunosorbent assay (ELISA) for guinea pig CCL5 protein. Diluted rabbit polyclonal anti-recombinant guinea pig (rgp)CCL5 in PBS + 0.05% Tween 20 (Sigma, St. Louis, MO) with 1% bovine albumin fraction V (Gemini, Woodland, CA) was added to Reacti-Bind™ Protein A coated plates (Pierce, Rockford, IL) and incubated overnight at 4°C. The following day the antibody solution was

washed four times with PBS + 0.05% Tween 20 (PBST). Recombinant gpCCL5 standards (40 – 1280 pg/ml) and supernatants from cell cultures were diluted in Macrophage-SFM and incubated for 3 h at 37°C. The wells were washed and then incubated with 375 pg/ml of biotinylated (EZ-Link™ Sulfo-NHS-LC-Biotin; Pierce, Rockford, IL) rgpCCL5 for one hour at 37°C. Wells were washed and detection of biotinylated CCL5 was performed by incubating with peroxidase-conjugated streptavidin (150µl/well of 833pg/ml) (Jackson ImmunoResearch Laboratories, Inc., West Grove, PA) for 1 h at 37°C. Plates were washed with PBST with a final wash of 0.1 M sodium acetate (pH 5.5). Colormetric analysis was determined by adding substrate 3, 3', 5, 5' – tetramethylbenzidine (TMB) (150µl/well) (BD Biosciences Pharmingen, San Diego, CA) and incubating in a dark environment for 15 minutes. Color development was stopped with the addition of 10% sulfuric acid, and plates were read on a Dynatech MR5000 automated plate reader (Dyantech Laboratories, Inc., Chantilly, VA) at 450nm. Sample concentrations were derived from the rgpCCL5 standard curve.

Statistical analysis. Analysis of variance was used to determine the significance of main treatment effects (vaccination status) and differences between time intervals within treatment groups. Mean differences between rgpCCL5 mRNA and protein isolated from BCG vaccinated and naive guinea pigs were tested at a 95% confidence interval using the Duncan post hoc analysis. The statistical tests were performed using SAS software (release 8.01; SAS Institute, Inc., Cary, NC).

RESULTS

Development of a gpCCL5 ELISA. We designed an ELISA that could detect gpCCL5 with high sensitivity considering the low physiological levels of CCL5 (pg-ng/ml) previously detected in other animal models (167, 182). The development of an ELISA involved the production of rgpCCL5, which was previously described (184), and polyclonal anti-rgpCCL5. Figure 16A illustrates rgpCCL5 cloned into pET30Xa/LIC vector and induced by 0.1mM IPTG (Fig. 16A, lane 4; uninduced, lane 3). Purified rgpCCL5 was obtained using reverse phase HPLC before and after cleavage with endopeptidase, Factor Xa (Fig. 16A, lane 5). Recombinant human CCL5 was used as a control (Fig. 16A, lane 7). In Figure 16B, the specificity of anti-serum (1:1000 dilution) from a rabbit immunized against gpCCL5 is displayed. It is apparent that the anti-serum binds to mature rgpCCL5 (Fig. 16B, lane 1-3).

Figure 17 illustrates the standard curve for the ELISA assay using a range of two-fold dilutions of rgpCCL5 and the rabbit anti-guinea pig CCL5 serum discussed above. The anti-rgpCCL5 antiserum was bound to a protein A-coated plate. Then biotinylated rgpCCL5 and unlabeled rgpCCL5 were allowed to compete for binding to the Fab portion of IgG on the plate as described in Materials and Methods. This standard curve was used to quantitate gpCCL5 levels in samples. The absence of unlabeled rgpCCL5 (0 pg/ml) resulted in a response greater than two standard deviations below the lowest concentration of rgpCCL5 used on the standard curve (40pg/ml) (data not shown).

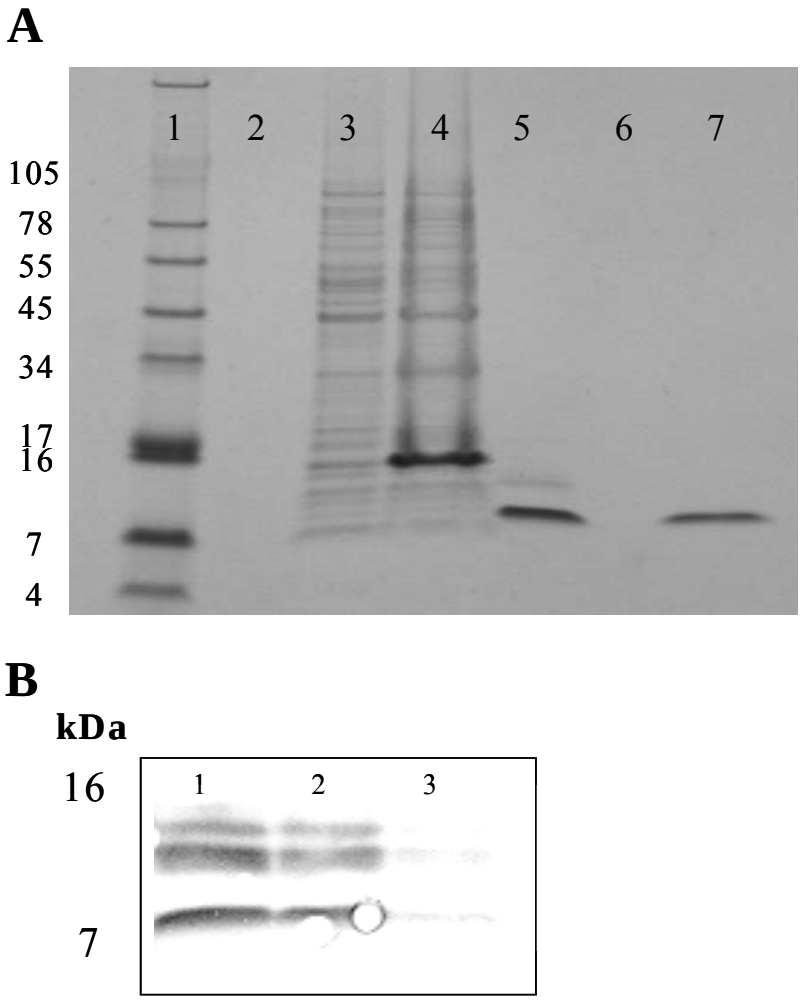

Figure 16: Specificity of rabbit anti-rgpCCL5 serum was tested by Western blot. In Panel A, a SDS-PAGE analysis was performed on the expression and purification of rgpCCL5 and compared to rhCCL5. The mature sequence of gpCCL5 was subcloned into pET30 Xa/LIC and was expressed using 0.1mM IPTG and further purified using reverse phase HPLC. The mature protein was achieved by a blunt cleavage of the 5' tag using Factor Xa leaving only the mature sequence. The mature product was further purified using reverse phase HPLC. Lane 1, low molecular weight ladder, lane 2, empty, lane 3, uninduced total *E. coli* protein, lane 4, cellular proteins from 0.1mM IPTG induction, lane 5, purified mature rgpCCL5, lane 6, empty, and lane 7, rhCCL5. In Panel B, purified rgpCCL5 was then used to immunize rabbits, and anti-serum (1:1000 dilution) was taken three months later. A Western blot was used to detect rgpCCL5 specificity. Lane 1-3, rgpCCL5 at two-fold dilutions.

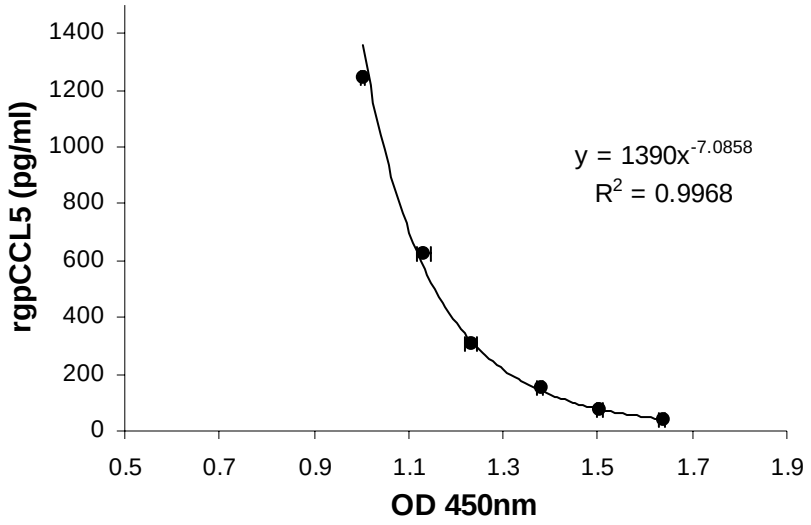

Figure 17: Standard curve for the guinea pig CCL5 ELISA. Protein A coated plates were incubated with rabbit anti-guinea pig CCL5 (same anti-serum as that tested in the western blot in figure one). Unlabelled recombinant CCL5 was used at two-fold dilutions to develop a standard curve. Biotinylated rgpCCL5 was then added to compete with unlabeled CCL5. Horseradish peroxidase was added followed by TMB substrate for 15' in the dark. The data points on the curve represent the average of quadruplicate wells $\pm$ SEM. The equation for the standard curve is depicted above with the R^2 value, which exceeds 0.99. The range of the standard curve is 40-1250pg/ml of CCL5 with 0pg/ml being two standard deviations lower than the 40pg/ml (data not shown).

Effects of BCG vaccination on gpCCL5 mRNA and protein production in resident alveolar macrophages infected with *M. tuberculosis*. Alveolar macrophages from naive and BCG-vaccinated guinea pigs were obtained as indicated above and infected with live virulent *M. tuberculosis* H37Rv (MOI 1:5) for 6, 12, 24, 48, and 72 h. At each time point, supernatants were collected and analyzed for gpCCL5 protein, and mRNA was isolated and analyzed using real-time PCR from cDNA obtained by reverse transcription. Figure 18 shows the difference in CCL5 mRNA and production by *M. tuberculosis*- infected alveolar macrophages obtained from BCG-vaccinated and naive guinea pigs. In Figure 18A, it is evident that infection of alveolar macrophages with virulent *M. tuberculosis* H37Rv stimulated the expression of CCL5 mRNA. This expression is seen immediately following 2 h infection of macrophages from BCG-vaccinated guinea pigs (t = 0 h) and peaks around 24 h. Alveolar macrophages obtained from naive guinea pigs had a delayed CCL5 mRNA response to *M. tuberculosis* with peak expression occurring at 48 h post-infection. Significance was not observed between treatment groups due to the high degree of variability. In Figure 18B, secretion of CCL5 protein was observed at levels ~ 100-200pg/ml as early as 12 h post-infection from both naive and BCG-vaccinated guinea pigs. Supernatants of alveolar macrophages obtained from BCG-vaccinated animals contained significantly higher levels ($p < 0.05$) of CCL5 protein at 72 h. It was also apparent that at 72 h post-infection, alveolar macrophages obtained from BCG-vaccinated guinea pigs secreted significantly elevated levels ($p < 0.05$) of CCL5 compared to all other time intervals observed within the same treatment group. In contrast, macrophages obtained from

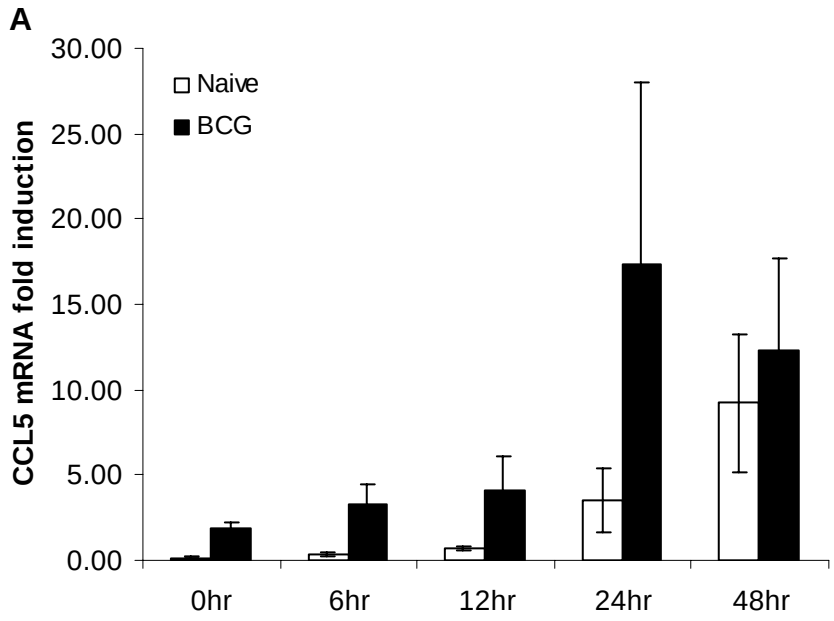

Figure 18: CCL5 mRNA and protein production is enhanced in alveolar macrophages isolated from BCG-vaccinated compared to naive guinea pigs. Alveolar macrophages from naive (white bars) and BCG-vaccinated (black bars) animals were isolated and infected with *M. tuberculosis* H37Rv (MOI 1:5) for 0, 6, 12, 24, 48, and 72 h. At each time point, total RNA was isolated from the macrophages and supernatants were aspirated and analyzed by ELISA. Panel A: Results were expressed as fold induction of mRNA, which was determined by normalizing CCL5 threshold cycle (C_t) values against HPRT values. This was further normalized against pooled mRNA from naive cells infected with *M. tuberculosis* at zero hours. Panel B: Supernatants from infected macrophages were analyzed for guinea pig CCL5 using ELISA. Data represent mean $\pm$ SEM of 3-4 experiments. An asterisk represents significance ($p < 0.05$) from all time points within a treatment group. A double asterisk represents significance ($p < 0.05$) between alveolar macrophages from naive and BCG-vaccinated animals at similar time points. ANOVA was used to analyze significance between groups.

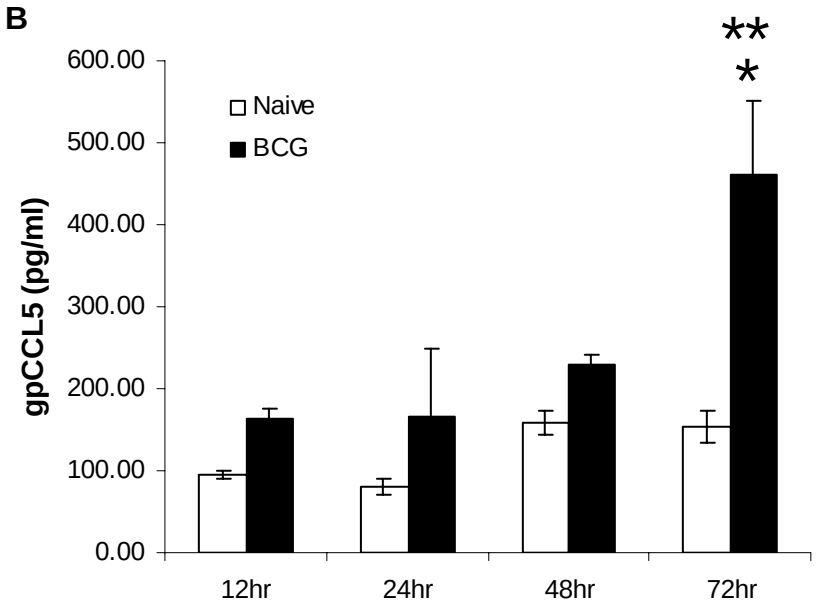

Figure 18 continued.

naive animals displayed no significant difference in CCL5 secretion over time in culture.

Effects of BCG vaccination on CCL5 mRNA and protein production in resident peritoneal macrophages infected with *M. tuberculosis.* Figure 19 illustrates the effects of BCG vaccination on CCL5 mRNA expression and protein secretion in resident peritoneal macrophages infected with virulent mycobacteria. In Figure 19A, peritoneal macrophages obtained from BCG-vaccinated guinea pigs exhibited similar results to alveolar macrophages immediately after infection (t = 0 h, 2 h post-infection) with heightened CCL5 mRNA levels, though not significant. There was no significant difference in CCL5 mRNA expression between uninfected macrophages from naive or BCG-vaccinated animals. However, as early as 6 h post-infection, peritoneal macrophages obtained from BCG-vaccinated animals displayed significantly ($p < 0.05$) elevated levels of CCL5 mRNA compared to cells obtained from naive animals. Levels of CCL5 mRNA steadily increased throughout the 48 h of infection in the BCG-vaccinated peritoneal macrophages. This contrasted with the relatively low levels of CCL5 mRNA observed in peritoneal macrophages obtained from naive animals throughout the infection. Secreted CCL5 protein from *M. tuberculosis* H37Rv-infected peritoneal macrophages (Fig. 19B) correlated with patterns seen at the transcriptional level. Infected macrophages obtained from naive guinea pigs never reached CCL5 protein levels higher than 350pg/ml, while CCL5 was secreted at significantly higher levels in resident peritoneal macrophages obtained from BCG-vaccinated at 48 and 72 h. At these time intervals post-infection, secreted CCL5 was significantly elevated ($p < 0.05$) compared to levels at 12 and 24h within the BCG-vaccinated group.

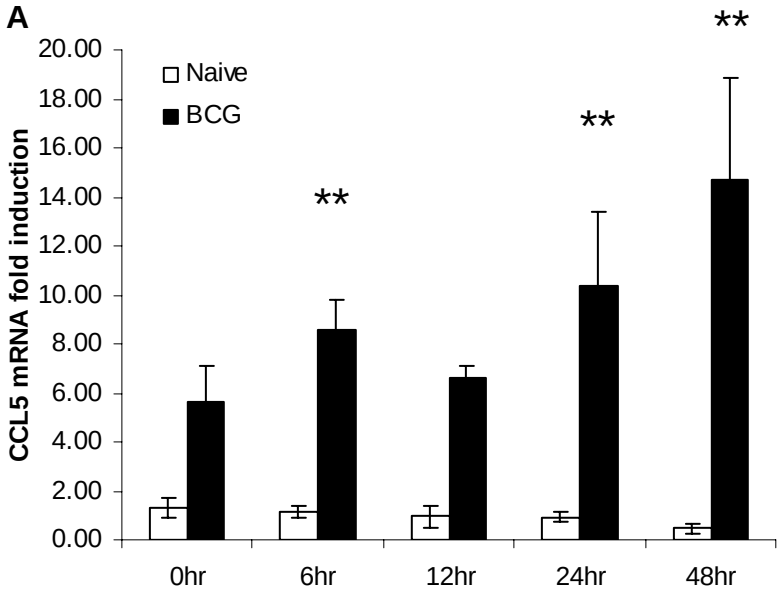

Figure 19: BCG-vaccination affects CCL5 mRNA and protein levels in guinea pig resident peritoneal macrophages. Resident peritoneal macrophages were isolated from naive (white bars) and BCG-vaccinated (black bars) guinea pigs and infected with *M. tuberculosis* H37Rv (MOI 1:5). At different time points (0, 6, 12, 24, 48, and 72 h), supernatants were collected and RNA was isolated from infected macrophages. The RNA was reverse transcribed into cDNA and real time PCR using SYBR Green was performed. Panel A: Results were expressed as fold induction of mRNA, which was determined by normalizing CCL5 threshold cycle (C_t) values against HPRT values. This was further normalized against pooled mRNA from naive cells infected with *M. tuberculosis* at zero hours. Panel B: Supernatants from infected macrophages were analyzed for guinea pig CCL5 using ELISA. Results are representative of the mean $\pm$ SEM of 4-5 separate experiments. Significant ($p < 0.05$) production of CCL5 protein from 12 and 24 h within treatment groups is denoted by an asterisk. Significance ($p < 0.05$) between naive and BCG-vaccinated at similar time points is depicted by a double asterisk. Significance was determined using ANOVA.

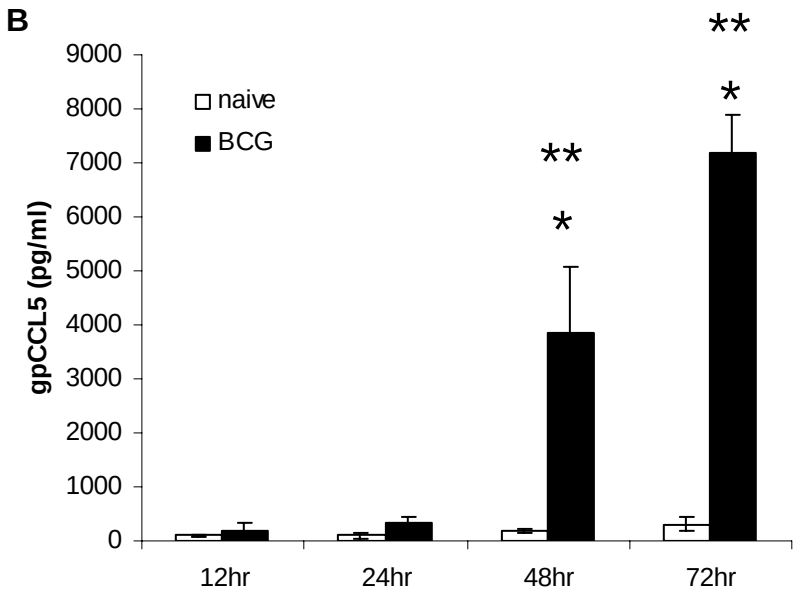

Figure 19 continued.

Effects of BCG vaccination on CCL5 mRNA and protein production in splenocytes infected with *M. tuberculosis*. Figure 20 illustrates the effect BCG-vaccination on CCL5 mRNA expression and protein secretion in infected splenocytes. In Figure 20A, a significant difference ($p < 0.05$) was demonstrated between CCL5 mRNA in uninfected splenocytes obtained directly from naive and BCG-vaccinated guinea pigs (time point = 0 h). In contrast to infected macrophages, CCL5 mRNA was significantly enhanced ($p < 0.05$) in *M. tuberculosis* infected splenocytes from naive guinea pigs at 12 and 24 h compared with time zero. Splenocytes from BCG-vaccinated animals exhibited a similar kinetic pattern with a significant enhancement ($p < 0.05$) of CCL5 mRNA at 24 h compared to zero hours. Surprisingly, these fold induction levels in CCL5 mRNA were approximately half the values of infected macrophages. It was also evident that CCL5 mRNA was significantly elevated ($p < 0.05$) at 24 h in *M. tuberculosis*-infected splenocytes obtained from BCG-vaccinated compared to naive guinea pigs. In Figure 20B, the secretion of CCL5 protein from infected splenocytes displayed novel kinetics. As early as 6 h post-infection, a measurable quantity of CCL5 protein (~ 1000 pg/ml) was detected. However, at this time point there was no difference between splenocytes obtained from BCG-vaccinated and naive guinea pigs. As the infection progressed, splenocytes from naive guinea pigs maintained the same levels of CCL5 protein as those observed at 6 h. In contrast, splenocytes from vaccinated animals displayed CCL5 kinetics similar to resident macrophage populations reaching significantly enhanced levels of CCL5 at 24, 48, and 72 h compared to 6 h after infection ($p < 0.05$). Additionally, significant differences between secreted CCL5 in

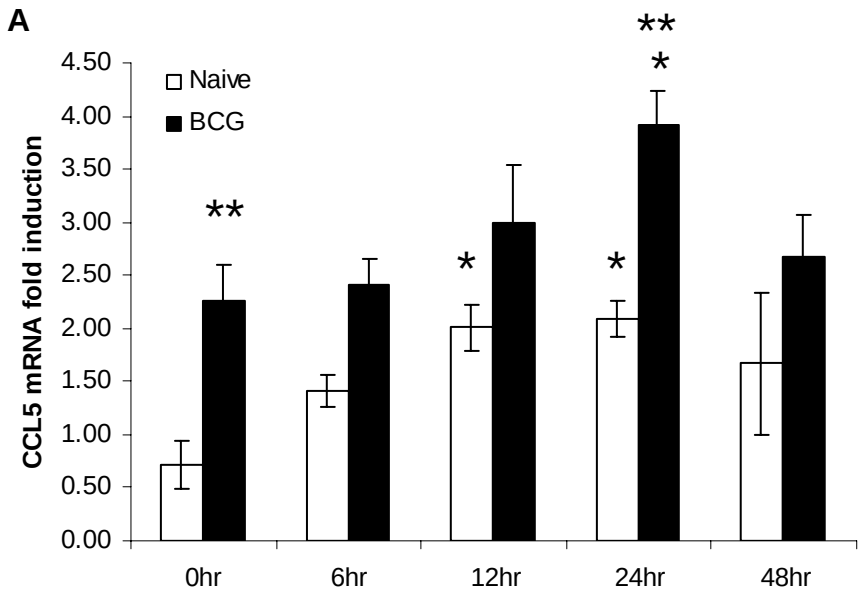

Figure 20: Vaccination with BCG affects CCL5 mRNA expression and protein production from splenocytes infected with *M. tuberculosis.* Splenocytes were obtained from naive (clear bars) and BCG-vaccinated (black bars) guinea pigs and infected with *M. tuberculosis* H37Rv (MOI 1:5) for various times (0, 6, 12, 24, 48, and 72 h). At each time point, total RNA was collected, reverse transcribed into cDNA, and real time PCR using SYBR Green was performed. Panel A: results were expressed as fold induction of mRNA, which was determined by normalizing CCL5 threshold cycle (C_t) values against HPRT values. This was further normalized against pooled mRNA from naive cells infected with *M. tuberculosis* at zero hours. Panel B: supernatants were collected from each sample and analyzed by ELISA to detect CCL5 protein levels. . Data represent mean $\pm$ SEM of 3-4 experiments. An asterisk represents significance ($p < 0.05$) between gpCCL5 values from the first time point displayed within treatment groups. A double asterisk represents significance ($p < 0.05$) between splenocytes from naive and BCG-vaccinated animals at similar time points. ANOVA was used to analyze significance between groups.

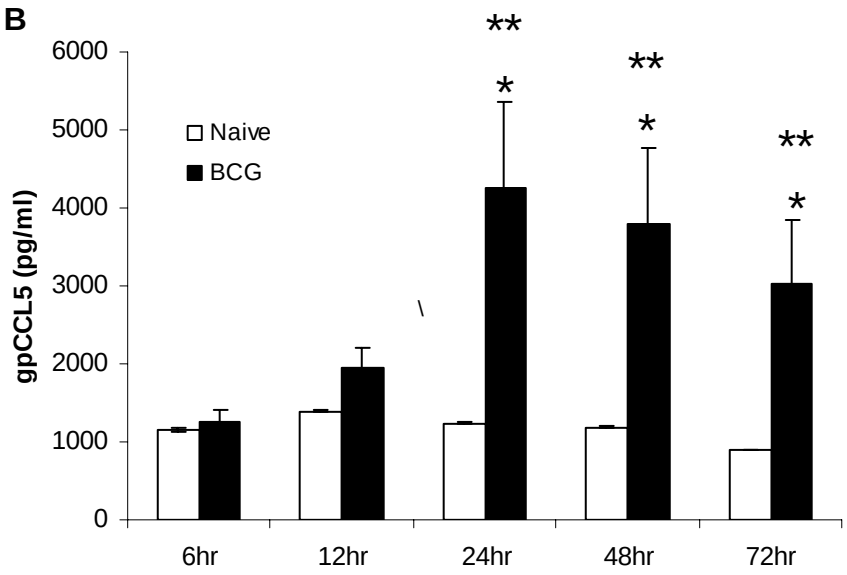

Figure 20 continued.

splenocytes obtained from naive and vaccinated guinea pigs were apparent after infecting the cells for 24, 48, and 72 h with *M. tuberculosis* H37Rv (MOI 1:5).

CCL5 mRNA expression and protein production during tuberculous pleurisy in the guinea pig. A model of tuberculous pleurisy has been well established in the guinea pig model (7, 8) and provides a method to assess the development of a mycobacterial-specific inflammatory response in BCG-vaccinated guinea pigs. A previous study showed peak levels of fluid accumulation in the pleural space at day 5 following intrapleural injections of killed mycobacteria (8). In Figure 21, pleural samples from days 1-5 were further analyzed for CCL5 mRNA expression in pleural exudate cells and secreted CCL5 protein in the pleural fluid. As shown in Figure 21A, significant levels ($p < 0.05$) of CCL5 mRNA were seen at days 3 and 4, with peak induction levels on day 4 expressing 100-fold greater levels than resident pleural cells obtained from BCG-vaccinated pleuritis-free (i.e., not injected with heat-killed *M. tuberculosis*) animals. Figure 21B demonstrates a similar trend with CCL5 protein in pleural fluid. Secreted protein peaked at days 3 and 4, reaching concentrations ~ 50,000 pg/ml. These CCL5 protein levels were greater than 6 – fold from all *in vitro M. tuberculosis*-infected leukocytes.

DISCUSSION

In this paper, data are presented which advance our understanding of the protective role of vaccination with *M. bovis* BCG in a highly relevant guinea pig model.

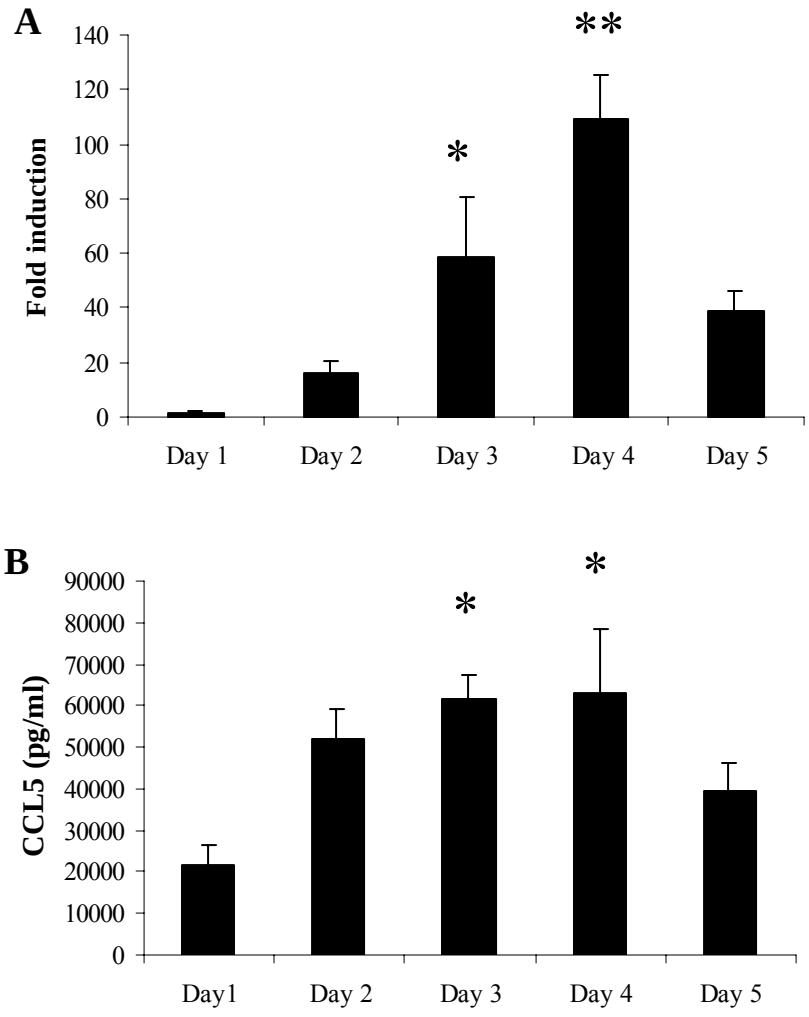

Figure 21: A kinetic study of CCL5 mRNA expression and protein production *in vivo* from guinea pigs following induction of tuberculous pleurisy. BCG-vaccinated guinea pigs were injected with heat killed *M. tuberculosis* H37Rv 5 wks post-vaccination and fluid in the pleural space was aspirated at daily intervals. Panel (A) total RNA was collected from pleural exudate cells, reverse transcribed to cDNA, and real-time PCR using SYBR Green was performed. Fold induction levels were derived from normalizing the CCL5 C_t values against HPRT values, and further normalizing against values derived from resident pleural cells obtained from BCG-vaccinated pleuritic-free animals. Panel B: CCL5 protein levels were measured in pleural fluids by ELISA. Data are representative of the mean $\pm$ SEM of 3-4 separate animals. An asterisk represents significance ($p < 0.05$) from day one. A double asterisk represents significance ($p < 0.05$) above all days. Significance was determined using ANOVA.

We examined the CCL5 response *in vitro* to *M. tuberculosis* infection in three distinct leukocyte populations from BCG-vaccinated and naïve guinea pigs, and *in vivo* during tuberculous pleurisy. For the first time, an ELISA assay was developed and used to quantify secreted guinea pig CCL5 protein production by infected macrophages.

We show that alveolar macrophages infected with *M. tuberculosis* have an enhanced expression of CCL5 mRNA regardless of vaccination status (fig. 18A). These results are similar to previous work in our lab, which demonstrated minimal effects of prior vaccination on expression of another CC chemokine, CCL2 (MCP-1), at the mRNA level in H37Rv-infected alveolar macrophages isolated from BCG-immunized and non-immunized guinea pigs (*118*). At the protein level, CCL5 was significantly elevated in alveolar macrophages harvested from BCG-immunized guinea pigs compared to non-immunized animals at 72 h post-*M. tuberculosis* infection (fig. 18B). This trend seems to replicate a previous study displaying enhanced levels of CXCL8, a member of the alpha (CXC) chemokine family, in alveolar macrophages harvested from BCG-vaccinated compared to naïve guinea pigs and infected with *M. tuberculosis* (*118*). The levels of CCL5 protein in our study were similar to CCL5 levels present in *M. tuberculosis* H37Ra-infected human alveolar macrophages *in vitro* at 72 h in one study (167). However, in another study, CCL5 protein exhibited 10-fold higher levels in supernatants from H37Ra- and H37Rv-infected human alveolar macrophages (174). One explanation for the discrepancy in this last experiment is that the MOI used was 100-fold higher, suggesting that a large bacterial load may be needed to elicit higher (ng/ml) levels of CCL5 protein from alveolar macrophages. The absence of published

murine and rabbit studies analyzing CCL5 production from alveolar macrophages infected with *M. tuberculosis* prevents us from making a more complete comparative analysis.

Resident peritoneal macrophages were infected with *M. tuberculosis* to compare their CCL5 response to that of alveolar macrophages. Resident peritoneal macrophages harvested from BCG-vaccinated guinea pigs had elevated levels of CCL5 mRNA in response to virulent infection, whereas CCL5 mRNA levels in macrophages isolated from naive animals were unaffected by *M. tuberculosis* infection. In this cell type, CCL5 mRNA was immediately enhanced, though not significantly, at 2 h post-incubation (0 h) with *M. tuberculosis* and followed a kinetic pattern peaking at 48 h post-infection. Significant differences between peritoneal macrophages harvested from BCG-vaccinated and naive guinea pigs were apparent as early as 6 h, and continued through 48 h post-infection (fig. 19A). These observations are similar to previous research done in our laboratory analyzing thioglycollate-induced peritoneal macrophages infected with *M. tuberculosis* (85). These earlier studies demonstrated a significant up-regulation of CCL5 mRNA in infected peritoneal exudate macrophages harvested from BCG-vaccinated guinea pigs compared to naïve animals, and confirmed the absence of a response by infected macrophages from naive animals. Guinea pig CCL5 protein production by *M. tuberculosis*-infected resident peritoneal macrophages from BCG-vaccinated animals exhibited similar kinetics to mRNA levels, with concentrations reaching significant differences at 48 and 72 h (fig. 19B). The absolute levels of CCL5 protein were substantially higher by more than 10-fold in resident peritoneal

macrophages isolated from BCG-vaccinated guinea pigs compared to alveolar macrophages.

The contribution of antigen-sensitized lymphocytes derived from *M. bovis* BCG vaccination was analyzed by measuring the expression of CCL5 in *M. tuberculosis*-infected splenocytes. This mixed cell population has been characterized previously when we reported a significant elevation of TNFα protein production in splenocytes obtained from BCG-vaccinated versus naive guinea pigs (106). In this study we demonstrate significant enhancement in CCL5 mRNA expression in uninfected (time = 0 h) splenocytes harvested from BCG-vaccinated guinea pigs compared to naive animals (Figure 20A). These results are similar to previous findings of increased CCL5 mRNA in $CD8^+$ T cells from lymph nodes in guinea pigs (98), and agree with previous data showing increased levels of CCL5 mRNA expression in murine memory T lymphocytes (191, 204). Significant differences in CCL5 mRNA levels between naive and vaccinated infected splenocytes were observed at 24 h (fig. 20A), but the levels of fold induction were drastically reduced compared to infected macrophages (fig. 18A and 19A). However, CCL5 protein production (~1000 pg/ml) appeared as early as 6 h post-infection in both splenocyte groups (fig. 20B) suggesting constitutive production of CCL5, which was independent of vaccination status. After day one, infected splenocytes from BCG-vaccinated animals displayed enhanced levels of secreted CCL5 protein whereas naive splenocytes produced relatively constant levels throughout the culture period. Rapid CCL5 secretion may be due to the presence of T lymphocytes, especially memory $CD8^+$ T cells. This theory is supported by findings that CCL5 is stored in

unique secretory compartments in memory and effector human $CD8^+$ T cells (30). Granules containing CCL5 in humans during chronic gastritis were seen more often in $CD8^+$ T cells than in $CD4^+$ T cells (143). It has also been shown by Dorner et al. that a greater percentage of murine $CD8^+$ T cells produce CCL5 compared to $CD4^+$ T cells on a single cell basis (55). Future studies will identify the precise cellular types responsible for the production of CCL5 in the spleens of guinea pigs.

A model of tuberculous pleurisy in the guinea pig was developed in our laboratory to study the cells and cytokines involved in the development of a mycobacterial-specific inflammatory exudate in a previously vaccinated animal (8, 154). Pleural tuberculosis is the most common extrapulmonary manifestation of tuberculosis in humans (138) and generally resolves without therapy (164) suggesting that the immune response in the pleural space is sufficient. In the present study, we have shown a significant increase in CCL5 mRNA expression from the pleural exudate cells (fig. 21A) and in secreted CCL5 protein in the pleural fluid (fig. 21B) of BCG-vaccinated guinea pigs following induction of tuberculous pleurisy. CCL5 mRNA levels were elevated from day one following induction during infection compared to uninduced resident pleural cells, and peaked on day 4. Similarly, Fine, et al. saw increased CCL5 mRNA peaking at 72 h and heightened levels of CCL5 protein throughout the experiment when they induced pleurisy in mice with methylated BSA, complete Freund's adjuvant, and *M. tuberculosi*s dried cell walls (60). CCL5 protein production peaked at 24 h in their experiment, which coincided with increased numbers of T lymphocytes and macrophages from 24 to 48 h. Due to the absence of time intervals

past 72 h, it is difficult to compare their results with ours. However, their peak levels of CCL5 mRNA correlated with our significantly enhanced levels at 72 h. The high production of CCL5 in the pleural inflammatory response could reflect the activity of numerous leukocyte and non-leukocyte populations. The primary cells involved in delayed-type hypersensitivity reactions include T lymphocytes and macrophages, which are both producers of CCL5 and chemotactic to CCL5. Recently it has been demonstrated that normal pleural mesothelial cells can express and secrete CCL5 in the presence of TNFα, and this effect is synergistically enhanced with IFNγ (92). This synergistic effect could have resulted in enhanced CCL5 mRNA stability suggesting an explanation for the prolonged elevated levels of CCL5 mRNA throughout the five days in our studies. It has also been shown that TNFα and IFNγ can induce CCL5 secretion in human endothelial cells (122) and lung fibroblasts (195). Since previous studies have demonstrated an induction of TNFα and IFNγ during tuberculosis pleurisy in humans and guinea pigs (8, 18, 19), it is reasonable to expect high levels of CCL5 throughout the inflammatory process, which is precisely what we observed (Figure 21B). The continued presence of CCL5 in tuberculous pleurisy may be beneficial for the development of delayed-type hypersensitivity reaction due to its ability to attract monocytes/macrophages and T lymphocytes (142, 175), especially of the Th1 phenotype (209). Chensue et al. have demonstrated the importance of CCL5 by neutralizing it with anti-CCL5, thus resulting in a diminished PPD-granuloma size in mice (35). At higher concentrations, CCL5 has been shown to activate T lymphocytes and induce proliferation in a mitogen-like manner (11, 14), as well as acting like an adjuvant to

induce proliferation of memory T lymphocytes (95). Future studies will be focused on dissecting the role of CCL5 in tuberculous pleurisy by neutralizing its effects *in vivo* and analyzing granuloma formation and leukocyte influx.

In summary, we know from previous studies that BCG provides solid protection against *M. tuberculosis* infections in the guinea pig (185, 186). Here we demonstrate enhanced expression and production of CCL5 in response to *in vitro M. tuberculosis* infection in three distinct leukocyte populations obtained from an antigen-induced inflammatory exudate in BCG-vaccinated guinea pigs compared to naive animals. Similarly, we observed elevated CCL5 protein and mRNA levels in the immune response against *M. tuberculosis* antigens as it progressed in pleuritic guinea pigs. Taken together, these results suggest that CCL5 is important in eliciting rapid effective immune responses against *M. tuberculosis.*

CHAPTER VI

THE ROLE OF CCL5 DURING TUBERCULOUS PLEURISY IN THE GUINEA PIG MODEL

INTRODUCTION

Tuberculous pleurisy remains one of the leading extrapulmonary manifestations of tuberculosis infections (3, 180). The development of the HIV/AIDS pandemic has resulted in an increase number of tuberculosis cases and, in some studies, increased cases of tuberculous pleurisy (67, 75). It is believed that this extrapulmonary disease usually arises as a result of a rupture of a tubercle in the subpleura from the primary infection leading to spewing of caseous discharge into the pleural space. This occurs in patients recently sensitized to mycobacterial antigens, resulting in a prompt, localized cell-mediated immune response in the pleural space and the appearance of acute symptoms (57). Untreated patients with tuberculous pleurisy usually resolve the infection within a month, suggesting that this is a self-limiting form of tuberculosis (57, 109) and that the intrapleural immune response is protective. Therefore, this localized, antigen-specific inflammatory response might provide a useful approach to understanding the role of a particular cytokine/chemokine during a protective immune response elicited against *M. tuberculosis.*

Previous studies have attempted to elucidate the cytokines/chemokines involved during this extrapulmonary tuberculous manifestation. In the concentrated pleural fluid (183) which accumulates throughout the course of tuberculous pleurisy, neutrophils

predominate during the early phase of disease with primarily lymphocytes in late effusions (109). IFNγ, TNFα, IL-1β, and TGFβ have been found in tuberculous pleural fluid, pleural macrophages, and/or mesothelial cells (18, 60, 83, 100, 183) in response to *M. tuberculosis*. Previous studies have also demonstrated a plethora of chemokines, including CXCL-8, CCL5, and CCL2, in association with tuberculous pleurisy (60, 92, 135, 149).

Chemokines partake in various biological activities, including chemotaxis of T lymphocytes (166, 175), macrophages (27), and neutrophils (119), $CD4^+$ T lymphocyte differentiation (217), enhancing T lymphocyte proliferation and IFNγ production (193), activating leukocyte reactive oxygen intermediates (36, 170), and granuloma formation (35, 48). These activities suggest an important role of these molecules during the delayed-type hypersensitivity reaction elicited in response to *M. tuberculosis.*

A guinea pig model of tuberculous pleurisy has been developed previously (154). In this study, the role of CCL5 was examined during tuberculous pleurisy in the guinea pig. The effect of altering CCL5 function by intrapleural injection of rgpCCL5 and anti-rgpCCL5 on the migration of leukocyte populations, cytokine/chemokine mRNA levels in pleural cells and within granulomas, and the histological nature of granulomas was examined. Together, these data contribute to our understanding of the role of CCL5 in the development and expression of a protective intrapleural immune response.

MATERIALS AND METHODS

Purified anti-rgpCCL5 IgG preparation. HiTrap™ Protein A HP (Amersham Biosciences, Uppsala, Sweden) columns were used to isolate rabbit anti-rgpCCL5 IgG from antiserum following the manufacturer's instructions. Isolated IgG samples were verified on SDS-PAGE gels under reducing and native conditions. Reducing conditions resulted in the presence of two bands, heavy (50kDa) and light (25kDa) chains, with one band (150kDa) present under native conditions. After verification of the isolation of IgG, the antibodies were passed through PD-10 desalting columns (Amersham Biosciences) and tested for neutralization properties via chemotaxis assays.

Animals and vaccination. Specific-pathogen-free, outbred, male and female Hartley guinea pigs from Charles River Breeding Laboratories, Inc. (Wilmington, MA) were housed in polycarbonate cages within an air-filtered environment under a 12 h light-dark cycle. Food (Ralston Purina, St. Louis, MO) and tap water were supplied to the animals ad libitum. Five-week old guinea pigs were vaccinated via intradermal injection of 0.1ml (10^3 CFU) of viable *Mycobacterium bovis* BCG (Danish 1331 strain, Statens Seruminstitut, Copenhagen, DK) into the left inguinal region. All procedures were reviewed and approved by the Texas A&M University Laboratory Animal Care Committee.

Mycobacterial preparations and pleurisy induction. *M. tuberculosis* H37Rv (ATCC 27294; American Type Culture Collection, Manassas, VA) and H37Ra (ATCC 25177) suspensions stored at –80°C were rapidly thawed, vortexed, and sonicated for 60s with an Ultrasonics sonicator (Heat Systems-Ultrasonics, Inc., Plainview, NY) at an

output setting of 8.0 to disperse clumps. Bacteria were heat-killed by incubation at 80°C for 2 h and resuspended in sterile, endotoxin free 0.9% sodium chloride solution (Sigma, St. Louis, MO) at a concentration of 2×10^7 CFU/ml. Five weeks after BCG-vaccination, guinea pigs were anesthetized by an intramuscular injection in the hind leg with 9-15mg/kg of ketamine and 0.75-1.25mg/kg of xylazine, and injected bilaterally into the pleural space with 1ml heat-killed *M. tuberculosis* in combination with either 0.9% sodium chloride solution, rgpCCL5 (6.7μg/side), rabbit IgG control (300μg/side) (ICN Pharmaceuticals, Inc., Aurora, OH), or rabbit anti-rgpCCL5 (300μg/side) following a previous protocol (154).

Necropsy and pleural cell isolation. Guinea pigs were anesthetized daily with the ketamine/xylazine mixture and 5 animals per group were given bilateral injections of 150μl of sterile PBS, rgpCCL5 (6.7μg /side), rabbit IgG control (300μg/side), or rabbit anti-rgpCCL5 (300μg/side). Four guinea pigs were not anesthetized after day 0 and were used as controls for the effect of daily anesthesia on the progression of tuberculosis pleurisy. At day 4, all guinea pigs were euthanized with an intraperitoneal overdose injection of sodium pentobarbital (100mg/ml) (Sleepaway Euthanasia Solution; Fort Dodge Laboratories, Inc., Fort Dodge, IA). The abdominal cavity was opened aseptically and fluid was collected from the pleural cavity by making a small incision in the top of the diaphragm and aspirating fluid with a syringe and 26gauge1 needle. After the majority of fluid was obtained the diaphragm was cut further until exposing the whole pleural cavity and any residual fluid was further aspirated. At this time, the severity of disease was scored according to the presence of granulomas as described in

Table 1. The groups receiving rabbit anti-rgpCCL5, rabbit IgG, and the control (with no anesthesia) had the pleural cavity washed with 10ml of PBS after the initial pleural fluid was collected. The pleural exudate was centrifuged at 200 × g for 15 min, and the fluid was transferred to a 15ml conical tube and centrifuged at 1,400 × g for 20 min to remove any remaining cells and stored at –80°C. Erythrocytes were lysed in the pleural cells using ACK lysis buffer (0.14M NH_4Cl, 1.0mM $KHCO_3$, 0.1mM Na_2EDTA [pH 7.2 – 7.4]) and washed twice with PBS. Pleural cells were then resuspended in 1ml of RPMI 1640 complete medium and enumerated on a hemacytometer by the trypan blue exclusion method (Gibco Life Technologies, Grand Island, NY).

Splenocyte preparation and T lymphocyte isolation. Spleens were removed and placed in RPMI-1640 medium supplemented with 10% FBS, 10μM 2-mercaptoethanol, and 2μM L-glutamine (RPMI complete medium (C-RPMI)). Spleens were homogenized and erythrocytes were lysed with ACK lysis buffer. Splenocytes were washed twice with PBS and resuspended in 2 ml of C-RPMI. T lymphocytes were further isolated by incubating the cells on a nylon wool column for 1 h at 37°C with 5% CO_2 following manufacturer's instructions (Polysciences Inc., Warrington, PA). The nonadherent cells were collected as the column was washed with 50ml of warm C-RPMI. Cells were centrifuged at 200 ×g for 10 min, followed by a PBS wash, and resuspended in RPMI + 0.1% bovine serum albumin (RPMI-BSA) at 5×10^6 cells/ml.

T lymphocyte chemotaxis. Chemotaxis was performed using ChemoTx (Neuroprobe, Inc., Gaithersburg, MD) disposable chemotaxis systems containing 5μm pore size polycarbonate filters, following modified instructions from the manufacturer.

Dilutions of rgpCCL5 and anti-rgpCCL5 were made in RPMI-BSA. Solutions containing anti-rgpCCL5 and rgpCCL5 were incubated for 30 min at 37°C preceding the addition of 300µl/well in a 96-well plate. The polycarbonate filter was then placed on the plate and checked to ensure that the fluid in each well was in contact with the filter. The cells were then added to the top of the filter in a 50µl volume containing 2.5×10^5 cells/well. Chemotaxis was performed at 37°C in 5% CO_2 for 2 h. The fluid on top of the filter was aspirated and cotton swabs were used to wipe off any cells remaining on the top of the filters. Plates were centrifuged for 430 × g for 10 minutes to dislodge any remaining cells bound to the underside of the filter. The filter plate was removed and 150ul aspirated from each well. A tetrazolium salt, 3-(4,5-dimethylthiazolyl-2)-2,5-diphenyltetrazolium bromide (MTT) (Sigma), was added at 5mg/ml to each well and allowed to incubate for 2 h at 37°C in 5% CO_2. Plates were centrifuged at 140 × g for 5 min and supernatants were aspirated. Warm lysis buffer (50% 2-2 Dimethylformamide and 20% SDS at pH 4.7) was added to each well and allowed to incubate for 4 h at 37°C and 5% CO_2. This colorimetric assay was then read at 570nm using a Dynatech MR5000 automated plate reader and analyzed with Biolinx Software, version 2.1 (Dynatech Laboratories, Inc., Chantilly, VA).

Flow cytometry. Pleural exudate cells were examined for cell surface expression of CD3, CD4, CD8, and MHC class II by flow cytometry as previously described (86). Briefly, 7.5×10^5 cells were blocked with normal goat IgG (1 mg/ml; Sigma) for 10 minutes, then washed with HBSS containing 10% FBS and stained with mouse anti-guinea pig CD3 (1:500), with mouse anti-guinea pig CD4 (1:500), with

mouse anti-guinea pig CD8 (1:1000), or with mouse anti-guinea pig MHC II (1:10; all from Serotec, Raleigh, NC) for 1 h on ice while shaking. Cells were washed 3 times in HBSS containing 10% FBS. The pellet was resuspended in FITC-conjugated AffiniPure goat anti-mouse IgG (1:50; Jackson ImmunoResearch Laboratories, Inc., West Grove, PA), and incubated for 1 h on ice while shaking. The cells were washed 2 times in HBSS containing 10% FBS, and resuspended in 300 μl HBSS containing 1% paraformaldehyde. The proportions of positive cells were determined with a FACSCalibur flow cytometer and Cell Quest software (Becton Dickinson, San Jose, CA). Controls included unstained and secondary antibody only stained cells, and the positive population was set such that less than 2% of the negative control was positive for green fluorescence.

Cellular differentiation. Pleural cells were resuspended at 2 x 10^6 cells/ml and 80μl of cells were centrifuged onto silanated glass slides (CSA-100; PGC Scientifics, Gaithersburg, MD) at 140 × g for 5 min (Cytospin 2; Shandon Southern Instrument, Inc., Sewickley, PA). Diff-Quik (Dade Behring Inc., Newark, DE) stains were performed on the cells and 600 cells/slide were analyzed using light microscopy to determine the relative proportions of different leukocyte populations. Dr. Karen Russell from Texas A&M University Department of Veterinary Pathobiology performed all of the differential counts without knowledge of the treatment groups associated with the studies.

Lymphoproliferation. Pleural cells were incubated in a 100μl volume (2×10^6 cells/ml) in 96-well plates at 37°C with 5% CO_2 with or without PPD (12.5 or 25 μg/ml)

for 96 h. [H^3] thymidine was added at 1 μCi/well for the final 6 h of incubation. Spontaneous proliferation was determined by plating the cells immediately (*ex vivo)* with [H^3] thymidine for 6 h. Pleural cells were harvested onto glass fiber filters, and proliferation was determined by the number of counts per minute with a liquid scintillation counter (LS8000; Beckman Instruments, Inc., Fullerton, CA). Data are presented as the mean cpm from each group for spontaneous proliferation and mean delta (PPD-stimulated cpm – unstimulated cpm) cpm for antigen-specific proliferation.

RNA isolation and real-time PCR on cytokine mRNA. RNA from pleural cells was obtained by centrifuging 5 x 10^5 cells, aspirating the supernatant, and lysing the cells with Buffer RLT (QIAGEN, Valencia, CA). Total RNA was isolated using the RNeasy kit (QIAGEN) with the addition of Rnase-free DNase (QIAGEN) according to the manufacturer's instructions. Granulomas from the pleural cavity were obtained and placed in ≥ 5 volumes of RNAlater (Ambion, Austin, TX) and stored at 4°. The PowerGen 125 PCR tissue homogenizing kit (Fischer Scientific, Pittsburgh, PA) was used to homogenize the granulomas. Total RNA from homogenates was isolated using RNeasy kit (QIAGEN). Reverse transcription was performed on total RNA using TaqMan Reverse Transcription Reagents (Applied Biosystems, Foster City, CA). Negative controls were performed to ensure PCR amplification of cDNA was not due to contaminating genomic DNA. Real-time PCR analysis was performed on the cDNA using SYBR Green I (Applied Biosystems) following a previously published protocol (*118*). Primer Express software (Applied Biosystems) was used to design primer sequences (see Table 2). The sequences for TNFα, CXCL8, and CCL2 primers were

previously described (8, *118*). Real-time PCR was performed using the Applied Biosystems Prism 7500 sequence detector following the manufacturer's instructions. Results were expressed as fold induction levels of mRNA, which was determined by normalizing cytokine/chemokine threshold cycle (C_t) values against HPRT values. This was further normalized against C_t values from pleural cells isolated from pleurisy-free (not given *M. tuberculosis* antigens) BCG-vaccinated guinea pigs.

Histopathology. Granulomas from the pleural cavity of pleuritic guinea pigs were obtained and fixed in 10% buffered formalin. Tissues were embedded in paraffin, sectioned at 5μm, and stained with hematoxylin and eosin (H & E) for histopathological examination and Ziehl-Neelsen staining to determine bacterial burdens within the granulomas. All tissue sections were scored based on their overall inflammatory severity/presence of cells or bacteria according to Table 4. The grading was performed by Dr. John Mackie, Veterinary Pathologist from Idexx Laboratories (Australia) without knowledge of the treatment group from which the samples were obtained.

Statistical analysis. For the chemotaxis assay, analysis of variance followed by Duncan's post hoc analysis was used to determine the statistical significance between rgpCCL5 concentrations. In the pleurisy studies, the same tests were used to compare the statistical significance of differences between guinea pigs treated with saline, rgpCCL5, IgG control, anti-rgpCCL5, or control without daily anesthesia for cytokine/chemokine mRNA expression levels. A two-tailed Student's t-test was used to determine statistical significance of differences between the rgpCCL5 versus saline groups, the anti-rgpCCL5 versus IgG control groups, and the saline versus control

groups (no anesthesia after day 0). All differences were considered significant at a 95% confidence interval. The statistical tests were performed using SAS software (release 8.01; SAS Institute, Inc., Cary, NC).

RESULTS

Neutralization properties of anti-rgpCCL5. Figure 22 illustrates chemotactic effects of rgpCCL5 on T lymphocytes isolated from BCG-vaccinated guinea pigs (Fig. 22A). Significant migration of T lymphocytes was observed at concentrations of rgpCCL5 greater than 125ng/ml. Neutralization of the chemotactic effect of rgpCCL5 (375ng/ml) was detected with a concentration gradient of anti-rgpCCL5 (Fig. 22B) with complete neutralization apparent at 100μg/ml of anti-rgpCCL5 after 2 h of chemotaxis.

Severity of tuberculous pleurisy. The role of gpCCL5 during tuberculous pleurisy was assessed by injecting heat-killed *M. tuberculosis* H37Rv, and giving daily intrapleural injections of saline, rgpCCL5, rabbit IgG control, or anti-rgpCCL5. The effect of daily anesthesia was evaluated by characterizing pleurisy from a group of BCG-vaccinated guinea pigs to which anesthesia had been given on day 0 for pleurisy induction. Figure 23 describes the disease severity score, based upon the criteria in Table 1, and fluid accumulation in the pleural cavities of BCG-vaccinated guinea pigs after 4 days with tuberculous pleurisy. Guinea pigs receiving daily injections of rgpCCL5 (6.25μg/side/day) presented with similar disease severity to those given daily injections of sterile saline (Fig. 23A). However, there was a significant ($p < 0.05$)

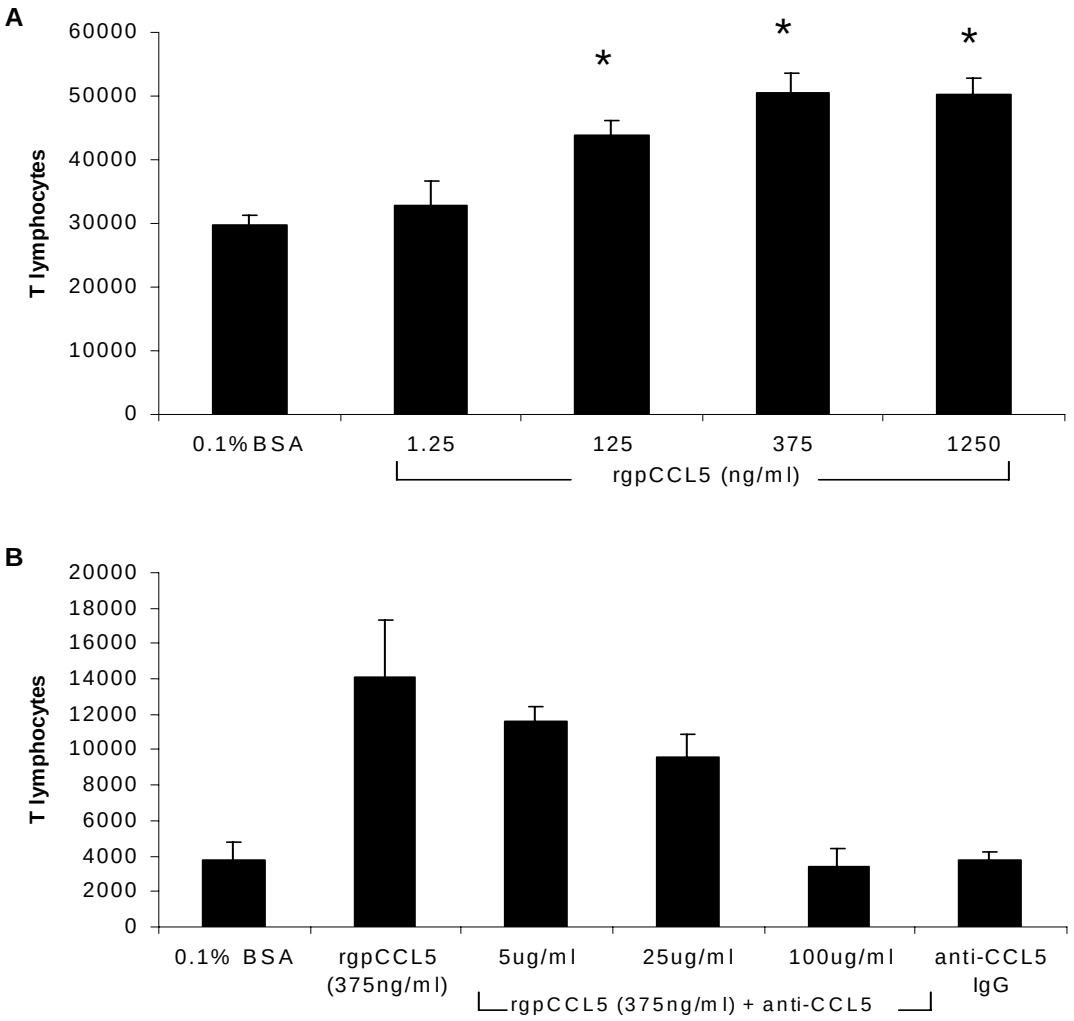

Figure 22: Chemotactic properties of rgpCCL5 to T lymphocytes and neutralization properties of anti-rgpCCL5. Cell migration was determined using the MTT viability assay after the cells were dislodged from the filters. Panel A displays migration of T lymphocytes from BCG-vaccinated guinea pigs to various concentrations of rgpCCL5. Results are representative of the mean $\pm$ SEM for three experiments, each containing quadruplicate wells per concentration tested. * Significant differences ($p < 0.05$) were seen in migration with rgpCCL5 concentrations compared to media alone using ANOVA. Panel B represents chemotaxis of T lymphocytes obtained from naive guinea pigs. Anti-rgpCCL5 IgG was incubated with rgpCCL5 for 30 min before addition to 96-well plate. Results are displayed as the mean $\pm$ SEM of quadruplicate wells from one experiment.

Table 1: Ranking of tuberculous pleurisy post-4 days induction

Disease severity ranking[a]	Characteristics of tuberculous pleurisy
1	Inflamed diaphragm/connective tissue; no granulomas
2	few/small granulomas
3	medium granulomas
4	severe granulomas

[a] Severity was determined by the size and quantity of granulomas inside the pleural cavity of BCG-vaccinated guinea pigs 4 days after pleurisy-induction.

Figure 23: The impact of altering local gpCCL5 activity on the severity of pleuritis in the guinea pig. Guinea pigs were injected into the pleural space with heat-killed *M. tuberculosis* (H37Rv). On day 4 of tuberculous pleurisy, the animals were euthanized and pleural fluid was aspirated and quantified. Severity was determined using the ranking system described in Table 1. Data in panel A represent the means $\pm$ SEM of five animals. Panel B and C represent the means $\pm$ SEM of four animals. Significance (* $p < 0.05$, ** $p < 0.01$) between treatment groups was determined by the Student's t test.

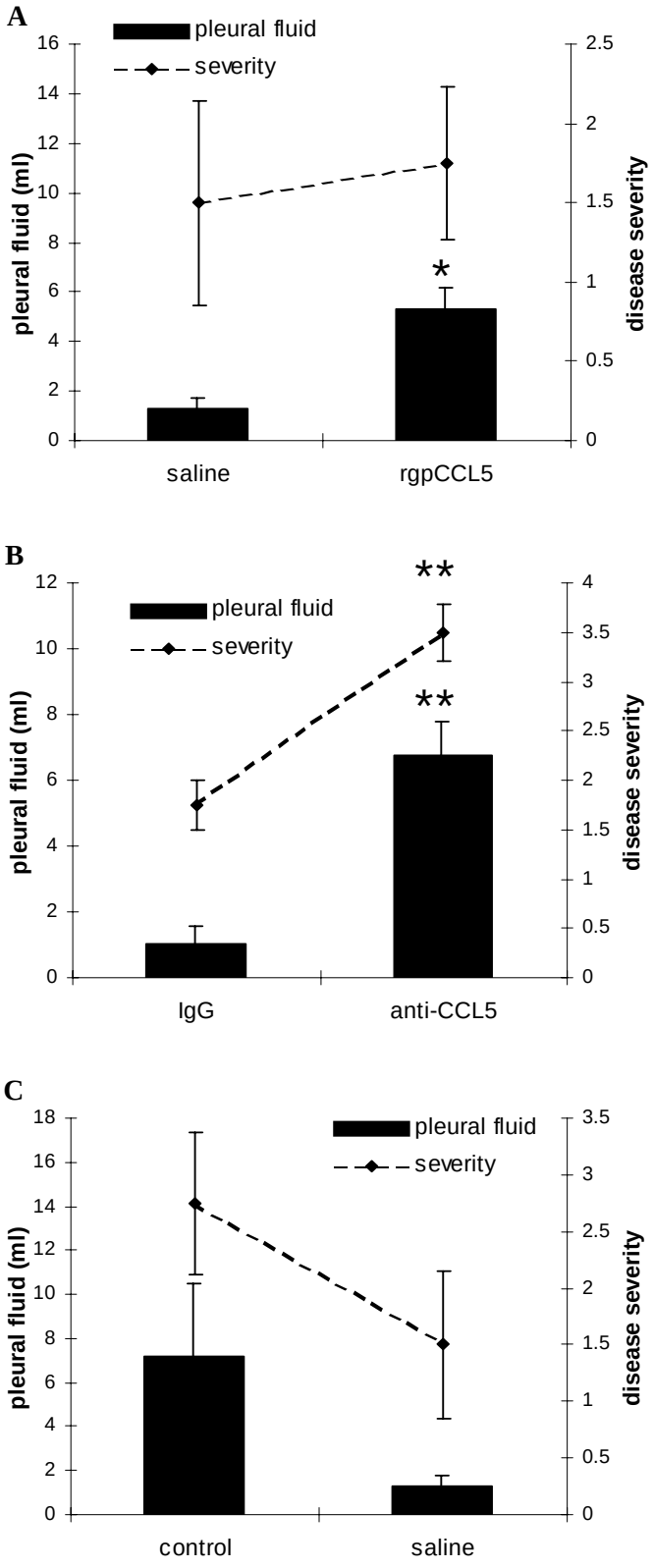
A
pleural fluid
severity
pleural fluid (ml)
disease severity
*
saline
rgpCCL5
B
pleural fluid
severity
pleural fluid (ml)
disease severity
**
**
IgG
anti-CCL5
C
pleural fluid
severity
pleural fluid (ml)
disease severity
control
saline

Elevation in the volume of pleural fluid obtained from the pleural cavity of guinea pigs given rgpCCL5 compared to saline alone. In Fig. 23B, guinea pigs receiving anti-rgpCCL5 (300μg/side/day) presented with significantly ($p < 0.01$) elevated pleural fluid levels and enhanced severity compared to animals given daily bilateral injections in the pleural cavity of rabbit IgG control (300μg/side/day). The effect of daily anesthesia on severity and fluid accumulation in animals infected with tuberculous pleurisy is illustrated in Fig. 23C. No significant difference was present between the two treatments groups in either disease severity or pleural fluid.

Effect of altering local CCL5 activity on leukocyte populations in the pleural cavity during tuberculous pleurisy. At 4 days post-pleurisy induction, pleural fluid was aspirated from the cavity and centrifuged to obtain pleural cells. Figure 24 illustrates the effect of adding exogenous CCL5 or neutralizing local CCL5 on the proportions of $CD3^+$, $CD4^+$, and $CD8^+$ T lymphocytes and MHC class II expressing cells as measured by flow cytometry. In Fig. 24A, a significant reduction ($p < 0.05$) of 15-20% was observed in the proportions of $CD3^+$ and $CD4^+$ T lymphocytes from pleurisy-infected BCG-vaccinated guinea pigs treated with daily injections of rgpCCL5. $CD8^+$ T lymphocytes appeared unaltered by the presence of exogenous rgpCCL5. In Fig. 24B and 24C, leukocytes from the pleural fluid were mixed with cells obtained from a 10ml PBS wash of the pleural cavity. Fig 24B demonstrates minimal differences in the proportion of T lymphocytes between animals treated with anti-CCL5 compared to control antibody isotype (IgG) alone. However, cells expressing MHC class II were significantly diminished ($p < 0.05$) in guinea pigs given daily injections of anti-rgpCCL5

Figure 24: The effect of CCL5 on T cell subpopulations and MHC II cells. Pleural cells were isolated on day 4 from pleurisy-induced BCG-vaccinated guinea pigs. The cells were labeled with anti-CD3, anti-CD4, anti-CD8, and anti-MHC class II. All data represent the mean $\pm$ SEM of 3-4 guinea pigs per treatment group. Panel A represents saline versus rgpCCL5-treated pleuritic guinea pigs. Anti-rgpCCL5 compared to control IgG-treated groups were represented in panel B, and panel C demonstrates the effect of daily anesthesia (saline) versus control (anesthesia only given on day 0) on T cell population in the pleural effusions. Labeled leukocytes were then quantified by flow cytometry. Significance (* $p < 0.05$, ** $p < 0.01$) was determined using the Student t test.

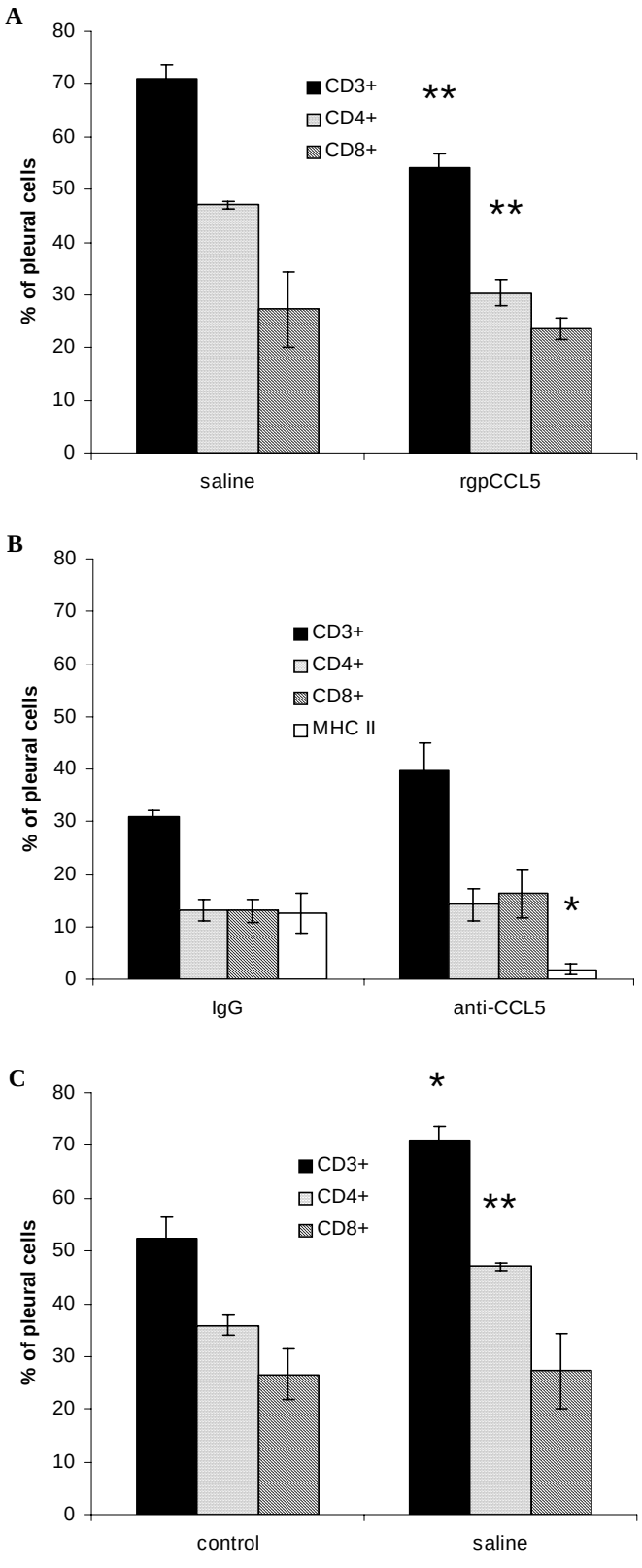
A
80
70
60
50
40
30
20
10
0
% of pleural cells
CD3+
CD4+
CD8+
**
**
saline
rgpCCL5
B
80
70
60
50
40
30
20
10
0
% of pleural cells
CD3+
CD4+
CD8+
MHC II
*
IgG
anti-CCL5
C
80
70
60
50
40
30
20
10
0
% of pleural cells
CD3+
CD4+
CD8+
*
**
control
saline

Compared to control IgG antibody. Pleuritic guinea pigs not anesthetized daily (control) displayed significantly diminished levels of CD3+ ($p < 0.05$) and CD4+ ($p < 0.01$) T lymphocytes (Fig. 24C) compared to saline treated groups with daily anesthesia.

Pleural cells were centrifuged onto glass slides and stained with Diff-Quik to enumerate different leukocyte populations, and the results are illustrated in Fig. 25. In Fig. 25A, lymphocytes were significantly diminished ($p < 0.05$) in animals treated with rgpCCL5 compared to saline, while treatment with rgpCCL5 resulted in a minimal differences in the other leukocyte populations compared to saline treated animals. In Fig. 25B, the pleural cells were obtained by mixing cells from the initial pleural fluid aspirate and cells from a 10ml PBS pleural wash. Macrophage populations were significantly depressed ($p < 0.05$) in animals treated with anti-rgpCCL5 compared to control antibody. An increase in the percentage of eosinophils was apparent in animals exposed to anti-rgpCCL5 compared to isotype control. Minimal differences were apparent regarding the other leukocyte populations. In Fig. 25C pleurisy-induced guinea pigs without daily anesthesia (control) presented percentages of leukocyte populations quite similar to the saline-treated group.

Proliferation of pleural cells. Pleural cells isolated from guinea pigs 4 days post-induction were analyzed for proliferative activity. As illustrated in Fig. 26, no difference was seen in spontaneous proliferation from cells isolated from rgpCCL5 or saline treated animals (Fig. 26A). Figure 26B shows a significant suppression ($p < 0.05$) of spontaneous proliferation *ex vivo* in cells isolated from anti-rgpCCL5-treated, compared to control IgG-treated, guinea pigs. In Fig. 26C, PPD-specific (25μg/ml)

Figure 25: Cellular differentiation of pleural cells between treatment groups. On day 4 of tuberculous pleurisy, pleural cells were extracted from BCG-vaccinated guinea pigs and centrifuged onto slides. Diff-Quik staining was performed on the slides to determine the proportions of different leukocyte subpopulations using light microscopy. Data represent the mean $\pm$ SEM of 3-4 animals per group. Panel A exhibits cellular populations in saline-treated compared to rgpCCL5-treated. Panel B compares cellular populations in anti-rgpCCL5 treated and IgG control treated groups. The effect of daily anesthesia and injections on cell populations in the pleural effusion is demonstrated in panel C, where the control group (receiving only one day with anesthesia and injection) is compared to the saline group (given daily injections and anesthesia). Significance (* $p < 0.05$) was determined using the Student's t test. Neut, neutrophil; Lymp, lymphocytes; Mac, macrophages; Eos, eosinophils; Kurl, Kurloff cells; R Lym, reactive lymphocytes.

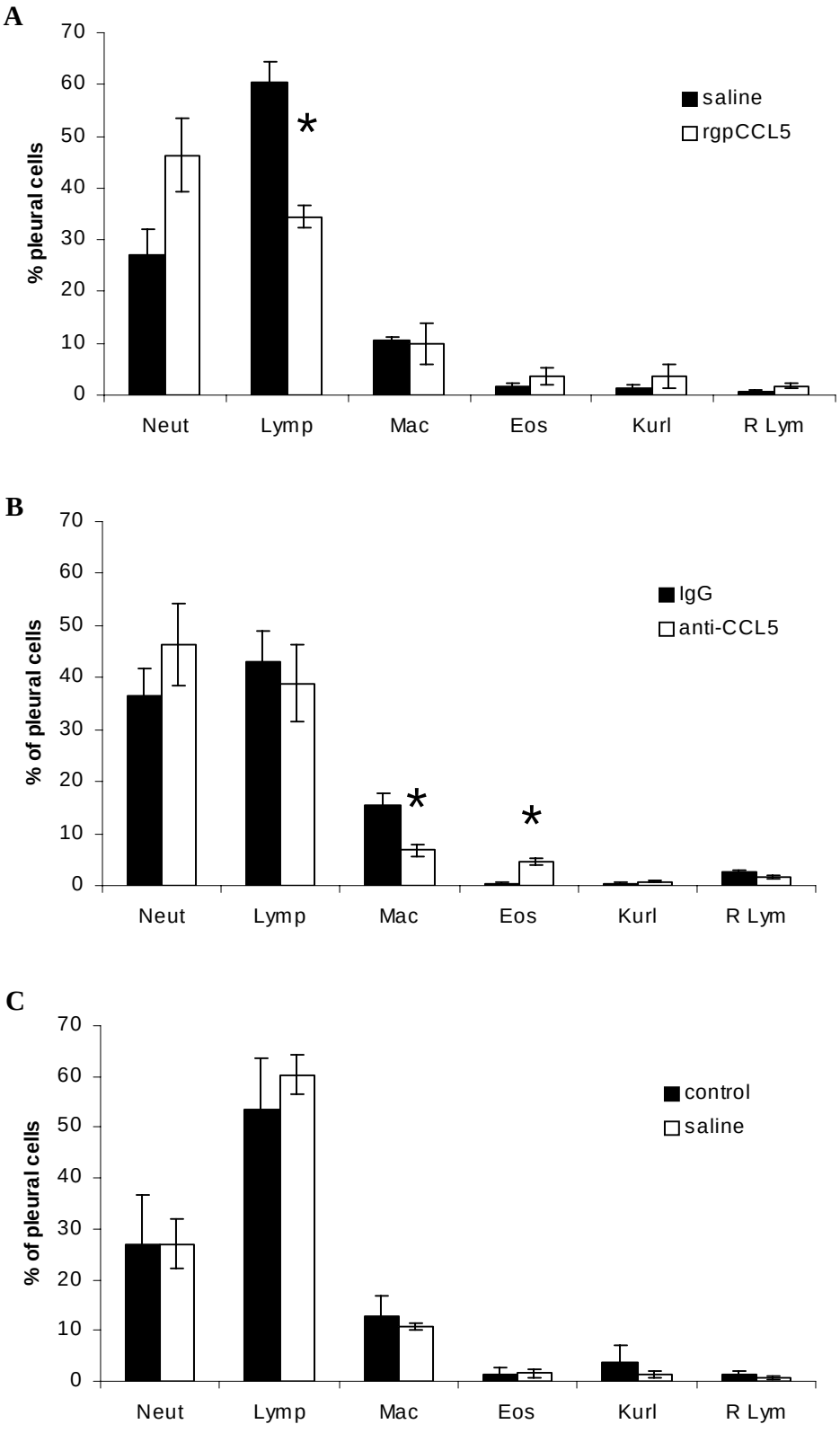
A
70
60
50
40
30
20
10
0
% pleural cells
saline
rgpCCL5
*
Neut
Lymp
Mac
Eos
Kurl
R Lym
B
70
60
50
40
30
20
10
0
% of pleural cells
IgG
anti-CCL5
*
*
Neut
Lymp
Mac
Eos
Kurl
R Lym
C
70
60
50
40
30
20
10
0
% of pleural cells
control
saline
Neut
Lymp
Mac
Eos
Kurl
R Lym

Figure 26: Effect of modifying local activity of CCL5 on pleural lymphocyte proliferation. Cells were obtained from the pleural cavity 4 days after induction. Panel A and B: cells were cultured immediately with [^{3}H] thymidine for 6 h to determine proliferative activity within the pleural cavity. Panel C: PPD-specific proliferation was determined in saline and rgpCCL5 treated guinea pigs after 72 h of antigen stimulation (PPD) with the addition of [^{3}H] thymidine the last 6 h. Results represent the mean cpm $\pm$ SEM of 3-4 animals per groups performed in triplicate. Significance (* $p < 0.05$) is depicted by an asterisk using Student's t test.

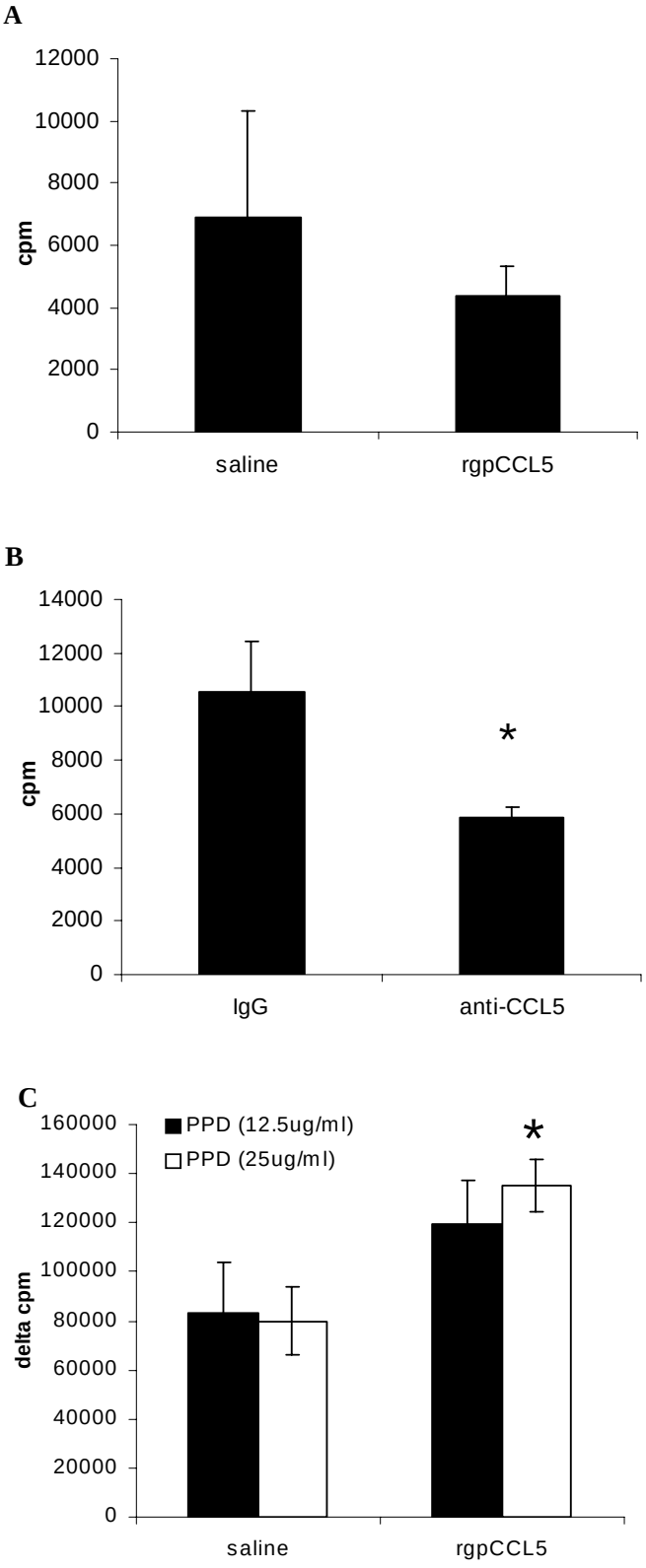
A
12000
10000
8000
6000
4000
2000
0
cpm
saline
rgpCCL5
B
14000
12000
10000
8000
6000
4000
2000
0
cpm
*
IgG
anti-CCL5
C
160000
140000
120000
100000
80000
60000
40000
20000
0
delta cpm
PPD (12.5ug/ml)
PPD (25ug/ml)
*
saline
rgpCCL5

Proliferation was significantly elevated ($p < 0.05$) in pleural cells isolated from rgpCCL5-treated compared to saline-treated animals.

Cytokine/chemokine mRNA expression in pleural cells. TNFα, IL-1β, IL-12p40, IFNγ, CCL2, CCL5, and CXCL8 mRNA were analyzed by isolating RNA from pleural cells obtained from BCG-vaccinated guinea pigs 4 days after pleurisy induction. Total RNA was reverse transcribed into cDNA and gene expression was determined using real-time PCR with primers described in Table 2, and the results are illustrated in Figs. 27-29. Expression of IFNγ mRNA in pleural cells was ~ 7 fold greater than all other cytokine levels tested in the saline treated group (Fig. 27A). On the contrary, animals treated with rgpCCL5 had similar IFNγ and IL-12p40 mRNA levels. Among the chemokines tested, CCL5 was expressed at levels 8 fold higher compared to CCL2 and CXCL8 expression (Fig. 27B). There was an absence of CCL2 expression in cells isolated from the pleural cavity of animals with tuberculous pleurisy (Fig. 27B) compared to pleural cells isolated from BCG-vaccinated guinea pigs without pleurisy. Comparative studies between treatment groups of pleuritic guinea pigs demonstrated significantly lower IFNγ ($p < 0.05$) and CCL5 ($p = 0.057$) mRNA levels in guinea pigs treated with rgpCCL5 compared to saline (Fig. 27A and 27B). Enhanced levels of IL-1β ($p < 0.05$) and IL-12p40 ($p < 0.05$) were detected in pleural exudate cells from pleuritic guinea pigs given daily injections of rgpCCL5 compared to saline alone (Fig. 27A). In Fig. 28A, mRNA from pleural cells obtained from initial pleural aspiration and PBS wash of the pleural cavity from guinea pigs given daily injections of isotype control (IgG) demonstrated enhanced IFNγ mRNA levels, like the saline group, at twice the

Table 2: Primers used for real-time PCR

Gene	Forward Primer[a]	Reverse Primer[a]
TNF alpha	5' - TTGATGGCAGAGAGAAGGTTGA - 3'	5' - CCTACCTGCTTCTCACCCATACC - 3'
IL-1 beta	5' - GGAGTCTCTACCAGCTCAACTTGG - 3'	5' - GCCCAGGCAACAGCTCTC - 3'
IL-12p40	5' - CCATTCGCTCCACGATGAG - 3'	5' - CCACAGTTTCATGCCACAAGA - 3'
IFN gamma	5' - GTTCCTCTGGTTCGGTGACA - 3'	5' - ATTTCGGTCAATGACGAGCAT - 3'
CCL5	5' - CCTTGCTTCTTTGCCTTGAAA - 3'	5' - CTGGCCCACTGCTTAGCAAT - 3'
CCL2	5' - CGAATGTTCAAAGGCTTTGAGGT - 3'	5' - TTGCCAAACTGGCACCAGAGAA - 3'
CXCL8	5' - CAGCTCCGAGACCAACTTTGT - 3'	5' - GGCAGCCTTCCTGCTCTCT - 3'
HPRT	5' - AGGTGTTTATCCCTCATGGACTAATT - 3'	5' - CCTCCCATCTCCTTCATCACAT - 3'

[a] Primers express software was used to design sequences for guinea pig genes to use in the real-time PCR assay using SYBR Green

Figure 27: Effect of rgpCCL5 on cytokine and chemokine mRNA in pleural cells obtained from BCG-vaccinated guinea pigs 4 days post induction. Total RNA was isolated, reverse transcribed, and cDNA was analyzed by real-time PCR. Results were expressed as fold induction of mRNA, which was determined by normalizing cytokine/chemokine threshold cycle (C_t) values against HPRT values. This was further normalized against mRNA from pleural cells obtained from pleurisy-free (no antigen injected) animals. Data represent mean $\pm$ SEM of 3-4 animals per group. Panel A: exhibits data comparing cytokine mRNA levels in saline-treated versus rgpCCL5-treated groups. Panel B: exhibits data comparing chemokine mRNA levels in saline-treated versus rgpCCL5-treated groups. Significance (* $p < 0.05$, ** $p < 0.01$) was determined using Student's t test.

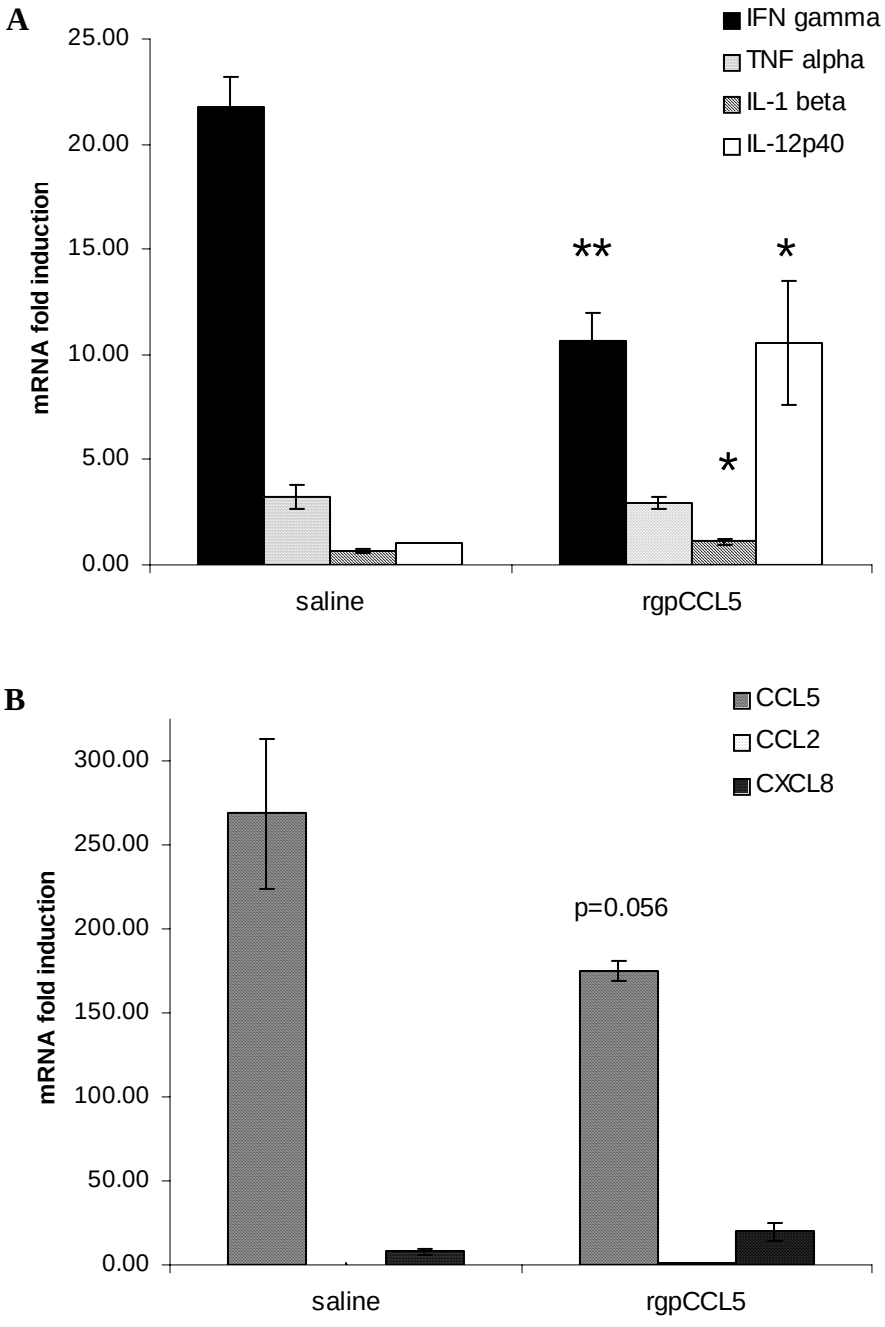
A
IFN gamma
TNF alpha
IL-1 beta
IL-12p40
mRNA fold induction
25.00
20.00
15.00
10.00
5.00
0.00
**
*
*
saline
rgpCCL5
B
CCL5
CCL2
CXCL8
mRNA fold induction
300.00
250.00
200.00
150.00
100.00
50.00
0.00
p=0.056
saline
rgpCCL5

Figure 28: Effect of anti-CCL5 on cytokine and chemokine mRNA in pleural cells obtained from BCG-vaccinated guinea pigs 4 days post-pleurisy induction. Total RNA was isolated, reverse transcribed, and cDNA was analyzed by real-time PCR. Results were expressed as fold induction of mRNA, which was determined by normalizing cytokine/chemokine threshold cycle (C_t) values against HPRT values. This was further normalized against mRNA from pleural cells obtained from pleurisy-free (no antigen injected) animals. Panel A: exhibits data comparing cytokine mRNA levels in IgG control treated compared to anti-rgpCCL5 treated groups. Panel B: exhibits data comparing chemokine mRNA levels in IgG control treated compared to anti-rgpCCL5 treated groups. Data represent mean $\pm$ SEM of 3-4 animals per group. Significance (* $p < 0.05$) was determined using Student's t test.

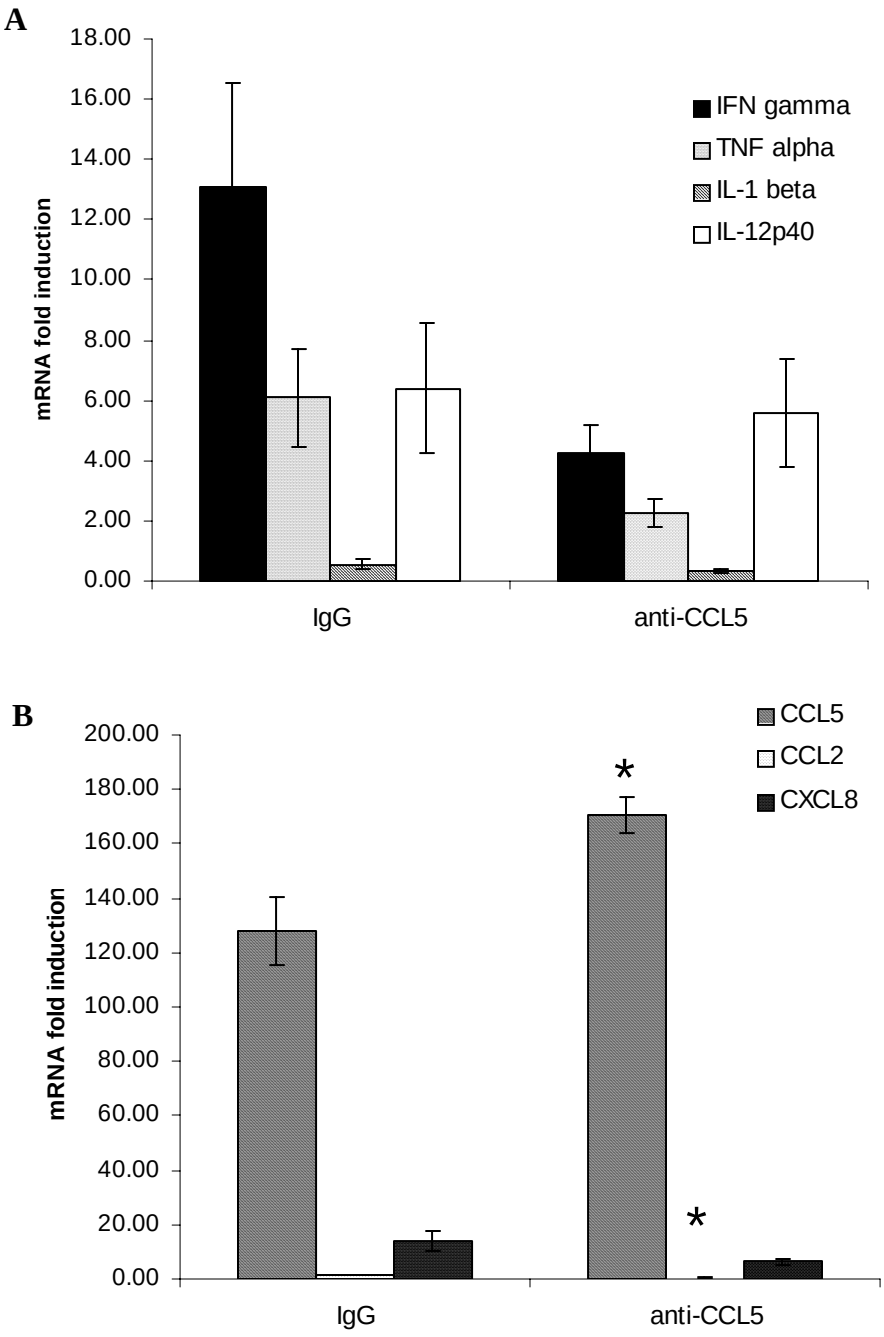
A
18.00
16.00
14.00
12.00
10.00
8.00
6.00
4.00
2.00
0.00
mRNA fold induction
IFN gamma
TNF alpha
IL-1 beta
IL-12p40
IgG
anti-CCL5
B
200.00
180.00
160.00
140.00
120.00
100.00
80.00
60.00
40.00
20.00
0.00
mRNA fold induction
CCL5
CCL2
CXCL8
*
*
IgG
anti-CCL5

Expression of all cytokines tested (Fig. 28A). Guinea pigs treated with anti-rgpCCL5 displayed similar expression levels between IFNγ and IL-12p40 (Fig. 28A). Approximately 10-fold greater CCL5 mRNA levels were observed compared to all other chemokine mRNA levels tested (Fig. 28B). Comparative studies illustrated reduced levels of CCL2 ($p < 0.05$), with decreasing trends, though not significant, in IFNγ ($p < 0.1$) and TNFα ($p < 0.1$) in animals treated with daily anti-rgpCCL5 compared to isotype control. Levels of CCL5 mRNA were significantly enhanced ($p < 0.05$) in guinea pig population given daily doses of anti-CCL5 compared to rabbit IgG isotype controls. Figures 29A and B display the cytokine/chemokine mRNA levels from pleurisy induced guinea pigs without daily anesthesia (control) compared to animals with daily anesthesia and injections (saline). Levels of IFNγ were significantly diminished ($p < 0.05$) in the control group compared to the saline group (Fig. 29A). Anesthesia treatment did not affect the other cytokine and chemokine mRNA levels (Fig. 29A and B).

Severity and cellular composition of granulomas. Granulomas were isolated from BCG-vaccinated guinea pigs 4 days after tuberculous pleurisy was induced. Figure 30 illustrates the overall severity of the inflammatory response (Fig. 30A) and cellular composition from histological examination (Fig. 30B) using a scoring method depicted in table 3. There were minimal differences between the treatment groups at this stage of the inflammatory process. During this early time period, granulomas were difficult to score resulting in variability within each slide. Though not significant, the anti-CCL5 treated group displayed the greatest overall severity among the treatment groups. In Fig. 30B the overall cellular composition throughout the histological sections were scored.

Figure 29: Effect of daily anesthesia on cytokine and chemokine mRNA in pleural cells obtained from BCG-vaccinated guinea pigs 4 days post-induction. Total RNA was isolated, reverse transcribed, and cDNA was analyzed by real-time PCR. Results were expressed as fold induction of mRNA, which was determined by normalizing cytokine/chemokine threshold cycle (C_t) values against HPRT values. This was further normalized against mRNA from pleural cells obtained from pleurisy-free (no antigen injected) animals. Panel A: exhibits data comparing cytokine mRNA levels in daily anesthesia (saline) group compared to day 0 anesthesia only (control). Panel B: exhibits data comparing chemokine mRNA levels in daily anesthesia (saline) group compared to day 0 anesthesia only (control). Data represent mean $\pm$ SEM of 3-4 animals per group. Significance (* $p < 0.05$) was determined using Student's t test.

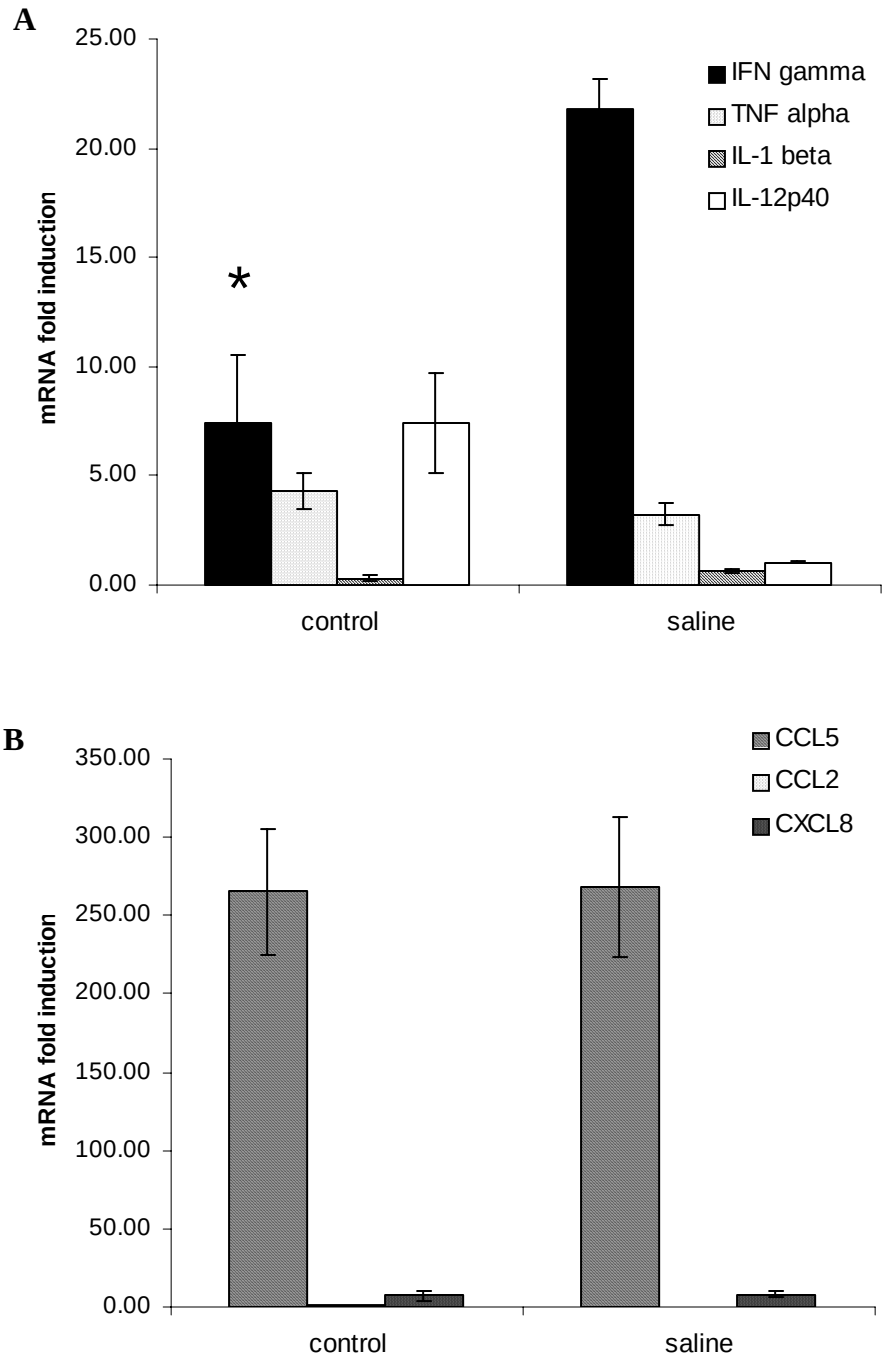
A
25.00
20.00
15.00
10.00
5.00
0.00
mRNA fold induction
IFN gamma
TNF alpha
IL-1 beta
IL-12p40
*
control
saline
B
350.00
300.00
250.00
200.00
150.00
100.00
50.00
0.00
mRNA fold induction
CCL5
CCL2
CXCL8
control
saline

Table 3: Scoring of granulomas 4 days post-induction

Severity ranking[a]	Characteristics of granuloma/cellular and bacilli accumulation
0	No change/presence
1	Minimal change/presence
2	Mild change/presence
3	Moderate change/presence
4	Severe change/presence

[a] An arbitrary system was designed to assess the overall inflammatory severity, the concentration of leukocyte populations, and bacterial burden within the granulomas.

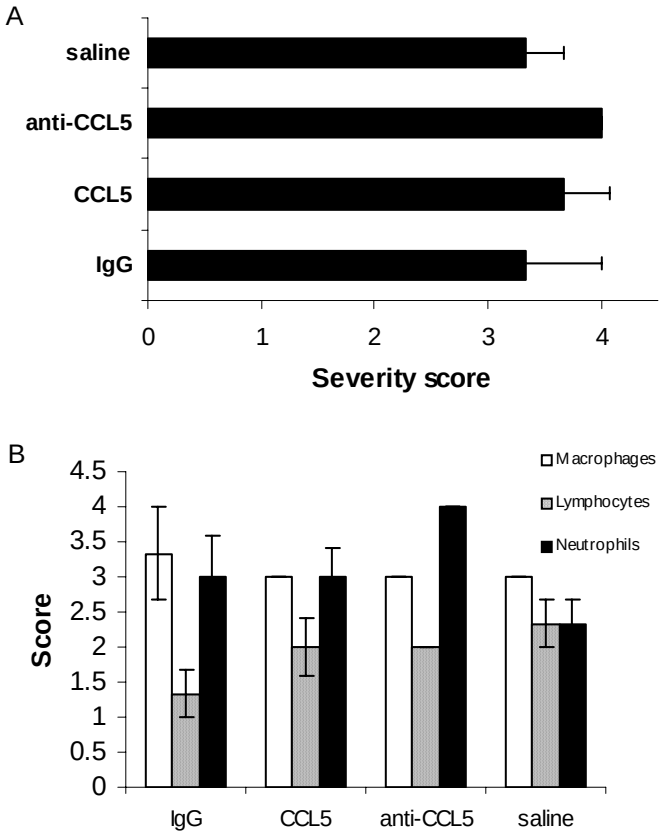

Figure 30: Characterization of granulomas derived after 4 days post-tuberculous pleurisy induction. Granulomatous tissue was sectioned and stained with H & E. The overall inflammatory severity was scored according to Table 3 and is displayed in panel A. Leukocyte populations were scored within the granulomatous tissue and characterized in panel B. Results represent the mean $\pm$ SEM of 3-4 animals per treatment group.

Once again, much variability was exhibited within each single animal. Overall there were no significant differences between cell populations in different treatment groups, however, the neutrophils seemed slightly elevated with about 1 score greater in the anti-CCL5 treated group compared to the other groups.

Cytokine/chemokine gene expression in granulomas isolated from tuberculous pleurisy. Total RNA was isolated from the whole granulomas, reverse transcribed, and analyzed via real-time PCR. Table 4 compares cytokine/chemokine mRNA expression in granulomas obtained from saline, rgpCCL5-treated, IgG (isotype controls)-treated, anti-rgpCCL5-treated, or control (only anesthetized on day 0 to induce pleurisy) groups. Minimal differences were observed between treatment groups given daily injections due to the large variability in gene expression within granulomas. However, a trend was apparent, with the rgpCCL5 treated group exhibiting the lowest TNFα and highest IL-12p40 mRNA levels compared to all the treatment groups given daily injections and anesthesia. Pleuritic guinea pigs receiving anti-rgpCCL5 exhibited the lowest IFNγ, IL-12p40, and CXCL8 mRNA expression of any treatment group. However, CCL2 mRNA expression was the highest in the group given daily doses of anti-rgpCCL5. The effect of daily anesthesia on mRNA in granulomas was demonstrated by significantly ($p < 0.05$) higher levels of IFNγ and IL-12p40 mRNA in granulomas obtained from pleurisy-induced guinea pigs not anesthetized daily compared to those undergoing daily anesthesia. IL-1β mRNA levels were also heightened ($p < 0.05$) in animals from the control group compared to all other groups, except saline-treated guinea pigs.

Table 4: Expression of cytokine and chemokine mRNA levels within granulomas isolated from pleurisy-induced guinea pigs

Gene	Saline[g]	rgpCCL5[g]	IgG[g]	Anti-rgpCCL5[g]	Control[g]
IFN gamma	5.68 ± 0.70[a]	6.50 ± 2.25[a]	9.11 ± 1.78[a]	4.57 ± 0.48[a]	31.50 ± 13.31[b]
IL-12p40	5.68 ± 0.46[c]	7.13 ± 0.98[c]	5.62 ± 1.08[c]	4.43 ± 1.45[c]	11.27 ± 1.45[d]
TNF alpha	5.68 ± 1.92	1.76 ± 0.65	3.15 ± 1.09	3.00 ± 1.43	6.06 ± 2.12
IL-1 beta	4.93 ± 2.23[e]	2.85 ± 1.19[f]	1.98 ± 1.31[f]	2.41 ± 0.68[f]	6.97 ± 0.60[e]
CCL5	28.82 ± 8.86	20.31 ± 6.67	21.83 ± 4.07	19.25 ± 6.31	35.99 ± 12.22
CCL2	7.45 ± 1.73	6.36 ± 2.17	6.58 ± 1.35	10.31 ± 1.73	8.83 ± 3.28
CXCL8	104.79 ± 40.02	71.37 ± 48.43	36.53 ± 17.45	29.77 ± 9.97	67.96 ± 8.68

[a] is significant ($p < 0.05$) from [b] groups

[c] is significant ($p < 0.05$) from [d] groups

[e] is significant ($p < 0.05$) from [f] groups

[g] At day 4 of pleurisy induction, granulomas were isolated, homogenized, and total RNA was isolated. Results were expressed as fold induction of mRNA, which was determined by normalizing cytokine/chemokine threshold cycle (Ct) values against HPRT values. This was further normalized against mRNA from pleural cells obtained from pleurisy-free (no antigen injected) animals. Data represent mean + SEM of 3-5 animals per group. Significance ($p < 0.05$) between all groups was performed using ANOVA.

Effect of gpCCL5 on *M. tuberculosis* within granulomas. Ziehl-Neelsen stains were performed on histological sections of granulomas obtained 4 days post-pleurisy induction. Figure 31 depicts *M. tuberculosis* numbers within the granulomas using the scoring method outlined in Table 3. This method of quantifying bacilli was highly variable within each group, resulting in the absence of statistical significance. However, it is important to note that the anti-CCL5 treated group demonstrated the highest bacterial burden within the granulomas compared to all other groups. The difference between the mean of rgpCCL5 treated and anti-CCL5 treated exceeded 1 score group. This comparison exhibits the largest bacillary difference when comparing all other groups. Histological sections from these two treatment groups after acid-fast stain are depicted in Fig. 32. Samples from each treatment group suggest rgpCCL5-treated animals (Fig. 32A and C) have diminished bacillary loads compared to anti-rgpCCL5 treated animals (Fig. 32B and D) within granulomas.

DISCUSSION

Tuberculous pleurisy remains one of the leading extrapulmonary manifestations of tuberculosis infections (3, 180). However, it presents usually as a self-limiting disease controlled by the host cell-mediated immune response. As a result, it serves as a potential model to dissect the important molecules involved in a local, protective antimycobacterial immune response. Our results support previous studies demonstrating the ability of CCL5 to be chemotactic to T lymphocytes (166, 175) at concentrations of 125-1250ng/ml (Fig. 22A). These chemotactic properties were neutralized when

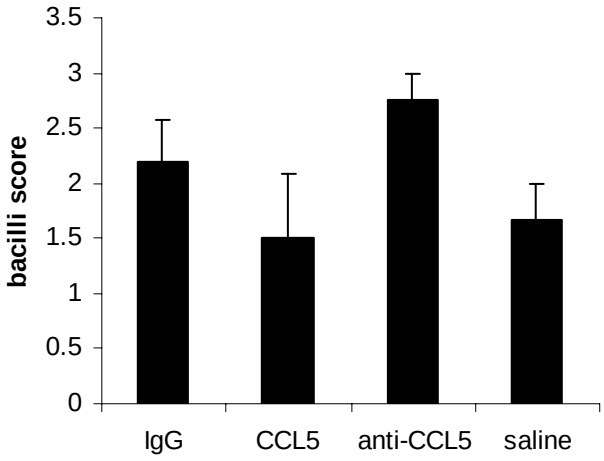

Figure 31: The effect of modifying local CCL5 activity on *M. tuberculosis* within the granuloma. Histological slides were prepared from granulomas on day 4 post-tuberculous pleurisy induction from BCG-vaccinated guinea pigs given various daily treatments including: rabbit IgG control, rgpCCL5, anti-rgpCCL5, or saline. Histological sections were acid-fast stained and scored according to the description depicted in Table 3. Results display the mean $\pm$ SEM of 3-4 animals per treatment group.

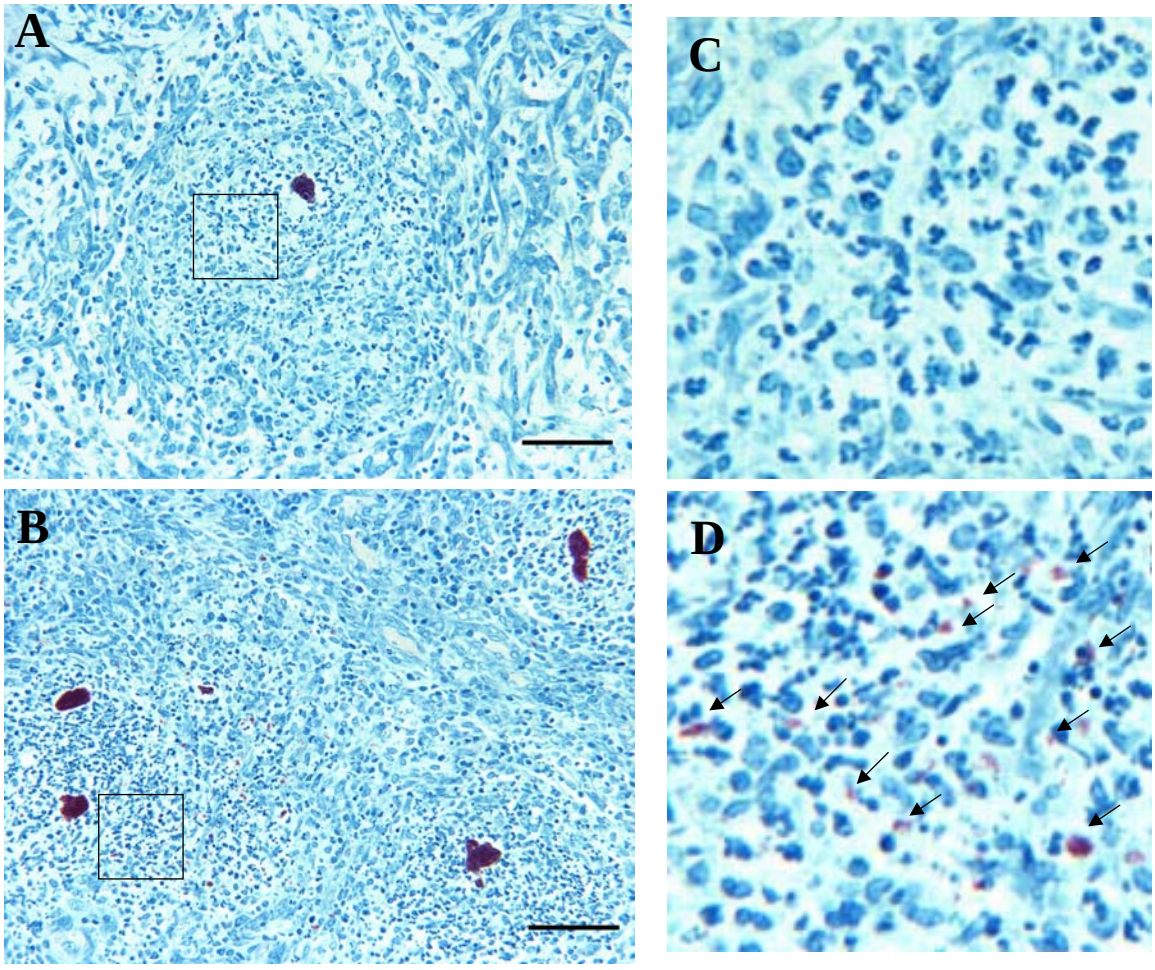

Figure 32: The effect of local modulation of CCL5 on bacillary loads within granulomas taken at day 4 post-pleurisy induction. BCG-vaccinated guinea pigs were induced with tuberculous pleurisy, and on day 4 granulomas were obtained and histological sections were acid-fast stained using Ziehl-Neelsen staining to determine bacterial burdens within granulomas. Panel A represents a granuloma from rgpCCL5-treated group (magnification ×200). Panel B represents a granuloma from anti-rgpCCL5 treated group (magnification ×200). Panel C and D are enlarged pictures of the localized areas depicted by squares in panels A and B respectively. Arrows were used in panels C and D to depict *M. tuberculosis* bacilli (pink) within granulomas.

RgpCCL5 was incubated with rabbit anti-rgpCCL5 in a dose dependent manner (Fig. 22B), with complete neutralization of rgpCCL5 (375ng/ml) observed at 100μg/ml of anti-rgpCCL5.

Characterization of the role of gpCCL5 during tuberculous pleurisy was determined by giving daily injections of rgpCCL5 or anti-rgpCCL5 for 4 days. Previous studies showed optimal CCL5 mRNA and protein concentrations were seen at 4 days (see Chapter IV) with optimal fluid levels accruing at days 4 and 5 (8). Pleuritic guinea pigs given rgpCCL5 at daily intervals had significantly elevated fluid levels compared to saline alone (Fig. 23A). These results coincided with elevated levels of cells in the pleural cavity in animals given rgpCCL5 daily (data not shown). The chemotactic effects of CCL5 on T lymphocytes (166, 175), monocytes/macrophages (27), neutrophils (147), and eosinophils (4) suggests a plausible explanation for the enhanced cells numbers in the pleural effusions. In the rgpCCL5 treated group, there was slight neutrophilia ($p < 0.1$) with a significant reduction in T lymphocytes ($p < 0.05$) (Fig. 24A and 25A). The presence of neutrophilia in the rgpCCL5-treated group supports previous studies demonstrating heightened neutrophils during inflammation when CCL5 is being over-expressed *in vivo* (4, 25). However, those studies also exhibit enhanced levels of T lymphocytes and monocyte/macrophages in rodents with CCL5 over-expression. Those results contradict our findings, but the levels of CCL5 in lungs from those studies were undetermined or less than 200pg/ml. Since we injected greater than 10,000-fold higher concentrations (6.25μg/side/day) of CCL5 into a localized area, these results are difficult to correlate. One explanation is that the rgpCCL5 concentration used in this study was

above the chemotactic concentration. Future studies will look at the effects of lower rgpCCL5 doses on leukocyte populations within the pleural cavity during the development of pleurisy in this model.

The absence of guinea pig reagents to determine if the T lymphocytes are of the memory phenotype leaves more unanswered questions regarding these results. In an attempt to address the presence of memory T lymphocytes, spontaneous and antigen-specific proliferation was measured. A lack of significant differences between rgpCCL5-treated and saline-treated groups in spontaneous proliferation (immediately *ex vivo*) might be due to the high levels of CCL5 already present in the pleural fluid (Chapter V, Fig. 6), or to the significantly elevated T lymphocyte population present in the saline group compared to the rgpCCL5 group. However, Fig. 26C exhibits significantly higher proliferation in pleural cells obtained from rgpCCL5 treated groups compared to saline alone when stimulated with PPD (25μg/ml). These results suggest that there was a heightened population of memory T lymphocytes in the group given rgpCCL5 daily, supporting a previous study demonstrating human memory T lymphocyte chemotaxis to CCL5 (175).

IFNγ mRNA expression levels were 10-fold greater in pleural effusion cells than in cells isolated from pleurisy-free BCG-vaccinated guinea pigs. These findings are in agreement with other studies showing heightened IFNγ mRNA levels in guinea pigs and humans with tuberculous pleuritis (8, 18). These enhanced levels are the result of local cell-mediated immunity in the pleural space, which was demonstrated by Allen et al. (6). Comparative studies between rgpCCL5 and saline treated groups during tuberculous

pleuritis demonstrated significantly lower levels of IFNγ mRNA in guinea pigs receiving daily doses of rgpCCL5 (Fig. 27A). Previous studies linking CCL5 with IFNγ production by human and murine antigen-specific $CD4^+$ and $CD8^+$ T lymphocytes cell lines (11, 110) contrast with the current findings. However, considering that the saline treated group had twice the percentage of T lymphocytes in the pleural effusion cell population and twice the IFNγ mRNA expression levels than the group treated with rgpCCL5, it would suggest the increase in IFNγ mRNA levels is due to the elevated percentage of T lymphocyte and not to enhanced mRNA levels on a per cell basis.

TNFα mRNA levels were elevated in all pleuritic BCG-vaccinated guinea pigs (Fig. 27A). These results agree with other studies showing heightened TNFα mRNA levels in pleural cells obtained from humans and guinea pigs with pleuritis (8, 18) and elevated TNFα protein levels in human tuberculous pleurisy (137). Comparative studies between rgpCCL5 and saline treated guinea pigs revealed no significant difference. The proinflammatory cytokine, IL-1β, mRNA levels were significantly enhanced in guinea pigs given daily doses of rgpCCL5 (Fig. 27A) though the fold induction levels in both groups were below 5. These findings agree with data demonstrating the ability of rgpCCL5 to enhance IL-1β mRNA in macrophages (113, 184). IL-1β protein in pleural effusions from humans with tuberculous pleuritis exhibited minimal levels usually below 200pg/ml (183).

Analysis of the Th1 cytokine subunit, IL-12p40 mRNA, revealed significantly higher levels in rgpCCL5 treated animals compared to saline alone (Fig. 27A). These are novel findings suggesting a role of rgpCCL5 in favoring a Th1 response, which has

been demonstrated previously in mice (54). The differences in cell populations do not seem to correlate proportionally with the 5-10 fold increase in IL-12p40 from the rgpCCL5-treated group, suggesting that rgpCCL5 enhances the expression of IL-12p40 mRNA in cells stimulated with daily injections of rgpCCL5 compared to saline alone. We have demonstrated enhanced IL-12p40 mRNA levels in resident and alveolar macrophages stimulated with ~1μg/ml rgpCCL5 (data not shown).

MRNA levels of CXCL8 and CCL5 appear to be heightened at day 4 after pleurisy induction in BCG-vaccinated guinea pigs (Fig. 27B), with CCL5 mRNA being expressed at levels greater than 10-fold higher compared to CXCL8 and CCL2. These results provide support for a previous study looking at pleurisy in mice. Fine et al. demonstrated a gradual reduction of numerous chemokines, including CCL2, from 6 h to 72 h except for CCL5, which displayed a gradual increase in mRNA expression through 72 h post-induction (60). Comparison between saline and rgpCCL5-treated animals illustrated lower trends, though not significant, of CXCL8 ($p < 0.1$) mRNA in guinea pigs given daily injections of rgpCCL5 (Fig. 27B). These data are supported by previous results in Chapter II regarding the ability of rgpCCL5 to upregulate CXCL8 mRNA in macrophages. It must also be noted that there was a slight increase, though not significant, in neutrophils in rgpCCL5 treated animals (Fig. 25A), suggesting this heightened expression could be due to the differences in cell populations in the pleural cavity. However, Pace et al. observed production of CXCL8 in patients with tuberculous pleurisy and correlated its presence with an enhanced T lymphocyte (not neutrophil) accumulation (146). These results are difficult to interpret due to an absence

of CXCL8 kinetics throughout the development of pleurisy. The reduced expression of CCL5 mRNA ($p = 0.056$) in the rgpCCL5-treated group might be due to the diminished presence of T lymphocytes in the pleural space or a downregulation by the host to limit the production of CCL5. Studies looking at protein levels of CXCL8 and CCL5 need to be performed before further conclusions can be made.

Due to the variation in the methodology for acquiring pleural cells, the anti-CCL5 and rabbit IgG control groups cannot be compared with data from the rgpCCL5- and saline-treated groups. There were significant differences between the anti-rgpCCL5 and IgG isotype control groups in pleural fluid and severity (Fig. 23B). The anti-rgpCCL5 group produced significantly more pleural fluid and had enhanced severity compared to the IgG isotype control. In conjunction with the data in Fig. 24 and 25 on the cellular composition in the pleural fluid and wash, these data suggest that anti-rgpCCL5 treatment blocked recruitment of MHC class II expressing cells (Fig. 24B), including macrophages (Fig. 25B), and enhanced the accumulation of eosinophils ($p < 0.05$) (Fig. 25B) compared to the IgG isotype control. The reduction in macrophages and other MHC class II expressing cells in the anti-CCL5 treated group supports the role of CCL5 in attracting these cells to the site of inflammation (27). Together, the presence of eosinophilia and reduced macrophages suggests diminished polarization towards a Th1 response.

Previous studies have demonstrated that CCL5 can induce spontaneous, as well as antigen-specific, proliferation in T lymphocytes (11, 14, 110, 121, 193). As a result, we looked at proliferation of lymphocytes directly coming out of the pleural cavity

(immediately *ex vivo*). A significant reduction of spontaneous proliferation was apparent in cells obtained from the anti-rgpCCL5 treated group (Fig. 26B), suggesting that CCL5 was involved in the proliferative responses occurring within the pleural cavity at day 4 following the induction of tuberculous pleurisy. In support of these findings, Makino et al., reported diminished polyclonal and antigen-specific T lymphocytes proliferation in CCL5 -/- mice compared to wild type mice (121). Lillard et al. also observed enhanced ova-specific T lymphocyte proliferation in mice receiving rCCL5 *in vivo* (110). PPD-specific proliferation was not performed in these experiments, but will be analyzed in future experiments to support this theory of CCL5's involvement in proliferative activity.

Previous studies have demonstrated the ability of CCL5 to affect cytokine/chemokine expression in different types of leukocytes (11, 35, 110, 113, 184). In the present study, we showed a trend, though not significant, toward reduced IFNγ mRNA expression from pleural cells obtained from the anti-CCL5 treated group (Fig. 28A). Unlike the large variation in T lymphocyte populations between rgpCCL5 and saline treated groups, the anti-CCL5 and IgG control groups had similar T lymphocyte populations. This findings confirm previous studies exhibiting the presence of CCL5 with heightened IFNγ expression and production (35, 110, 121). Chensue et al. reported enhanced IFNγ production in type1 granulomas in mice treated with rhCCL5. Another study performed by Makino et al. exhibited diminished IFNγ production by antigen-specific T lymphocytes from CCL5 -/- mice.

The proinflammatory cytokine TNFα exhibited slightly diminished mRNA levels, though not significant, in animals treated with anti-CCL5 (Fig. 28A). These results may be due to a reduction in macrophages, and an increase in neutrophils and eosinophils (Fig. 25B). In Chapter II, it was demonstrated that rgpCCL5 stimulated alveolar and peritoneal macrophages to enhance TNFα mRNA and protein levels, further supporting these findings.

Chemokine levels were also affected by neutralization of CCL5. CCL5 mRNA was significantly enhanced ($p < 0.05$) in the group given anti-rgpCCL5 (Fig. 28B) suggesting that the animals were trying to compensate for the low levels of CCL5. CCL2 was significantly ($p < 0.05$) diminished in animals treated with anti-CCL5, however, the expression levels were similar to those seen in pleural cells obtained from pleurisy-free (not injected with antigen) BCG-vaccinated guinea pigs.

The role of CCL5 in granuloma formation is not well understood. We demonstrated similar overall inflammatory severity in the granulomas between the treatment groups, with the anti-rgpCCL5-treated animals displaying slightly higher severity compared to the other groups, though not statistically significant (Fig. 30A). This increase in severity among the anti-CCL5 treated guinea pigs correlates with slightly enhanced neutrophilia (Fig. 28B), as compared to other groups. These granulomas were in the early phase of development and, as a result, were difficult to score and had a range of variability resulting in a lack of significance. Previously, Chensue infused rhCCL5 (20μg/day) into mice two days before challenging the mice with PPD-coated beads (35). These animals displayed no differences in cellular

composition and granuloma size on day 3. Likewise, when they infused anti-mCCL5 into mice injected with PPD-coated beads, they observed no effect on cellular composition. This correlated with our results exhibiting limited differences in leukocyte populations within the granulomas containing altered CCL5 protein levels. However, leukocyte numbers were not quantified and multiple days were not analyzed, thus limiting our abilities to make further conclusions.

The levels of cytokine and chemokine mRNA inside the granulomas were quite variable, with no statistical significance displayed between the four treated groups. However, the rgpCCL5-treated animals groups had the highest levels of IL-12p40 mRNA over all other groups with daily anesthesia. Animals treated with anti-rgpCCL5 daily displayed the lowest levels of IFNγ, IL-12p40, and CXCL8 mRNA compared to other groups receiving daily injections and anesthesia. Although not significant due to the small number of animals tested and large variability, the trend seems to confirm studies correlating CCL5's presence with enhanced levels of these inflammatory genes (54, 121, 184). It is interesting to note that all the leukocyte populations were similar within the granulomas except neutrophils, which predominated in the anti-CCL5 treated group. However, this group also had the lowest CXCL8 mRNA expression, suggesting CCL5 may be linked to CXCL8 expression, which is supported by the findings in Chapter II demonstrating rgpCCL5's ability to elevate CXCL8 expression in macrophages.

The lower levels of cytokine and chemokine mRNA in the anti-rgpCCL5 treated group related to enhanced bacillary loads, though not significant, within granulomas

(Fig. 31 and 32) compared to all other groups receiving daily anesthesia. These results are supported by a previous study performed by Saukkonen et al. that demonstrated enhanced *M. tuberculosis* viability within human alveolar macrophages co-cultured with anti-hCCL5 (174). The largest variation in bacterial burdens between groups was observed in the rgpCCL5 and anti-rgpCCL5 treated groups (Fig. 31 and 32), suggesting that CCL5 has a role in *M. tuberculosis* viability. Future studies will be focused on deciphering these protective mechanisms elicited by gpCCL5, and its role in tuberculous pleurisy as the granulomas mature.

CHAPTER VII

CONCLUSIONS

One third of the world's population remains infected with *M. tuberculosis* with an annual mortality reaching ~ 2 million deaths. In this dissertation, our goal was to understand the role of gpCCL5 during a tuberculosis infection in the guinea pig model and the effect that BCG-vaccination has on its production. Our first aim of these studies was to produce and characterize rgpCCL5 and anti-rgpCCL5. We subcloned the mature guinea pig cDNA into pET30Xa/LIC vector, transformed the vector into an *E. coli* strain, and expressed it using IPTG. The protein was refolded, purified using reverse phase HPLC, cleaved to obtain mature rgpCCL5, and re-purified over a C4 column using reverse phase HPLC. The recombinant protein was chemotactic for both T lymphocytes and peritoneal exudate cells with an optimal concentration ~ 1350ng/ml. We injected rabbits with rgpCCL5 and obtained rabbit polyclonal anti-rgpCCL5 serum, which bound rgpCCL5 on a Western blot. This antibody neutralized the chemotactic effect for T lymphocytes.

We demonstrated the ability of rgpCCL5 (~ 1μg/ml) to significantly stimulate TNFα, IL-1β, CCL2, and CXCL8 mRNA and TNFα protein in peritoneal and alveolar macrophages. These results suggest that rgpCCL5 is not only attracting leukocytes to the site of inflammation, but enhancing numerous inflammatory cytokines and chemokines in preparation for an antigenic encounter. We demonstrated that the pre-stimulation of cells with rgpCCL5 resulted in diminished levels of chemokines and

cytokines when cells were exposed subsequently to LPS. Future studies will elucidate the affect of rgpCCL5 pre-treatment on macrophages stimulated with mycobacterial antigens.

Previous studies have demonstrated the mitogenic and antigen-specific proliferative activities of CCL5 at various concentrations (14, 110, 193). In preliminary studies reported in Chapter III, we saw limited effects of rgpCCL5 on splenocyte proliferation to both mitogenic and antigenic (PPD) stimuli. However, in Chapter VI pleural effusion cells exhibited a significant reduction in spontaneous proliferation *ex vivo* from pleuritic guinea pigs given anti-rgpCCL5 compared to IgG controls, and the rgpCCL5 treated group demonstrated elevated antigen (PPD)-specific proliferation compared to saline alone. These data suggest gpCCL5 is involved in T lymphocyte proliferation and further *in vitro* studies need to be performed to examine isolated T lymphocytes exposed to varying concentrations of rgpCCL5 alone or in combination with PPD.

Saukkonen et al. reported enhanced *M. tuberculosis* viability in human alveolar macrophages co-cultured with anti-CCL5 (174). We observed minimal effects of rgpCCL5 on *M. tuberculosis* viability within peritoneal and alveolar macrophages. Preliminary studies did show that macrophages isolated from BCG-vaccinated guinea pigs controlled *M. tuberculosis* better than macrophages from naive animals. Jackett et al. demonstrated enhanced H_2O_2 from macrophages isolated from BCG-vaccinated compared to naive guinea pigs 3 days after intravenous infection with *M. tuberculosis* (H37Ra) (84). These findings led us to examine a possible influence of gpCCL5 on

H_2O_2 production. Our preliminary studies failed to demonstrate a correlation with H_2O_2 production and gpCCL5 stimulation in *M. tuberculosis*-infected macrophages. In summary, this ability of CCL5 to alter intracellular *M. tuberculosis* viability still remains to be elucidated in the guinea pig model.

BCG-vaccination induces effective protection against *M. tuberculosis* in the guinea pig, therefore, we characterized variations in host immunity between naive and BCG-vaccinated guinea pigs. Levels of IL-12p40 mRNA were elevated significantly in *M. tuberculosis*-infected alveolar macrophages from BCG-vaccinated compared to naive guinea pigs. We also demonstrated increased IL-12p40 mRNA levels at early culture intervals in alveolar macrophages infected with virulent *M. tuberculosis* (H37Rv) compared to an attenuated strain (H37Ra). This pattern was reversed later in the infection (post-18 h). These results further support previous studies demonstrating the role of IL-12/IL-23 in providing protection against *M. tuberculosis* (2, 39, 78).

For the first time, we quantified gpCCL5 protein levels using an ELISA developed from rabbit polyclonal anti-rgpCCL5 serum. Significantly enhanced levels of CCL5 mRNA and protein were observed in alveolar and peritoneal macrophages, as well as splenocytes, infected with virulent *M. tuberculosis* (H37Rv) *in vitro.* These results supported a previous study performed in our laboratory exhibiting increased CCL5 mRNA in peritoneal exudate cells obtained from BCG-vaccinated guinea pigs compared to naive animals and infected with *M. tuberculosis* (85). It also supports previous studies demonstrating heightened CCL5 production in human alveolar macrophages infected with *M. tuberculosis* (167). We looked at the production of gpCCL5 *in vivo*

during tuberculous pleurisy and demonstrated significantly elevated levels of gpCCL5 mRNA in pleural exudate cells and protein in the pleural fluid as the infection progressed reaching peak levels on day 4.

These results prompted us to look further into the effect of modifying local activity of gpCCL5 during tuberculous pleurisy. We induced tuberculous pleurisy in BCG-vaccinated guinea pigs and administered daily bilateral injections of either rgpCCL5, saline, anti-rgpCCL5, or IgG isotype control. On day 4 post-induction, the animals were exsanguinated, and pleural fluid/cells and granulomas were collected. Exogenous addition of large concentrations of rgpCCL5 (6.7μg/side/day) compared to saline during tuberculous pleurisy resulted in elevated leukocyte migration and pleural fluid accumulation. Cellular accumulation exhibited slight neutrophilia, correlating with enhanced CXCL8 mRNA expression in rgpCCL5-treated guinea pigs, and a diminished percentage of T lymphocytes, which was proportional to the reduced IFNγ mRNA levels in the pleural exudate cells. Although saline-treated animals had significantly more T lymphocytes than rgpCCL5-treated animals, when pleural exudate cells were stimulated with PPD, those cells from the rgpCCL5-treated group exhibited significantly elevated proliferation. This group also had elevated levels of IL-12p40 and IL-1β mRNA compared to saline alone. Neutralizing local activity of gpCCL5 with anti-rgpCCL5 treatment resulted in significantly elevated severity of inflammation, with suppressed macrophage, but elevated eosinophil, accumulation. This suggests a polarization towards a Th2 , rather than a Th1, response. In support of this conclusion, IFNγ and TNFα were diminished in anti-rgpCCL5-treated guinea pigs compared to IgG controls.

Diminished spontaneous proliferation was also observed in the pleural effusion cells from animals receiving anti-rgpCCL5. A tendency toward increased bacillary loads in the granulomas from anti-rgpCCL5 supports the conclusion that neutralizing CCL5 resulted in an inefficient or delayed cell-mediated immune response. Cytokine/chemokine mRNA expression levels were not significantly different among treatment groups due to the small number of animals and large variability between them, however, anti-rgpCCL5 treated animals had the lowest levels of mRNA for IL-12p40 and IFNγ, both of which are associated with a Th1 response.

These studies suggest an important role of CCL5 in leukocyte activation and protection against *M. tuberculosis* infections. From these data and previous data, Figure 33 demonstrates numerous pathways throughout a *M. tuberculosis* infection in which CCL5 may be involved. Further studies assessing the production of CCL5 *in vivo* following virulent pulmonary infection are needed, as are studies of the requirement for CCL5 in granuloma architecture. If these studies provide further evidence supporting an essential protective role of CCL5 during a *M. tuberculosis* infection, it would be beneficial to design new tuberculosis vaccines which stimulate elevated CCL5 production when the host was confronted with the bacillus. Another possible mode of protection might be to deliver CCL5 in conjunction with a tuberculosis vaccine as an adjuvant. Previously studies have displayed synergistic protection when expressing CCL5 with HIV DNA vaccines (211).

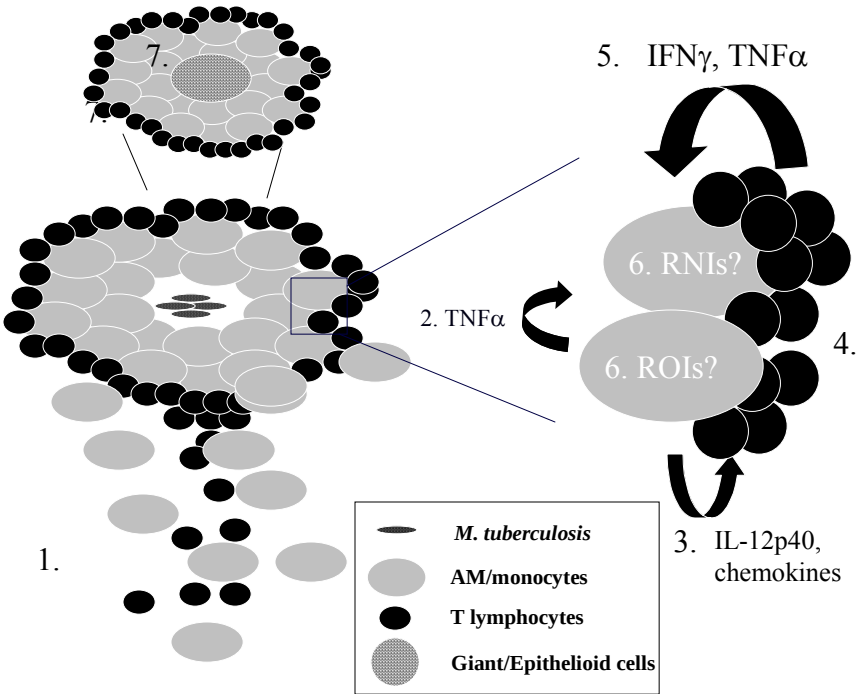

Figure 33: Summary: The putative role(s) of CCL5 during *M. tuberculosis* infection. From these data and previous studies analyzing the role of CCL5 in the immune response elicited against tuberculosis, we suggest 7 areas of CCL5 involvement during infection. Stage 1: First, CCL5 is chemotactic to T lymphocytes, especially of the memory phenotype, and monocyte/macrophages into inflammatory foci. Stage 2: Next, CCL5 stimulates macrophage TNFα production, which activates macrophages in a paracrine and autocrine fashion. Stage 3: Then, CCL5 induces release of chemokines and Th1 cytokines from macrophages, which results in T lymphocyte migration and differentiation of Th0 cells into Th1 lymphocytes. Stage 4: Next, CCL5 enhances IL-2 production, resulting in lymphocyte proliferation and Stage 5: the release of macrophages activating cytokines, IFNγ and TNFα. Stage 6: This activation of macrophages with IFNγ and TNFα may result in elevated production of ROIs and RNIs, which have displayed anti-mycobacterial properties. Stage7: Finally, the production of IFNγ and TNFα aids in macrophage fusion resulting in epithelioid and giant cell formations at the foci of the granuloma. These cells types display an enhanced anti-mycobacterial activity, resulting in diminished bacterial viability.

REFERENCES

1. **Adams, L. B., M. C. Dinauer, D. E. Morgenstern, and J. L. Krahenbuhl.** 1997. Comparison of the roles of reactive oxygen and nitrogen intermediates in the host response to *Mycobacterium tuberculosis* using transgenic mice. Tuber Lung Dis **78:**237-246.

2. **Akahoshi, M., H. Nakashima, K. Miyake, Y. Inoue, S. Shimizu, Y. Tanaka, K. Okada, T. Otsuka, and M. Harada.** 2003. Influence of interleukin-12 receptor beta1 polymorphisms on tuberculosis. Hum Genet **112:**237-243.

3. **Aktogu, S., A. Yorgancioglu, K. Cirak, T. Kose, and S. M. Dereli.** 1996. Clinical spectrum of pulmonary and pleural tuberculosis: a report of 5,480 cases. Eur Respir J **9:**2031-2035.

4. **Alam, R., S. Stafford, P. Forsythe, R. Harrison, D. Faubion, M. A. Lett-Brown, and J. A. Grant.** 1993. RANTES is a chemotactic and activating factor for human eosinophils. J Immunol **150:**3442-3448.

5. **Algood, H. M., P. L. Lin, D. Yankura, A. Jones, J. Chan, and J. L. Flynn.** 2004. TNF influences chemokine expression of macrophages *in vitro* and that of CD11b+ cells *in vivo* during *Mycobacterium tuberculosis* infection. J Immunol **172:**6846-6857.

6. **Allen, J. C., and M. A. Apicella.** 1968. Experimental pleural effusion as a manifestation of delayed hypersensitivity to tuberculin PPD. J Immunol **101:**481-487.

7. **Allen, S. S., L. Cassone, T. M. Lasco, and D. N. McMurray.** 2004. Effect of neutralizing transforming growth factor beta1 on the immune response against *Mycobacterium tuberculosis* in guinea pigs. Infect Immun **72:**1358-1363.

8. **Allen, S. S., and D. N. McMurray.** 2003. Coordinate cytokine gene expression *in vivo* following induction of tuberculous pleurisy in guinea pigs. Infect Immun **71:**4271-4277.

9. **Alves-Rosa, F., M. Vulcano, M. Beigier-Bompadre, G. Fernandez, M. Palermo, and M. A. Isturiz.** 2002. Interleukin-1beta induces *in vivo* tolerance to lipopolysaccharide in mice. Clin Exp Immunol **128:**221-228.

10. **Appay, V., A. Brown, S. Cribbes, E. Randle, and L. G. Czaplewski.** 1999. Aggregation of RANTES is responsible for its inflammatory properties. Characterization of nonaggregating, noninflammatory RANTES mutants. J Biol Chem **274:**27505-27512.

11. **Appay, V., P. R. Dunbar, V. Cerundolo, A. McMichael, L. Czaplewski, and S. Rowland-Jones.** 2000. RANTES activates antigen-specific cytotoxic T lymphocytes in a mitogen-like manner through cell surface aggregation. Int Immunol **12:**1173-1182.

12. **Appay, V., and S. L. Rowland-Jones.** 2001. RANTES: a versatile and controversial chemokine. Trends Immunol **22:**83-87.

13. **Arbelaez, M. P., K. E. Nelson, and A. Munoz.** 2000. BCG vaccine effectiveness in preventing tuberculosis and its interaction with human immunodeficiency virus infection. Int J Epidemiol **29:**1085-1091.

14. **Bacon, K. B., B. A. Premack, P. Gardner, and T. J. Schall.** 1995. Activation of dual T cell signaling pathways by the chemokine RANTES. Science **269:**1727-1730.

15. **Bainton, D. F.** 1981. The discovery of lysosomes. J Cell Biol **91:**66s-76s.

16. **Balasubramanian, V., E. H. Wiegeshaus, and D. W. Smith.** 1994. Mycobacterial infection in guinea pigs. Immunobiology **191:**395-401.

17. **Balish, E., R. D. Wagner, A. Vazquez-Torres, J. Jones-Carson, C. Pierson, and T. Warner.** 1999. Mucosal and systemic candidiasis in IL-8Rh-/- BALB/c mice. J Leukoc Biol **66:**144-150.

18. **Barnes, P. F., S. J. Fong, P. J. Brennan, P. E. Twomey, A. Mazumder, and R. L. Modlin.** 1990. Local production of tumor necrosis factor and IFN-gamma in tuberculous pleuritis. J Immunol **145:**149-154.

19. **Barnes, P. F., S. Lu, J. S. Abrams, E. Wang, M. Yamamura, and R. L. Modlin.** 1993. Cytokine production at the site of disease in human tuberculosis. Infect Immun **61:**3482-3489.

20. **Bermudez, L. E., and J. Goodman.** 1996. *Mycobacterium tuberculosis* invades and replicates within type II alveolar cells. Infect Immun **64:**1400-1406.

21. **Bermudez, L. E., F. J. Sangari, P. Kolonoski, M. Petrofsky, and J. Goodman.** 2002. The efficiency of the translocation of *Mycobacterium tuberculosis* across a bilayer of epithelial and endothelial cells as a model of the

alveolar wall is a consequence of transport within mononuclear phagocytes and invasion of alveolar epithelial cells. Infect Immun **70:**140-146.

22. **Bischoff, S. C., M. Krieger, T. Brunner, A. Rot, V. von Tscharner, M. Baggiolini, and C. A. Dahinden.** 1993. RANTES and related chemokines activate human basophil granulocytes through different G protein-coupled receptors. Eur J Immunol **23:**761-767.

23. **Bose, M., P. Farnia, S. Sharma, D. Chattopadhya, and K. Saha.** 1999. Nitric oxide dependent killing of *Mycobacterium tuberculosis* by human mononuclear phagocytes from patients with active tuberculosis. Int J Immunopathol Pharmacol **12:**69-79.

24. **Botha, T., and B. Ryffel.** 2003. Reactivation of latent tuberculosis infection in TNF-deficient mice. J Immunol **171:**3110-3118.

25. **Braciak, T. A., K. Bacon, Z. Xing, D. J. Torry, F. L. Graham, T. J. Schall, C. D. Richards, K. Croitoru, and J. Gauldie.** 1996. Overexpression of RANTES using a recombinant adenovirus vector induces the tissue-directed recruitment of monocytes to the lung. J Immunol **157:**5076-5084.

26. **Byrd, T. F.** 1998. Multinucleated giant cell formation induced by IFN-gamma/IL-3 is associated with restriction of virulent *Mycobacterium tuberculosis* cell to cell invasion in human monocyte monolayers. Cell Immunol **188:**89-96.

27. **Campbell, E. M., A. E. Proudfoot, T. Yoshimura, B. Allet, T. N. Wells, A. M. White, J. Westwick, and M. L. Watson.** 1997. Recombinant guinea pig and human RANTES activate macrophages but not eosinophils in the guinea pig. J Immunol **159:**1482-1489.

28. **Carter, A. B., M. M. Monick, and G. W. Hunninghake.** 1998. Lipopolysaccharide-induced NF-kappaB activation and cytokine release in human alveolar macrophages is PKC-independent and TK- and PC-PLC-dependent. Am J Respir Cell Mol Biol **18:**384-391.

29. **Casola, A., A. Henderson, T. Liu, R. P. Garofalo, and A. R. Brasier.** 2002. Regulation of RANTES promoter activation in alveolar epithelial cells after cytokine stimulation. Am J Physiol Lung Cell Mol Physiol **283:**L1280-1290.

30. **Catalfamo, M., T. Karpova, J. McNally, S. V. Costes, S. J. Lockett, E. Bos, P. J. Peters, and P. A. Henkart.** 2004. Human CD8+ T cells store RANTES in a unique secretory compartment and release it rapidly after TcR stimulation. Immunity **20:**219-230.

31. **Cauthen, G. M., A. Pio, and H. G. ten Dam.** 2002. Annual risk of tuberculous infection. 1988. Bull World Health Organ **80:**503-511; discussion 501-502.

32. **Centers for Disease Control and Prevention.** 2004. Tuberculosis associated with blocking agents against tumor necrosis factor-alpha--California, 2002-2003. MMWR Morb Mortal Wkly Rep **53:**683-686.

33. **Chang, T. L., C. J. Gordon, B. Roscic-Mrkic, C. Power, A. E. Proudfoot, J. P. Moore, and A. Trkola.** 2002. Interaction of the CC-chemokine RANTES with glycosaminoglycans activates a p44/p42 mitogen-activated protein kinase-dependent signaling pathway and enhances human immunodeficiency virus type 1 infectivity. J Virol **76:**2245-2254.

34. **Chensue, S. W., K. Warmington, J. H. Ruth, N. Lukacs, and S. L. Kunkel.** 1997. Mycobacterial and schistosomal antigen-elicited granuloma formation in IFN-gamma and IL-4 knockout mice: analysis of local and regional cytokine and chemokine networks. J Immunol **159:**3565-3573.

35. **Chensue, S. W., K. S. Warmington, E. J. Allenspach, B. Lu, C. Gerard, S. L. Kunkel, and N. W. Lukacs.** 1999. Differential expression and cross-regulatory function of RANTES during mycobacterial (type 1) and schistosomal (type 2) antigen-elicited granulomatous inflammation. J Immunol **163:**165-173.

36. **Chihara, J., H. Yamada, T. Yamamoto, D. Kurachi, N. Hayashi-Kameda, K. Honda, H. Kayaba, and O. Urayama.** 1998. Priming effect of RANTES on eosinophil oxidative metabolism. Allergy **53:**1178-1182.

37. **Ciesielski, C. J., E. Andreakos, B. M. Foxwell, and M. Feldmann.** 2002. TNFalpha-induced macrophage chemokine secretion is more dependent on NF-kappaB expression than lipopolysaccharides-induced macrophage chemokine secretion. Eur J Immunol **32:**2037-2045.

38. **Colditz, G. A., T. F. Brewer, C. S. Berkey, M. E. Wilson, E. Burdick, H. V. Fineberg, and F. Mosteller.** 1994. Efficacy of BCG vaccine in the prevention of tuberculosis. Meta-analysis of the published literature. Jama **271:**698-702.

39. **Cooper, A. M., A. Kipnis, J. Turner, J. Magram, J. Ferrante, and I. M. Orme.** 2002. Mice lacking bioactive IL-12 can generate protective, antigen-specific cellular responses to mycobacterial infection only if the IL-12 p40 subunit is present. J Immunol **168:**1322-1327.

40. **Cremer, I., J. Ghysdael, and V. Vieillard.** 2002. A non-classical ISRE/ISGF3 pathway mediates induction of RANTES gene transcription by type I IFNs. FEBS Lett **511:**41-45.

41. **Dahl, K. E., H. Shiratsuchi, B. D. Hamilton, J. J. Ellner, and Z. Toossi.** 1996. Selective induction of transforming growth factor beta in human monocytes by lipoarabinomannan of *Mycobacterium tuberculosis*. Infect Immun **64:**399-405.

42. **Darwin, K. H., S. Ehrt, J. C. Gutierrez-Ramos, N. Weich, and C. F. Nathan.** 2003. The proteasome of *Mycobacterium tuberculosis* is required for resistance to nitric oxide. Science **302:**1963-1966.

43. **de la Rosa, G., N. Longo, J. L. Rodriguez-Fernandez, A. Puig-Kroger, A. Pineda, A. L. Corbi, and P. Sanchez-Mateos.** 2003. Migration of human blood dendritic cells across endothelial cell monolayers: adhesion molecules and chemokines involved in subset-specific transmigration. J Leukoc Biol **73:**639-649.

44. **de Waal Malefyt, R., J. Abrams, B. Bennett, C. G. Figdor, and J. E. de Vries.** 1991. Interleukin 10(IL-10) inhibits cytokine synthesis by human monocytes: an autoregulatory role of IL-10 produced by monocytes. J Exp Med **174:**1209-1220.

45. **Denis, M.** 1991. Killing of *Mycobacterium tuberculosis* within human monocytes: activation by cytokines and calcitriol. Clin Exp Immunol **84:**200-206.

46. **Dentener, M. A., V. Bazil, E. J. Von Asmuth, M. Ceska, and W. A. Buurman.** 1993. Involvement of CD14 in lipopolysaccharide-induced tumor necrosis factor-alpha, IL-6 and IL-8 release by human monocytes and alveolar macrophages. J Immunol **150:**2885-2891.

47. **deSchoolmeester, M. L., M. C. Little, B. J. Rollins, and K. J. Else.** 2003. Absence of CC chemokine ligand 2 results in an altered Th1/Th2 cytokine balance and failure to expel Trichuris muris infection. J Immunol **170:**4693-4700.

48. **Devergne, O., A. Marfaing-Koka, T. J. Schall, M. B. Leger-Ravet, M. Sadick, M. Peuchmaur, M. C. Crevon, K. J. Kim, T. T. Schall, and T. Kim.** 1994. Production of the RANTES chemokine in delayed-type hypersensitivity reactions: involvement of macrophages and endothelial cells. J Exp Med **179:**1689-1694.

49. **Dinarello, C. A.** 1997. Proinflammatory and anti-inflammatory cytokines as mediators in the pathogenesis of septic shock. Chest **112:**321S-329S.

50. **Ding, A. H., and C. F. Nathan.** 1987. Trace levels of bacterial lipopolysaccharide prevent interferon-gamma or tumor necrosis factor-alpha

from enhancing mouse peritoneal macrophage respiratory burst capacity. J Immunol **139:**1971-1977.

51. **Ding, A. H., C. F. Nathan, and D. J. Stuehr.** 1988. Release of reactive nitrogen intermediates and reactive oxygen intermediates from mouse peritoneal macrophages. Comparison of activating cytokines and evidence for independent production. J Immunol **141:**2407-2412.

52. **Ding, Z., K. Xiong, and T. B. Issekutz.** 2000. Regulation of chemokine-induced transendothelial migration of T lymphocytes by endothelial activation: differential effects on naive and memory T cells. J Leukoc Biol **67:**825-833.

53. **Dorger, M., S. Munzing, A. M. Allmeling, K. Messmer, and F. Krombach.** 2001. Phenotypic and functional differences between rat alveolar, pleural, and peritoneal macrophages. Exp Lung Res **27:**65-76.

54. **Dorner, B. G., A. Scheffold, M. S. Rolph, M. B. Huser, S. H. Kaufmann, A. Radbruch, I. E. Flesch, and R. A. Kroczek.** 2002. MIP-1alpha, MIP-1beta, RANTES, and ATAC/lymphotactin function together with IFN-gamma as type 1 cytokines. Proc Natl Acad Sci U S A **99:**6181-6186.

55. **Dorner, B. G., S. Steinbach, M. B. Huser, R. A. Kroczek, and A. Scheffold.** 2003. Single-cell analysis of the murine chemokines MIP-1alpha, MIP-1beta, RANTES and ATAC/lymphotactin by flow cytometry. J Immunol Methods **274:**83-91.

56. **Dye, C., S. Scheele, P. Dolin, V. Pathania, and M. C. Raviglione.** 1999. Consensus statement. Global burden of tuberculosis: estimated incidence, prevalence, and mortality by country. WHO Global Surveillance and Monitoring Project. JAMA **282:**677-686.

57. **Ellner, J. J., P. F. Barnes, R. S. Wallis, and R. L. Modlin.** 1988. The immunology of tuberculous pleurisy. Semin Respir Infect **3:**335-342.

58. **Fenton, M. J., and M. W. Vermeulen.** 1996. Immunopathology of tuberculosis: roles of macrophages and monocytes. Infect Immun **64:**683-690.

59. **Ferlito, M., O. G. Romanenko, S. Ashton, F. Squadrito, P. V. Halushka, and J. A. Cook.** 2001. Effect of cross-tolerance between endotoxin and TNF-alpha or IL-1beta on cellular signaling and mediator production. J Leukoc Biol **70:**821-829.

60. **Fine, J. S., A. Rojas-Triana, J. V. Jackson, L. W. Engstrom, G. S. Deno, D. J. Lundell, and L. A. Bober.** 2003. Impairment of leukocyte trafficking in a murine pleuritis model by IL-4 and IL-10. Inflammation **27:**161-174.

61. **Flynn, J. L., and J. Chan.** 2001. Immunology of tuberculosis. Annu Rev Immunol **19:**93-129.

62. **Flynn, J. L., J. Chan, K. J. Triebold, D. K. Dalton, T. A. Stewart, and B. R. Bloom.** 1993. An essential role for interferon gamma in resistance to *Mycobacterium tuberculosis* infection. J Exp Med **178:**2249-2254.

63. **Flynn, J. L., M. M. Goldstein, J. Chan, K. J. Triebold, K. Pfeffer, C. J. Lowenstein, R. Schreiber, T. W. Mak, and B. R. Bloom.** 1995. Tumor necrosis factor-alpha is required in the protective immune response against *Mycobacterium tuberculosis* in mice. Immunity **2:**561-572.

64. **Foey, A. D., S. L. Parry, L. M. Williams, M. Feldmann, B. M. Foxwell, and F. M. Brennan.** 1998. Regulation of monocyte IL-10 synthesis by endogenous IL-1 and TNF-alpha: role of the p38 and p42/44 mitogen-activated protein kinases. J Immunol **160:**920-928.

65. **Fok, J. S., R. S. Ho, P. K. Arora, G. E. Harding, and D. W. Smith.** 1976. Host-parasite relationships in experimental airborne tuberculosis. V. Lack of hematogenous dissemination of *Mycobacterium tuberculosis* to the lungs in animals vaccinated with Bacille Calmette-Guerin. J Infect Dis **133:**137-144.

66. **Fraker, D. L., M. C. Stovroff, M. J. Merino, and J. A. Norton.** 1988. Tolerance to tumor necrosis factor in rats and the relationship to endotoxin tolerance and toxicity. J Exp Med **168:**95-105.

67. **Frye, M. D., C. J. Pozsik, and S. A. Sahn.** 1997. Tuberculous pleurisy is more common in AIDS than in non-AIDS patients with tuberculosis. Chest **112:**393-397.

68. **Fuller, C. L., J. L. Flynn, and T. A. Reinhart.** 2003. In situ study of abundant expression of proinflammatory chemokines and cytokines in pulmonary granulomas that develop in cynomolgus macaques experimentally infected with *Mycobacterium tuberculosis*. Infect Immun **71:**7023-7034.

69. **Fulton, S. A., J. V. Cross, Z. T. Toossi, and W. H. Boom.** 1998. Regulation of interleukin-12 by interleukin-10, transforming growth factor-beta, tumor necrosis factor-alpha, and interferon-gamma in human monocytes infected with *Mycobacterium tuberculosis* H37Ra. J Infect Dis **178:**1105-1114.

70. **Gangadharam, P. R., and P. F. Pratt.** 1983. *In vitro* response of murine alveolar and peritoneal macrophages to Mycobacterium intracellulare. Am Rev Respir Dis **128:**1044-1047.

71. **Garcia-Perez, B. E., R. Mondragon-Flores, and J. Luna-Herrera.** 2003. Internalization of *Mycobacterium tuberculosis* by macropinocytosis in non-phagocytic cells. Microb Pathog **35:**49-55.

72. **Gaynor, C. D., F. X. McCormack, D. R. Voelker, S. E. McGowan, and L. S. Schlesinger.** 1995. Pulmonary surfactant protein A mediates enhanced phagocytosis of *Mycobacterium tuberculosis* by a direct interaction with human macrophages. J Immunol **155:**5343-5351.

73. **Hart, P. D., and I. Sutherland.** 1977. BCG and vole bacillus vaccines in the prevention of tuberculosis in adolescence and early adult life. Br Med J **2:**293-295.

74. **Henderson, R. A., S. C. Watkins, and J. L. Flynn.** 1997. Activation of human dendritic cells following infection with *Mycobacterium tuberculosis*. J Immunol **159:**635-643.

75. **Hill, A. R., S. Premkumar, S. Brustein, K. Vaidya, S. Powell, P. W. Li, and B. Suster.** 1991. Disseminated tuberculosis in the acquired immunodeficiency syndrome era. Am Rev Respir Dis **144:**1164-1170.

76. **Hirsch, C. S., R. Hussain, Z. Toossi, G. Dawood, F. Shahid, and J. J. Ellner.** 1996. Cross-modulation by transforming growth factor beta in human tuberculosis: suppression of antigen-driven blastogenesis and interferon gamma production. Proc Natl Acad Sci U S A **93:**3193-3198.

77. **Hirsch, C. S., T. Yoneda, L. Averill, J. J. Ellner, and Z. Toossi.** 1994. Enhancement of intracellular growth of *Mycobacterium tuberculosis* in human monocytes by transforming growth factor-beta 1. J Infect Dis **170:**1229-1237.

78. **Holscher, C., R. A. Atkinson, B. Arendse, N. Brown, E. Myburgh, G. Alber, and F. Brombacher.** 2001. A protective and agonistic function of IL-12p40 in mycobacterial infection. J Immunol **167:**6957-6966.

79. **Honda, K., and J. Chihara.** 1999. Eosinophil activation by eotaxin--eotaxin primes the production of reactive oxygen species from eosinophils. Allergy **54:**1262-1269.

80. **Hoogewerf, A. J., G. S. Kuschert, A. E. Proudfoot, F. Borlat, I. Clark-Lewis, C. A. Power, and T. N. Wells.** 1997. Glycosaminoglycans mediate cell surface oligomerization of chemokines. Biochemistry **36:**13570-13578.

81. **Hoshino, Y., D. B. Tse, G. Rochford, S. Prabhakar, S. Hoshino, N. Chitkara, K. Kuwabara, E. Ching, B. Raju, J. A. Gold, W. Borkowsky, W. N. Rom, R. Pine, and M. Weiden.** 2004. *Mycobacterium tuberculosis*-induced CXCR4 and chemokine expression leads to preferential X4 HIV-1 replication in human macrophages. J Immunol **172:**6251-6258.

82. **Hu, B., J. H. Jennings, J. Sonstein, J. Floros, J. C. Todt, T. Polak, and J. L. Curtis.** 2003. Resident murine alveolar and peritoneal macrophages differ in adhesion of apoptotic thymocytes. Am J Respir Cell Mol Biol **30:**687-693.

83. **Hua, C. C., L. C. Chang, Y. C. Chen, and S. C. Chang.** 1999. Proinflammatory cytokines and fibrinolytic enzymes in tuberculous and malignant pleural effusions. Chest **116:**1292-1296.

84. **Jackett, P. S., P. W. Andrew, V. R. Aber, and D. B. Lowrie.** 1981. Hydrogen peroxide and superoxide release by alveolar macrophages from normal and BCG-vaccinated guinea-pigs after intravenous challenge with *Mycobacterium tuberculosis*. Br J Exp Pathol **62:**419-428.

85. **Jeevan, A., T. Yoshimura, G. Foster, and D. N. McMurray.** 2002. Effect of *Mycobacterium bovis* BCG vaccination on interleukin-1 beta and RANTES mRNA expression in guinea pig cells exposed to attenuated and virulent mycobacteria. Infect Immun **70:**1245-1253.

86. **Jeevan, A., T. Yoshimura, K. E. Lee, and D. N. McMurray.** 2003. Differential expression of gamma interferon mRNA induced by attenuated and virulent *Mycobacterium tuberculosis* in guinea pig cells after *Mycobacterium bovis* BCG vaccination. Infect Immun **71:**354-364.

87. **Jiang, Y., D. I. Beller, G. Frendl, and D. T. Graves.** 1992. Monocyte chemoattractant protein-1 regulates adhesion molecule expression and cytokine production in human monocytes. J Immunol **148:**2423-2428.

88. **Jones, B. W., K. A. Heldwein, T. K. Means, J. J. Saukkonen, and M. J. Fenton.** 2001. Differential roles of Toll-like receptors in the elicitation of proinflammatory responses by macrophages. Ann Rheum Dis **60 Suppl 3:**iii6-iii12.

89. **Juffermans, N. P., S. Florquin, L. Camoglio, A. Verbon, A. H. Kolk, P. Speelman, S. J. van Deventer, and T. van Der Poll.** 2000. Interleukin-1

signaling is essential for host defense during murine pulmonary tuberculosis. J Infect Dis **182:**902-908.

90. **Juffermans, N. P., A. Verbon, S. J. van Deventer, H. van Deutekom, J. T. Belisle, M. E. Ellis, P. Speelman, and T. van der Poll.** 1999. Elevated chemokine concentrations in sera of human immunodeficiency virus (HIV)-seropositive and HIV-seronegative patients with tuberculosis: a possible role for mycobacterial lipoarabinomannan. Infect Immun **67:**4295-4297.

91. **Kapp, A., G. Zeck-Kapp, W. Czech, and E. Schopf.** 1994. The chemokine RANTES is more than a chemoattractant: characterization of its effect on human eosinophil oxidative metabolism and morphology in comparison with IL-5 and GM-CSF. J Invest Dermatol **102:**906-914.

92. **Katayama, H., A. Yokoyama, N. Kohno, K. Sakai, K. Hiwada, H. Yamada, and K. Hirai.** 2002. Production of eosinophilic chemokines by normal pleural mesothelial cells. Am J Respir Cell Mol Biol **26:**398-403.

93. **Kaufmann, A., D. Gemsa, and H. Sprenger.** 2000. Differential desensitization of lipopolysaccharide-inducible chemokine gene expression in human monocytes and macrophages. Eur J Immunol **30:**1562-1567.

94. **Kawai, T., M. Seki, K. Hiromatsu, J. W. Eastcott, G. F. Watts, M. Sugai, D. J. Smith, S. A. Porcelli, and M. A. Taubman.** 1999. Selective diapedesis of Th1 cells induced by endothelial cell RANTES. J Immunol **163:**3269-3278.

95. **Kim, J. J., J. S. Yang, T. Dentchev, K. Dang, and D. B. Weiner.** 2000. Chemokine gene adjuvants can modulate immune responses induced by DNA vaccines. J Interferon Cytokine Res **20:**487-498.

96. **Kinjo, Y., K. Kawakami, K. Uezu, S. Yara, K. Miyagi, Y. Koguchi, T. Hoshino, M. Okamoto, Y. Kawase, K. Yokota, K. Yoshino, K. Takeda, S. Akira, and A. Saito.** 2002. Contribution of IL-18 to Th1 response and host defense against infection by *Mycobacterium tuberculosis*: a comparative study with IL-12p40. J Immunol **169:**323-329.

97. **Kisich, K. O., M. Higgins, G. Diamond, and L. Heifets.** 2002. Tumor necrosis factor alpha stimulates killing of *Mycobacterium tuberculosis* by human neutrophils. Infect Immun **70:**4591-4599.

98. **Klunner, T., T. Bartels, M. Vordermeier, R. Burger, and H. Schafer.** 2001. Immune reactions of CD4- and CD8-positive T cell subpopulations in spleen and lymph nodes of guinea pigs after vaccination with Bacillus Calmette Guerin. Vaccine **19:**1968-1977.

99. **Kopydlowski, K. M., C. A. Salkowski, M. J. Cody, N. van Rooijen, J. Major, T. A. Hamilton, and S. N. Vogel.** 1999. Regulation of macrophage chemokine expression by lipopolysaccharide *in vitro* and *in vivo*. J Immunol **163:**1537-1544.

100. **Kurasawa, T., and K. Shimokata.** 1991. Cooperation between accessory cells and T lymphocytes in patients with tuberculous pleurisy. Chest **100:**1046-1052.

101. **Kurashima, K., N. Mukaida, M. Fujimura, M. Yasui, Y. Nakazumi, T. Matsuda, and K. Matsushima.** 1997. Elevated chemokine levels in bronchoalveolar lavage fluid of tuberculosis patients. Am J Respir Crit Care Med **155:**1474-1477.

102. **Ladel, C. H., C. Blum, A. Dreher, K. Reifenberg, M. Kopf, and S. H. Kaufmann.** 1997. Lethal tuberculosis in interleukin-6-deficient mutant mice. Infect Immun **65:**4843-4849.

103. **Lankford, C. S., and D. M. Frucht.** 2003. A unique role for IL-23 in promoting cellular immunity. J Leukoc Biol **73:**49-56.

104. **Laochumroonvorapong, P., S. Paul, C. Manca, V. H. Freedman, and G. Kaplan.** 1997. Mycobacterial growth and sensitivity to H2O2 killing in human monocytes *in vitro*. Infect Immun **65:**4850-4857.

105. **Lasco, T. M., L. Cassone, H. Kamohara, T. Yoshimura, T. Yamamoto, and D. N. McMurray.** 2004. Evaluating the role of tumor necrosis factor-alpha in experimental pulmonary tuberculosis in the guinea pig. Infect Immun in press.

106. **Lasco, T. M., T. Yamamoto, T. Yoshimura, S. S. Allen, L. Cassone, and D. N. McMurray.** 2003. Effect of *Mycobacterium bovis* BCG vaccination on Mycobacterium-specific cellular proliferation and tumor necrosis factor alpha production from distinct guinea pig leukocyte populations. Infect Immun **71:**7035-7042.

107. **Laurence, J. S., A. C. LiWang, and P. J. LiWang.** 1998. Effect of N-terminal truncation and solution conditions on chemokine dimer stability: nuclear magnetic resonance structural analysis of macrophage inflammatory protein 1 beta mutants. Biochemistry **37:**9346-9354.

108. **Leemans, J. C., S. Florquin, M. Heikens, S. T. Pals, R. van der Neut, and T. Van Der Poll.** 2003. CD44 is a macrophage binding site for *Mycobacterium tuberculosis* that mediates macrophage recruitment and protective immunity against tuberculosis. J Clin Invest **111:**681-689.

109. **Levine, H., P. B. Szanto, and D. W. Cugell.** 1968. Tuberculous pleurisy. An acute illness. Arch Intern Med **122:**329-332.

110. **Lillard, J. W., Jr., P. N. Boyaka, D. D. Taub, and J. R. McGhee.** 2001. RANTES potentiates antigen-specific mucosal immune responses. J Immunol **166:**162-169.

111. **Lin, Y., M. Zhang, and P. F. Barnes.** 1998. Chemokine production by a human alveolar epithelial cell line in response to *Mycobacterium tuberculosis*. Infect Immun **66:**1121-1126.

112. **Liu, L., F. P. Mul, T. W. Kuijpers, R. Lutter, D. Roos, and E. F. Knol.** 1996. Neutrophil transmigration across monolayers of endothelial cells and airway epithelial cells is regulated by different mechanisms. Ann N Y Acad Sci **796:**21-29.

113. **Locati, M., U. Deuschle, M. L. Massardi, F. O. Martinez, M. Sironi, S. Sozzani, T. Bartfai, and A. Mantovani.** 2002. Analysis of the gene expression profile activated by the CC chemokine ligand 5/RANTES and by lipopolysaccharide in human monocytes. J Immunol **168:**3557-3562.

114. **Lopez, M., L. M. Sly, Y. Luu, D. Young, H. Cooper, and N. E. Reiner.** 2003. The 19-kDa *Mycobacterium tuberculosis* protein induces macrophage apoptosis through Toll-like receptor-2. J Immunol **170:**2409-2416.

115. **Losa Garcia, J. E., F. M. Rodriguez, M. R. Martin de Cabo, M. J. Garcia Salgado, J. P. Losada, L. G. Villaron, A. J. Lopez, and J. L. Arellano.** 1999. Evaluation of inflammatory cytokine secretion by human alveolar macrophages. Mediators Inflamm **8:**43-51.

116. **Losana, G., C. Bovolenta, L. Rigamonti, I. Borghi, F. Altare, E. Jouanguy, G. Forni, J. L. Casanova, B. Sherry, M. Mengozzi, G. Trinchieri, G. Poli, F. Gerosa, and F. Novelli.** 2002. IFN-gamma and IL-12 differentially regulate CC-chemokine secretion and CCR5 expression in human T lymphocytes. J Leukoc Biol **72:**735-742.

117. **Lozes, E., K. Huygen, J. Content, O. Denis, D. L. Montgomery, A. M. Yawman, P. Vandenbussche, J. P. Van Vooren, A. Drowart, J. B. Ulmer, and M. A. Liu.** 1997. Immunogenicity and efficacy of a tuberculosis DNA vaccine encoding the components of the secreted antigen 85 complex. Vaccine **15:**830-833.

118. **Lyons, M. J., T. Yoshimura, and D. N. McMurray.** 2002. *Mycobacterium bovis* BCG vaccination augments interleukin-8 mRNA expression and protein

production in guinea pig alveolar macrophages infected with *Mycobacterium tuberculosis*. Infect Immun **70:**5471-5478.

119. **Lyons, M. J., T. Yoshimura, and D. N. McMurray.** 2004. Interleukin (IL)-8 (CXCL8) induces cytokine expression and superoxide formation by guinea pig neutrophils infected with *Mycobacterium tuberculosis*. Tuberculosis (Edinb) **84:**283-292.

120. **Maghazachi, A. A., A. Al-Aoukaty, and T. J. Schall.** 1996. CC chemokines induce the generation of killer cells from CD56+ cells. Eur J Immunol **26:**315-319.

121. **Makino, Y., D. N. Cook, O. Smithies, O. Y. Hwang, E. G. Neilson, L. A. Turka, H. Sato, A. D. Wells, and T. M. Danoff.** 2002. Impaired T cell function in RANTES-deficient mice. Clin Immunol **102:**302-309.

122. **Marfaing-Koka, A., O. Devergne, G. Gorgone, A. Portier, T. J. Schall, P. Galanaud, and D. Emilie.** 1995. Regulation of the production of the RANTES chemokine by endothelial cells. Synergistic induction by IFN-gamma plus TNF-alpha and inhibition by IL-4 and IL-13. J Immunol **154:**1870-1878.

123. **Marfaing-Koka, A., M. Maravic, M. Humbert, P. Galanaud, and D. Emilie.** 1996. Contrasting effects of IL-4, IL-10 and corticosteroids on RANTES production by human monocytes. Int Immunol **8:**1587-1594.

124. **Martin, W. J., 2nd, J. F. Downing, M. D. Williams, R. Pasula, H. L. Twigg, 3rd, and J. R. Wright.** 1995. Role of surfactant protein A in the pathogenesis of tuberculosis in subjects with human immunodeficiency virus infection. Proc Assoc Am Physicians **107:**340-345.

125. **Matsukawa, A., N. W. Lukacs, C. M. Hogaboam, S. W. Chensue, and S. L. Kunkel.** 2001. III. Chemokines and other mediators, 8. Chemokines and their receptors in cell-mediated immune responses in the lung. Microsc Res Tech **53:**298-306.

126. **McDonough, K. A., Y. Kress, and B. R. Bloom.** 1993. Pathogenesis of tuberculosis: interaction of *Mycobacterium tuberculosis* with macrophages. Infect Immun **61:**2763-2773.

127. **McMurray, D. N.** 1994. Guinea Pig Model of Tuberculosis, p. 135-147. *In* B. R. Bloom (ed.), Tuberculosis: Pathogenesis, Protection, and Control. American Society of Microbiology, Washington, DC.

128. **McMurray, D. N., F. M. Collins, A. M. Dannenberg, Jr., and D. W. Smith (ed.).** 1996. Pathogenesis of Experimental Tuberculosis in Animal Models, vol. 215. Springer-Verlag Berlin.

129. **McMurray, D. N., G. Dai, and S. Phalen.** 1999. Mechanisms of vaccine-induced resistance in a guinea pig model of pulmonary tuberculosis. Tuber Lung Dis **79:**261-266.

130. **Means, T. K., R. P. Pavlovich, D. Roca, M. W. Vermeulen, and M. J. Fenton.** 2000. Activation of TNF-alpha transcription utilizes distinct MAP kinase pathways in different macrophage populations. J Leukoc Biol **67:**885-893.

131. **Means, T. K., S. Wang, E. Lien, A. Yoshimura, D. T. Golenbock, and M. J. Fenton.** 1999. Human toll-like receptors mediate cellular activation by *Mycobacterium tuberculosis*. J Immunol **163:**3920-3927.

132. **Mederle, I., R. Le Grand, B. Vaslin, E. Badell, B. Vingert, D. Dormont, B. Gicquel, and N. Winter.** 2003. Mucosal administration of three recombinant *Mycobacterium bovis* BCG-SIVmac251 strains to cynomolgus macaques induces rectal IgAs and boosts systemic cellular immune responses that are primed by intradermal vaccination. Vaccine **21:**4153-4166.

133. **Medvedev, A. E., K. M. Kopydlowski, and S. N. Vogel.** 2000. Inhibition of lipopolysaccharide-induced signal transduction in endotoxin-tolerized mouse macrophages: dysregulation of cytokine, chemokine, and toll-like receptor 2 and 4 gene expression. J Immunol **164:**5564-5574.

134. **Medzhitov, R., P. Preston-Hurlburt, E. Kopp, A. Stadlen, C. Chen, S. Ghosh, and C. A. Janeway, Jr.** 1998. MyD88 is an adaptor protein in the hToll/IL-1 receptor family signaling pathways. Mol Cell **2:**253-258.

135. **Mohammed, K. A., N. Nasreen, M. J. Ward, K. K. Mubarak, F. Rodriguez-Panadero, and V. B. Antony.** 1998. Mycobacterium-mediated chemokine expression in pleural mesothelial cells: role of C-C chemokines in tuberculous pleurisy. J Infect Dis **178:**1450-1456.

136. **Mohan, V. P., C. A. Scanga, K. Yu, H. M. Scott, K. E. Tanaka, E. Tsang, M. M. Tsai, J. L. Flynn, and J. Chan.** 2001. Effects of tumor necrosis factor alpha on host immune response in chronic persistent tuberculosis: possible role for limiting pathology. Infect Immun **69:**1847-1855.

137. **Momi, H., W. Matsuyama, K. Inoue, M. Kawabata, K. Arimura, H. Fukunaga, and M. Osame.** 2002. Vascular endothelial growth factor and proinflammatory cytokines in pleural effusions. Respir Med **96:**817-822.

138. **Morehead, R. S.** 1998. Tuberculosis of the pleura. South Med J **91:**630-636.

139. **Mukaida, N.** 2000. Interleukin-8: an expanding universe beyond neutrophil chemotaxis and activation. Int J Hematol **72:**391-398.

140. **Nelson, P. J., H. T. Kim, W. C. Manning, T. J. Goralski, and A. M. Krensky.** 1993. Genomic organization and transcriptional regulation of the RANTES chemokine gene. J Immunol **151:**2601-2612.

141. **Nelson, P. J., B. D. Ortiz, J. M. Pattison, and A. M. Krensky.** 1996. Identification of a novel regulatory region critical for expression of the RANTES chemokine in activated T lymphocytes. J Immunol **157:**1139-1148.

142. **O'Brien, A. D., T. J. Standiford, P. J. Christensen, S. E. Wilcoxen, and R. Paine, 3rd.** 1998. Chemotaxis of alveolar macrophages in response to signals derived from alveolar epithelial cells. J Lab Clin Med **131:**417-424.

143. **Ohtani, N., H. Ohtani, T. Nakayama, H. Naganuma, E. Sato, T. Imai, H. Nagura, and O. Yoshie.** 2004. Infiltration of CD8+ T cells containing RANTES/CCL5+ cytoplasmic granules in actively inflammatory lesions of human chronic gastritis. Lab Invest **84:**368-375.

144. **Oppmann, B., R. Lesley, B. Blom, J. C. Timans, Y. Xu, B. Hunte, F. Vega, N. Yu, J. Wang, K. Singh, F. Zonin, E. Vaisberg, T. Churakova, M. Liu, D. Gorman, J. Wagner, S. Zurawski, Y. Liu, J. S. Abrams, K. W. Moore, D. Rennick, R. de Waal-Malefyt, C. Hannum, J. F. Bazan, and R. A. Kastelein.** 2000. Novel p19 protein engages IL-12p40 to form a cytokine, IL-23, with biological activities similar as well as distinct from IL-12. Immunity **13:**715-725.

145. **Orme, I. M., D. N. McMurray, and J. T. Belisle.** 2001. Tuberculosis vaccine development: recent progress. Trends Microbiol **9:**115-118.

146. **Pace, E., M. Gjomarkaj, M. Melis, M. Profita, M. Spatafora, A. M. Vignola, G. Bonsignore, and C. H. Mody.** 1999. Interleukin-8 induces lymphocyte chemotaxis into the pleural space. Role of pleural macrophages. Am J Respir Crit Care Med **159:**1592-1599.

147. **Pan, Z. Z., L. Parkyn, A. Ray, and P. Ray.** 2000. Inducible lung-specific expression of RANTES: preferential recruitment of neutrophils. Am J Physiol Lung Cell Mol Physiol **279:**L658-666.

148. **Parham, C., M. Chirica, J. Timans, E. Vaisberg, M. Travis, J. Cheung, S. Pflanz, R. Zhang, K. P. Singh, F. Vega, W. To, J. Wagner, A. M. O'Farrell, T. McClanahan, S. Zurawski, C. Hannum, D. Gorman, D. M. Rennick, R. A.**

Kastelein, R. de Waal Malefyt, and K. W. Moore. 2002. A receptor for the heterodimeric cytokine IL-23 is composed of IL-12Rbeta1 and a novel cytokine receptor subunit, IL-23R. J Immunol **168:**5699-5708.

149. **Park, J. S., Y. S. Kim, Y. K. Jee, N. H. Myong, and K. Y. Lee.** 2003. Interleukin-8 production in tuberculous pleurisy: role of mesothelial cells stimulated by cytokine network involving tumour necrosis factor-alpha and interleukin-1 beta. Scand J Immunol **57:**463-469.

150. **Pasula, R., J. F. Downing, J. R. Wright, D. L. Kachel, T. E. Davis, Jr., and W. J. Martin, 2nd.** 1997. Surfactant protein A (SP-A) mediates attachment of *Mycobacterium tuberculosis* to murine alveolar macrophages. Am J Respir Cell Mol Biol **17:**209-217.

151. **Pasula, R., P. Wisniowski, and W. J. Martin, 2nd.** 2002. Fibronectin facilitates *Mycobacterium tuberculosis* attachment to murine alveolar macrophages. Infect Immun **70:**1287-1292.

152. **Pearl, J. E., B. Saunders, S. Ehlers, I. M. Orme, and A. M. Cooper.** 2001. Inflammation and lymphocyte activation during mycobacterial infection in the interferon-gamma-deficient mouse. Cell Immunol **211:**43-50.

153. **Petit-Bertron, A. F., C. Fitting, J. M. Cavaillon, and M. Adib-Conquy.** 2003. Adherence influences monocyte responsiveness to interleukin-10. J Leukoc Biol **73:**145-154.

154. **Phalen, S. W., and D. N. McMurray.** 1993. T-lymphocyte response in a guinea pig model of tuberculous pleuritis. Infect Immun **61:**142-145.

155. **Pieters, J.** 2001. Entry and survival of pathogenic mycobacteria in macrophages. Microbes Infect **3:**249-255.

156. **Platzer, C., C. Meisel, K. Vogt, M. Platzer, and H. D. Volk.** 1995. Up-regulation of monocytic IL-10 by tumor necrosis factor-alpha and cAMP elevating drugs. Int Immunol **7:**517-523.

157. **Proudfoot, A. E., T. M. Handel, Z. Johnson, E. K. Lau, P. LiWang, I. Clark-Lewis, F. Borlat, T. N. Wells, and M. H. Kosco-Vilbois.** 2003. Glycosaminoglycan binding and oligomerization are essential for the *in vivo* activity of certain chemokines. Proc Natl Acad Sci U S A **100:**1885-1890.

158. **Qiu, B., K. A. Frait, F. Reich, E. Komuniecki, and S. W. Chensue.** 2001. Chemokine expression dynamics in mycobacterial (type-1) and schistosomal

(type-2) antigen-elicited pulmonary granuloma formation. Am J Pathol **158:**1503-1515.

159. **Rathanaswami, P., M. Hachicha, M. Sadick, T. J. Schall, and S. R. McColl.** 1993. Expression of the cytokine RANTES in human rheumatoid synovial fibroblasts. Differential regulation of RANTES and interleukin-8 genes by inflammatory cytokines. J Biol Chem **268:**5834-5839.

160. **Reiling, N., C. Holscher, A. Fehrenbach, S. Kroger, C. J. Kirschning, S. Goyert, and S. Ehlers.** 2002. Cutting edge: Toll-like receptor (TLR)2- and TLR4-mediated pathogen recognition in resistance to airborne infection with *Mycobacterium tuberculosis*. J Immunol **169:**3480-3484.

161. **Roach, D. R., A. G. Bean, C. Demangel, M. P. France, H. Briscoe, and W. J. Britton.** 2002. TNF regulates chemokine induction essential for cell recruitment, granuloma formation, and clearance of mycobacterial infection. J Immunol **168:**4620-4627.

162. **Roche, P. W., J. A. Triccas, and N. Winter.** 1995. BCG vaccination against tuberculosis: past disappointments and future hopes. Trends Microbiol **3:**397-401.

163. **Rollins, B. J., A. Walz, and M. Baggiolini.** 1991. Recombinant human MCP-1/JE induces chemotaxis, calcium flux, and the respiratory burst in human monocytes. Blood **78:**1112-1116.

164. **Roper, W. H., and J. J. Waring.** 1955. Primary serofibrinous pleural effusion in military personnel. Am Rev Tuberc **71:**616-634.

165. **Roscic-Mrkic, B., M. Fischer, C. Leemann, A. Manrique, C. J. Gordon, J. P. Moore, A. E. Proudfoot, and A. Trkola.** 2003. RANTES (CCL5) uses the proteoglycan CD44 as an auxiliary receptor to mediate cellular activation signals and HIV-1 enhancement. Blood **102:**1169-1177.

166. **Roth, S. J., T. G. Diacovo, M. B. Brenner, J. P. Rosat, J. Buccola, C. T. Morita, and T. A. Springer.** 1998. Transendothelial chemotaxis of human alpha/beta and gamma/delta T lymphocytes to chemokines. Eur J Immunol **28:**104-113.

167. **Sadek, M. I., E. Sada, Z. Toossi, S. K. Schwander, and E. A. Rich.** 1998. Chemokines induced by infection of mononuclear phagocytes with mycobacteria and present in lung alveoli during active pulmonary tuberculosis. Am J Respir Cell Mol Biol **19:**513-521.

168. **Salez, L., M. Singer, V. Balloy, C. Creminon, and M. Chignard.** 2000. Lack of IL-10 synthesis by murine alveolar macrophages upon lipopolysaccharide exposure. Comparison with peritoneal macrophages. J Leukoc Biol **67:**545-552.

169. **Samson, M., O. Labbe, C. Mollereau, G. Vassart, and M. Parmentier.** 1996. Molecular cloning and functional expression of a new human CC-chemokine receptor gene. Biochemistry **35:**3362-3367.

170. **Sannohe, S., T. Adachi, K. Hamada, K. Honda, Y. Yamada, N. Saito, C. H. Cui, H. Kayaba, K. Ishikawa, and J. Chihara.** 2003. Upregulated response to chemokines in oxidative metabolism of eosinophils in asthma and allergic rhinitis. Eur Respir J **21:**925-931.

171. **Sato, E., K. L. Simpson, M. B. Grisham, S. Koyama, and R. A. Robbins.** 1999. Effects of reactive oxygen and nitrogen metabolites on RANTES- and IL-5-induced eosinophil chemotactic activity *in vitro*. Am J Pathol **155:**591-598.

172. **Sato, K., T. Akaki, and H. Tomioka.** 1998. Differential potentiation of anti-mycobacterial activity and reactive nitrogen intermediate-producing ability of murine peritoneal macrophages activated by interferon-gamma (IFN-gamma) and tumour necrosis factor-alpha (TNF-alpha). Clin Exp Immunol **112:**63-68.

173. **Sato, K., H. Tomioka, T. Shimizu, T. Gonda, F. Ota, and C. Sano.** 2002. Type II alveolar cells play roles in macrophage-mediated host innate resistance to pulmonary mycobacterial infections by producing proinflammatory cytokines. J Infect Dis **185:**1139-1147.

174. **Saukkonen, J. J., B. Bazydlo, M. Thomas, R. M. Strieter, J. Keane, and H. Kornfeld.** 2002. Beta-chemokines are induced by *Mycobacterium tuberculosis* and inhibit its growth. Infect Immun **70:**1684-1693.

175. **Schall, T. J., K. Bacon, K. J. Toy, and D. V. Goeddel.** 1990. Selective attraction of monocytes and T lymphocytes of the memory phenotype by cytokine RANTES. Nature **347:**669-671.

176. **Schindler, R., B. D. Clark, and C. A. Dinarello.** 1990. Dissociation between interleukin-1 beta mRNA and protein synthesis in human peripheral blood mononuclear cells. J Biol Chem **265:**10232-10237.

177. **Schindler, R., J. Mancilla, S. Endres, R. Ghorbani, S. C. Clark, and C. A. Dinarello.** 1990. Correlations and interactions in the production of interleukin-6 (IL-6), IL-1, and tumor necrosis factor (TNF) in human blood mononuclear cells: IL-6 suppresses IL-1 and TNF. Blood **75:**40-47.

178. **Schlesinger, L. S., C. G. Bellinger-Kawahara, N. R. Payne, and M. A. Horwitz.** 1990. Phagocytosis of *Mycobacterium tuberculosis* is mediated by human monocyte complement receptors and complement component C3. J Immunol **144:**2771-2780.

179. **Schlesinger, L. S., T. M. Kaufman, S. Iyer, S. R. Hull, and L. K. Marchiando.** 1996. Differences in mannose receptor-mediated uptake of lipoarabinomannan from virulent and attenuated strains of *Mycobacterium tuberculosis* by human macrophages. J Immunol **157:**4568-4575.

180. **Seibert, A. F., J. Haynes, Jr., R. Middleton, and J. B. Bass, Jr.** 1991. Tuberculous pleural effusion. Twenty-year experience. Chest **99:**883-886.

181. **Seiler, P., P. Aichele, S. Bandermann, A. E. Hauser, B. Lu, N. P. Gerard, C. Gerard, S. Ehlers, H. J. Mollenkopf, and S. H. Kaufmann.** 2003. Early granuloma formation after aerosol *Mycobacterium tuberculosis* infection is regulated by neutrophils via CXCR3-signaling chemokines. Eur J Immunol **33:**2676-2686.

182. **Shi, S., C. Nathan, D. Schnappinger, J. Drenkow, M. Fuortes, E. Block, A. Ding, T. R. Gingeras, G. Schoolnik, S. Akira, K. Takeda, and S. Ehrt.** 2003. MyD88 primes macrophages for full-scale activation by interferon-gamma} yet mediates few responses to *Mycobacterium tuberculosis*. J Exp Med **198:**987-997.

183. **Silva-Mejias, C., F. Gamboa-Antinolo, L. F. Lopez-Cortes, M. Cruz-Ruiz, and J. Pachon.** 1995. Interleukin-1 beta in pleural fluids of different etiologies. Its role as inflammatory mediator in empyema. Chest **108:**942-945.

184. **Skwor, T. A., H. Cho, C. Cassidy, T. Yoshimura, and D. N. McMurray.** 2004. Recombinant guinea pig CCL5 (RANTES) differentially modulates cytokine production in alveolar and peritoneal macrophages. J Leukoc Biol **76.**

185. **Smith, D. W., Harding G. E.** 1978. Influence of BCG vaccination on the bacillemic phase of experimental airborne tuberculosis in guinea pigs, p. 85-90. *In* R. J. Montali (ed.), Mycobacterial Infections of Zoo Animals. Smithsonian Institution Press, Washington DC.

186. **Smith, D. W., D. N. McMurray, E. H. Wiegeshaus, A. A. Grover, and G. E. Harding.** 1970. Host-parasite relationships in experimental airborne tuberculosis. IV. Early events in the course of infection in vaccinated and nonvaccinated guinea pigs. Am Rev Respir Dis **102:**937-949.

187. **Song, A., A. Patel, K. Thamatrakoln, C. Liu, D. Feng, C. Clayberger, and A. M. Krensky.** 2002. Functional domains and DNA-binding sequences of RFLAT-

1/KLF13, a Kruppel-like transcription factor of activated T lymphocytes. J Biol Chem **277:**30055-30065.

188. **Sozzani, S., M. Locati, D. Zhou, M. Rieppi, W. Luini, G. Lamorte, G. Bianchi, N. Polentarutti, P. Allavena, and A. Mantovani.** 1995. Receptors, signal transduction, and spectrum of action of monocyte chemotactic protein-1 and related chemokines. J Leukoc Biol **57:**788-794.

189. **Stellato, C., L. A. Beck, G. A. Gorgone, D. Proud, T. J. Schall, S. J. Ono, L. M. Lichtenstein, and R. P. Schleimer.** 1995. Expression of the chemokine RANTES by a human bronchial epithelial cell line. Modulation by cytokines and glucocorticoids. J Immunol **155:**410-418.

190. **Sugawara, I., H. Yamada, Y. Kazumi, N. Doi, K. Otomo, T. Aoki, S. Mizuno, T. Udagawa, Y. Tagawa, and Y. Iwakura.** 1998. Induction of granulomas in interferon-gamma gene-disrupted mice by avirulent but not by virulent strains of *Mycobacterium tuberculosis*. J Med Microbiol **47:**871-877.

191. **Swanson, B. J., M. Murakami, T. C. Mitchell, J. Kappler, and P. Marrack.** 2002. RANTES production by memory phenotype T cells is controlled by a posttranscriptional, TCR-dependent process. Immunity **17:**605-615.

192. **Tachibana, K., G. J. Chen, D. S. Huang, P. Scuderi, and R. R. Watson.** 1992. Production of tumor necrosis factor alpha by resident and activated murine macrophages. J Leukoc Biol **51:**251-255.

193. **Taub, D. D., S. M. Turcovski-Corrales, M. L. Key, D. L. Longo, and W. J. Murphy.** 1996. Chemokines and T lymphocyte activation: I. Beta chemokines costimulate human T lymphocyte activation *in vitro*. J Immunol **156:**2095-2103.

194. **Teitelbaum, R., W. Schubert, L. Gunther, Y. Kress, F. Macaluso, J. W. Pollard, D. N. McMurray, and B. R. Bloom.** 1999. The M cell as a portal of entry to the lung for the bacterial pathogen *Mycobacterium tuberculosis*. Immunity **10:**641-650.

195. **Teran, L. M., M. Mochizuki, J. Bartels, E. L. Valencia, T. Nakajima, K. Hirai, and J. M. Schroder.** 1999. Th1- and Th2-type cytokines regulate the expression and production of eotaxin and RANTES by human lung fibroblasts. Am J Respir Cell Mol Biol **20:**777-786.

196. **Trajkovic, V., G. Singh, B. Singh, S. Singh, and P. Sharma.** 2002. Effect of *Mycobacterium tuberculosis*-specific 10-kilodalton antigen on macrophage release of tumor necrosis factor alpha and nitric oxide. Infect Immun **70:**6558-6566.

197. **Tso, H. W., Y. L. Lau, C. M. Tam, H. S. Wong, and A. K. Chiang.** 2004. Associations between IL12B Polymorphisms and Tuberculosis in the Hong Kong Chinese Population. J Infect Dis **190:**913-919.

198. **Turner, L., S. G. Ward, and J. Westwick.** 1995. RANTES-activated human T lymphocytes. A role for phosphoinositide 3-kinase. J Immunol **155:**2437-2444.

199. **van Crevel, R., T. H. Ottenhoff, and J. W. van der Meer.** 2002. Innate immunity to *Mycobacterium tuberculosis*. Clin Microbiol Rev **15:**294-309.

200. **Vankayalapati, R., B. Wizel, S. E. Weis, B. Samten, W. M. Girard, and P. F. Barnes.** 2000. Production of interleukin-18 in human tuberculosis. J Infect Dis **182:**234-239.

201. **VanOtteren, G. M., T. J. Standiford, S. L. Kunkel, J. M. Danforth, M. D. Burdick, L. V. Abruzzo, and R. M. Strieter.** 1994. Expression and regulation of macrophage inflammatory protein-1 alpha by murine alveolar and peritoneal macrophages. Am J Respir Cell Mol Biol **10:**8-15.

202. **Verbon, A., N. Juffermans, S. J. Van Deventer, P. Speelman, H. Van Deutekom, and T. Van Der Poll.** 1999. Serum concentrations of cytokines in patients with active tuberculosis (TB) and after treatment. Clin Exp Immunol **115:**110-113.

203. **Villalta, F., Y. Zhang, K. E. Bibb, J. C. Kappes, and M. F. Lima.** 1998. The cysteine-cysteine family of chemokines RANTES, MIP-1alpha, and MIP-1beta induce trypanocidal activity in human macrophages via nitric oxide. Infect Immun **66:**4690-4695.

204. **Walzer, T., A. Marcais, F. Saltel, C. Bella, P. Jurdic, and J. Marvel.** 2003. Cutting edge: immediate RANTES secretion by resting memory CD8 T cells following antigenic stimulation. J Immunol **170:**1615-1619.

205. **Wang, M. J., K. C. Jeng, and P. C. Shih.** 1999. Differential expression of inducible nitric oxide synthase gene by alveolar and peritoneal macrophages in lipopolysaccharide-hyporesponsive C3H/HeJ mice. Immunology **98:**497-503.

206. **Wang, Y., C. G. Kelly, J. T. Karttunen, T. Whittall, P. J. Lehner, L. Duncan, P. MacAry, J. S. Younson, M. Singh, W. Oehlmann, G. Cheng, L. Bergmeier, and T. Lehner.** 2001. CD40 is a cellular receptor mediating mycobacterial heat shock protein 70 stimulation of CC-chemokines. Immunity **15:**971-983.

207. **Wang, Y., C. G. Kelly, M. Singh, E. G. McGowan, A. S. Carrara, L. A. Bergmeier, and T. Lehner.** 2002. Stimulation of Th1-polarizing cytokines, C-C chemokines, maturation of dendritic cells, and adjuvant function by the peptide binding fragment of heat shock protein 70. J Immunol **169:**2422-2429.

208. **Wanidworanun, C., and W. Strober.** 1993. Predominant role of tumor necrosis factor-alpha in human monocyte IL-10 synthesis. J Immunol **151:**6853-6861.

209. **Weber, C., K. S. Weber, C. Klier, S. Gu, R. Wank, R. Horuk, and P. J. Nelson.** 2001. Specialized roles of the chemokine receptors CCR1 and CCR5 in the recruitment of monocytes and T(H)1-like/CD45RO(+) T cells. Blood **97:**1144-1146.

210. **Wickremasinghe, M. I., L. H. Thomas, C. M. O'Kane, J. Uddin, and J. S. Friedland.** 2004. Transcriptional mechanisms regulating alveolar epithelial cell-specific CCL5 secretion in pulmonary tuberculosis. J Biol Chem **279:**27199-27210.

211. **Xin, K. Q., Y. Lu, K. Hamajima, J. Fukushima, J. Yang, K. Inamura, and K. Okuda.** 1999. Immunization of RANTES expression plasmid with a DNA vaccine enhances HIV-1-specific immunity. Clin Immunol **92:**90-96.

212. **Xu, K., and C. L. Geczy.** 2000. IFN-gamma and TNF regulate macrophage expression of the chemotactic S100 protein S100A8. J Immunol **164:**4916-4923.

213. **Yoshimura, T.** 1993. cDNA cloning of guinea pig monocyte chemoattractant protein-1 and expression of the recombinant protein. J Immunol **150:**5025-5032.

214. **Yoshimura, T., and D. G. Johnson.** 1993. cDNA cloning and expression of guinea pig neutrophil attractant protein-1 (NAP-1). NAP-1 is highly conserved in guinea pig. J Immunol **151:**6225-6236.

215. **Zhang, X., and D. N. McMurray.** 1998. Suppression of lymphoproliferation by alveolar macrophages in the guinea pig. Tuber Lung Dis **79:**119-126.

216. **Zimmerli, S., S. Edwards, and J. D. Ernst.** 1996. Selective receptor blockade during phagocytosis does not alter the survival and growth of *Mycobacterium tuberculosis* in human macrophages. Am J Respir Cell Mol Biol **15:**760-770.

217. **Zou, W., J. Borvak, F. Marches, S. Wei, P. Galanaud, D. Emilie, and T. J. Curiel.** 2000. Macrophage-derived dendritic cells have strong Th1-polarizing potential mediated by beta-chemokines rather than IL-12. J Immunol **165:**4388-4396.

VITA

TROY ARTHUR SKWOR

ADDRESS:

Texas A&M University System Health Science Center
Department of Medical Microbiology & Immunology
Rm 407 Reynolds Medical Building
College Station, TX 77843-1114
(979)845-3679

EDUCATION:

December 2004	Doctor of Philosophy, Medical Sciences Department of Medical Microbiology & Immunology Texas A&M University College Station, TX
May 1999	Bachelor of Science, Medical Microbiology & Immunology College of Letters and Science University of Wisconsin – Madison Madison, WI

PUBLICATIONS AND POSTER PRESENTATIONS:

Skwor, T. A., H. Cho, C. Cassidy, T. Yoshimura, and D. N. McMurray. 2004. Recombinant guinea pig CCL5 (RANTES) differentially modulates cytokine production in alveolar and peritoneal macrophages. J Leukoc Biol. (in press).

Skwor, T. A., S. Seberry, L. Berghman, and D. N. McMurray. 2004. Effect of BCG vaccination on CCL5 (RANTES) production *in vitro* and *in vivo* in response to *Mycobacterium tuberculosis* in the guinea pig. Infect Immun. (submitted).

Jeevan, A., C. T. McFarland, T. Yoshimura, T. Skwor, T. Lasco, and D. N. McMurray. 2004. Production and characterization of guinea pig recombinant IFN gamma: Effect on MHC II expression and growth of *Mycobacterium tuberculosis* in macrophages. International Symposium on Emerging Trends in Tuberculosis Research 2004, New Delhi, India.

Skwor, T.A. and D. N. McMurray. 2003. Vaccination enhances IL-12p40 mRNA levels in guinea pig alveolar macrophages infected with *Mycobacterium tuberculosis.* US-Japan Tuberculosis and Leprosy Research Conference 2003, Newark, NJ